

Spray and Combustion Characteristics in Biodiesel Fuels

November 2019

Annisa Bhikuning

ABSTRACT

Recently biodiesel has becoming more attractive because the environmental benefits and it is made from renewable resources. Commonly, biodiesel is made from the trans-esterification process using methanol or alcohol and catalyst KOH/ NaOH to produce the biodiesel. The uses of biodiesel in the diesel engine have some advantages such as high cetane number, oxidation stability and can reduce the emissions. However, higher viscosity, boiling temperatures and surface tension in biodiesel may affect the spray characteristics compared to diesel oil. To overcome the unbeneficial in biodiesel, therefore, the new approaches in fuel design have been studied. In this study, the fuels were design to a new method that high-boiling point fuel in jatropha methyl ester is mixed to n-tridecane which is a low-boiling point fuel in order to improve the properties in jatropha methyl ester. Moreover, the emulsions fuel research is also conducted in this study to improve the micro-explosions in the fuel. Furthermore, biodiesel from waste cooking oil and bio hydro-finned diesel oil are also investigated.

In this study, the tested fuels are jatropha methyl ester (JME) blended to n-tridecane by volume (25:75, 50:50, 75:25 and 0:100), biodiesel fuel 100% (BDF) , bio hydro-fined diesel oil (BHD), and biodiesel water emulsions (BWE). Adding the n-tridecane in jatropha methyl ester can improve the fuel properties in the fuel. Higher percentage of n-tridecane in jatropha methyl ester can improve the boiling point; reduce the viscosity and surface tension. Moreover, bio hydro-fined diesel oil (BHD) is a second generation fuels which is not using the trans-esterification process but using hydro finning process shows improved the density and viscosity while biodiesel fuel (BDF) shows higher in viscosity, density and boiling point. Moreover, biodiesel water emulsions is made from waste cooking oil 5%, water 10%, diesel oil 100% and emulsions 18.7% shows higher viscosity, density and lower in caloric value compared to diesel oil.

In this study, the investigation of fuels are divided into several analyses. Firstly, non-evaporating sprays were conducted in the room temperature with different injection pressures (50, 100, and 150 MPa) and evaporating sprays were at 400,500, and 600 K. The spray tip penetration, cone angle, and sauter mean diameter were taken into account. The results show that biodiesel fuel (BDF) which is high in viscosity, density and high boiling point when it conducted in the evaporating condition in high injection pressure can make improved in spray characteristic. This happened because at high injection pressure the BDF can be improved in atomization makes spray characteristics nearly the same as low boiling fuels.

Secondly, Laser Induced Scattering (LIS) were conducted only in room temperature with injection pressure of 100 MPa for JME, and 50, 100, and 150 MPa for BHD, BDF, and tridecane. LIS is effected by the viscosity, density and surface tension in the fuel. Higher viscosity fuels show higher in liquid phase penetration. However, liquid length is not effected by injection pressure because at higher injection pressure has the longer liquid length. Nevertheless, the longer liquid length affects liquid impingement in diesel engine and also increase the emissions (unburned carbon) due to incomplete combustion occurred.

Thirdly, experiments in the combustion and emissions were conducted in diesel engine 4 stroke, direct injection, and single cylinder for different EGR rates and different injection pressures. The fuels are Diesel Oil (JIS), BHD and BDF. The results show that EGR is effective in reducing NO_x emissions but it is not recommended to conduct in partial load due to increase in CO, THC, and smoke emissions. Moreover, BHD shows a good result in thermal efficiency. The thermal efficiency in BHD can reached to 2.28 to 8.1% as compared to JIS and BDF. As fuel injection pressure increases, the brake thermal efficiency decreases and the fuel consumption decreases. This is because at high injection pressure a good atomization can be achieved and the combustion characteristics can be improved.

Lastly, the testing using biodiesel water emulsion was conducted in Yanmar diesel engine, four cylinder 4 stoke in different loads. The biodiesel water emulsion was compared to diesel oil and biodiesel blends with diesel oil. The results show that at high load and low load biodiesel water emulsion can increase the thermal efficiency up to 8.04% - 9.79% than diesel oil. This happened due to the micro-explosions in the fuel that high boiling fuel (biodiesel fuel) is mixed with low boiling material (water) with the emulsion. The water inside the fuel is vaporized earlier than biodiesel, which makes micro-explosions happened to improve the combustion characteristics and reduced in the emissions.

ACKNOWLEDGEMENTS

In the name of Allah, the Most Gracious, the Most Merciful.

Firstly and foremost, all praise in the world is to Allah, the All Mighty, for the blessings and strengths to finish this research and thesis.

I would like to express my sincere gratitude to Professor Jiro Senda and Professor Eriko Matsumura who give their guidance, their valuable time and encourage me to complete the research to fulfill my doctoral in Mechanical Engineering Department, Doshisha University.

I would also like to express my gratitude to the Directorate General of Higher Education Ministry of Education Culture of Indonesia (DIKTI), Regional Higher Education Service Institution (LLDIKTI III)- Jakarta and Trisakti University for their supports.

Also, I would like to thank to my biomass fuel teams and friends. Ryusuke Sagawa, Naoki Matsumoto, Kohsuke Nishiura, Ryunosuke Sugawara, Xin Li, and Shoi Koshikawa. Thank you very much for helping me in conducting the experiments and also thank you for your time and your support.

I would like to special thanks for my husband, Yapri Rizal who support me, encourage me, and help me in many conditions to finish my study. Also many thanks to my children, Baihaqi Ramadhan and Khadeeja Prisa Azzahra for their support, their loving and always give a nice smile to me.

Lastly, I would like to say thank you for my parents and family, who always support and pray for me so that I have a huge motivation in finishing my doctoral study.

November, 22nd 2019

Annisa Bhikuning

PREFACE

Biodiesel is one of the alternative fuel in the future. The use in biodiesel was started long time ago when Rudolf Diesel (1858-1913), the inventor of the engine that had some interested in biodiesels. He visualized that pure vegetable oils could power early diesel engines for agriculture, where petroleum was not available at the time. However, the biodiesel industry and research have been established in the Europe in the early of 1980s.

The viscosity in vegetable oils is higher than diesel fuel. High viscosity causes poor atomization of the fuel in the engine's combustion chambers and effects in operational problems such as engine deposits. Therefore, to overcome this. There are four methods in producing biodiesel; blending with diesel fuel, trans-esterification, pyrolysis and the micro-emulsions.

In this study, the tested fuels are from jatropha methyl ester (JME) and biodiesel fuel (BDF) which are from trans-esterification process using a catalyst KOH. Bio-hydro fined diesel oil (BHD) is a second generation oil made from hydro finning process, it is one of the pyrolysis process , and biodiesel water emulsions is using the micro-emulsions process that the combination between biodiesel, water and the emulsions.

The author had an experience in the experiment of running the diesel water emulsions into the diesel engine. The experimental study was carried under diesel water emulsions and conducted in one hour for performance tested and 17 hours for endurance tested. The results show that after the endurance test, at 60% load, water-diesel emulsion has 11% efficient than diesel oil. However, in minimum loads (idle, 20%, and 40%), before and after endurance tested diesel oil has more efficient compared to diesel-water emulsion. Moreover, the emissions show that after endurance test, at all loads, water-diesel emulsion can reduce NOx emission and opacity to 3.2% (20% load). In maximum load (80%), water-diesel emulsion can reduce emissions from NOx and CO up to 42% to 23.7%, as compared to diesel oil. These results show that emulsion fuel research can be considered as alternative technology in improving the combustion and reduced the emissions.

Bio-hydro fined diesel oil (BHD) is using hydro fined process that using hydrogen and Ni-Mo as a catalyst. The fuel properties in BHD oil is nearly the same as diesel oil. The oil based of BHD is from used cooking oil that collected in Kyoto area. The advantage in BHD is the oxygen content 0.4% in the fuel that

can improved the combustion characteristics and also reduce the emissions. While, the diesel oil has no oxygen content and makes the emissions higher than BHD.

The fuel design approach was also been studied. The method is mixing between low boiling point fuel (tridecane) with higher boiling fuel (jatropha methyl ester), so that the fuel properties in the fuel can be improved. Pure jatropha methyl ester has high viscosity, density, and surface tension that can lead poor atomization of the fuel in the diesel combustion. By mixing with low boiling point fuel (tridecane) with pure jatropha metyl ester makes the viscosity, density and surface tension are better than before. Therefore, this can achieved in good spray characteristics, better atomization of the fuel and reduced in the emissions.

The finding of a good method to find better biodiesel is important to study. There are many methods can be used to produce the biodiesel. The good achievements are better viscosity, density, surface tension and high cetane number in the biodiesel, therefore, the fuel can be run in the diesel engine in long period time without any fears in engine deposits. Moreover, the important is having good atomization of the fuel that can improve the combustion characteristics in the diesel engine.

Annisa Bhikuning

TABLE OF CONTENTS

	PAGE
ABSTRACT	i
ACKNOWLEDGEMENTS	iii
PREFACE	iv
TABLE OF CONTENTS	vi
LIST OF TABLES	xiii
LIST OF FIGURES	xiv
Chapter 1. Introduction	1
1.1. Introduction	1
1.2. Background of the Research	2
1.3. Objectives of the study	3
1.4. Organization of the thesis	4
Chapter 2. Literature Review	7
2.1. Introduction	7
2.2. Spray Characteristics	8
2.2.1. Spray Tip Penetration	9
2.2.2. Spray cone angle	13
2.2.3. Sauter Mean Diameter	16
2.2.4. Evaporating Spray	19
2.3. Fuel Design approach for Spray Combustion Control	19
2.3.1. Flash Boiling Process for Single Component	19
2.3.2. Flash Boiling for Two Component Solution	21
2.3.3. The Design of Fuel	22
2.4. References	24

Chapter 3. Emulsion Fuel Research	28
3.1 Introduction	28
3.2. Water-diesel emulsions	29
3.3 Water-biodiesel emulsions	30
3.4. Micro-explosions	31
3.5. Case studies in water-diesel emulsions	32
3.5.1. Experimental conditions	33
3.5.2. Results	33
3.5.3. Conclusions	33
3.6. References	34
Chapter 4. Biodiesel Production	36
4.1. Introduction	36
4.2. Chemical Structure	36
4.3. The Production of Biodiesel	37
4.3.1. Blending Oil	37
4.3.2. Trans-esterification	38
4.3.3. Micro-emulsions	41
4.3.4. Phyrolysis	42
4.4. Simulation of Biodiesel Production	42
4.5. Conclusions	45
4.6. References	46
Chapter 5. Fuel Analysis	48
5.1. Introduction	48
5.2. Fuel Preparation for JME Blending with n-Tridecane	48
5.2.1. Fuel Properties	48
5.2.2. Density	48
5.2.3. Viscosity	49
5.2.4. Flash Point	50
5.2.5. Cetane Number	51
5.2.6. Copper Strip Corrosion	51

5.2.7. Distillation	52
5.2.8. FTIR Analysis	53
5.2.9. Tridecane	53
5.2.10. JME 25% (Jatropha Methyl Ester 25% and n-Tridecane 75%)	54
5.2.11. JME 50% (Jatropha Methyl Ester 50% and n-Tridecane 50%)	55
5.2.12. JME 75% (JatrophaMethyl Ester 75% and n-Tridecane 25%)	56
5.3. Chemical Analysis of Biodiesel-Water Emulsions	57
5.3.1 Fuel Preparation	57
5.3.2. Density	57
5.3.3. Kinematic Viscosity	58
5.3.4. Flash Point	59
5.3.5. Cetane Index	59
5.3.6. Caloric Value	60
5.3.7. Distillation	61
5.3.8. FTIR Analysis	62
5.4 Chemical Analysis of Bio Hydro-Fined Diesel Oil (BHD) and Biodiesel Fuel (BDF)	64
5.4.1. Fuel Preparation	64
5.4.2. Density	65
5.4.3. Viscosity	65
5.4.4. Distillation	65
5.5. Conclusions	66
5.7. References	66
Chapter 6. Non-Evaporating Spray Characteristics	69
6.1. Introduction	69
6.2. Fuel Design Method	69
6.3. Experimental Method	70
6.4. Non-evaporating Spray from Jatropha Methyl Ester (JME) and its blends	71
6.4.1. Fuel Properties	71
6.4.2. Experimental Conditions	72
6.4.3 Results and discussions	72

6.4.3.1. Spray Tip Penetration	73
6.4.3.2. Spray Angle	75
6.4.3.3. Sauter Mean Diameter (SMD)	77
6.5 Non-evaporating Spray from Bio-hydro Fined Diesel Oil (BHD) and Biodiesel Fuel (BDF)	79
6.5.1. Fuel Properties	79
6.5.2. Experimental Conditions	79
6.5.3. Results and Discussions	80
6.5.3.1. Spray Characteristics	81
6.5.3.2. Sauter Mean Diameter (SMD)	82
6.6. Conclusions	83
6.7. References	83
Chapter 7. Evaporating Characteristics	85
7.1 Introduction	85
7.2. Experimental Method	85
7.3. Experimental Conditions	85
7.4. Results and Discussion	86
7.4.1 Evaporating Spray from Jatropha Methyl Ester (JME) and its blends	86
7.4.1.2. Fuel Distillations and Spray Image	86
7.4.1.3. Spray Tip Penetration	87
7.4.1.4. Spray Angle	88
7.4.2. Evaporating Spray from Bio-Hydro Fined Diesel (BHD) and Biodiesel Fuel (BDF)	88
7.4.2.1. Fuel Distillation and Spray Image	88
7.4.2.2. Spray Characteristics	90
7.4.2.3. Sauter Mean Diameter	91
7.5. Conclusion	93
7.6. References	93

Chapter 8. Laser Induced Scattering	95
8.1. Introduction	95
8.2. Experimental Method	96
8.3. Experimental Condition	97
8.4. Result and Discussion	98
8.4.1. Jatropha Methyl Ester (JME) and its Blends	98
8.4.1.1. Spray Characteristics	99
8.4.1.2 Spray Angle (JME25, JME50, and JME75)	100
8.4.2. Bio-Hydro Fined Diesel Oil (BHD), Waste Cooking Oil (WCO), Tridecane ($C_{13}H_{28}$)	102
8.4.2.1 Spray Characteristics	103
8.4.2.2. Spray Angle (Tridecane, BHD, and WCO)	104
8.4.2.3. The Effect of Liquid Length with Different Injection Pressures	105
8.5. Conclusion	106
8.6. References	106
Chapter 9. Combustion, Emissions and Heat Balance Analysis	108
9.1. Introduction	108
9.2. Materials and Method	108
9.2.1. Materials	108
9.2.2. Experimental Method	109
9.3. Experimental Results	112
9.3.1. Engine Performances	112
9.3.1.1. Brake Specific Fuel Consumption (BSFC)	112
9.3.1.2. Thermal Efficiency	113
9.3.1.3. Brake Mean Effective Pressure	114
9.3.2. Emissions Characteristics	115
9.3.2.1. Carbon monoxide (CO)	115
9.3.2.2. Nitrogen oxides (NO _x)	116
9.3.2.3. Hydro Carbon Emissions (THC)	117
9.3.2.4. Smoke	118
9.3.3. Engine Combustion Analysis	119

9.3.3.1. Peak Cylinder Pressures and Heat Release	119
9.3.4. Correlation between Combustion Phasing and EGR Rate	121
9.3.5. Correlation between Combustion Phasing and Fuel Properties	122
9.3.6. Correlation between Combustion Phasing and Combustion Duration	123
9.3.5. Heat Balance Analysis	124
9.4. Experimental Results in Different Injection Pressure	128
9.4.1 Experimental Condition	128
9.4.2 Results and Discussions	128
9.4.2.1 Combustion Characteristics	128
9.4.2.2. Heat Release Rate and Cylinder Pressures	130
9.4.2.3. Emissions	131
9.4.2.4. Correlation between Combustion Phasing	132
9.5. Conclusions	133
9.6. References	133
Chapter 10. Combustion and Emission Characteristics in Biodiesel Water Emulsions	136
10.1. Introduction	136
10.2. Materials and Method	136
10.2.1. Materials	136
10.2.2. Experimental Method	136
10.3. Results and Discussions	138
10.3.1. Engine Performance and emissions	139
10.3.1.1. Specific Fuel Consumption	139
10.3.1.2. Thermal Efficiency	140
10.3.2. Emissions	141
10.3.2.1. CO Emission	141
10.3.2.2. CO ₂ Emission	142
10.3.2.3. Smoke Opacity	142
10.4. Conclusions	143
10.5. References	144

Chapter 11. Conclusions	145
11.1. Summary of the Present Work	145
11.2. Contributions from the Present Work	147
11.3. Direction for Future Work	147

LIST OF TABLES

	Page
Table 2.1. Fuel Properties of diesel fuel (DF), palm methyl ester (PME), jatropha methyl ester (JME) and its blends	10
Table 2.2. Comparison between spray structure of biodiesel and diesel fuel	12
Table 2.3. The Comparison of SMD from biodiesel palm oil	18
Table 2.4. Fuel design approach [46]	22
Table 4.2. Rapeseed Fatty Acid Oil Profile and Properties [12]	40
Table 4.3. Physical Properties [23]	44
Table 6.1. The fuel properties	71
Table 6.2. The experimental conditions in non-evaporating spray	72
Table 6.3. Fuel Properties	79
Table 6.4. The Experimental Conditions	79
Table 7.1. The experimental conditions in all Fuels	85
Table 8.1. Experimental Conditions of Laser Induced Scattering (LIS)	97
Table 9.1. Fuel properties from various fuels	109
Table 9.2. Engine specifications	109
Table 9.3. Experimental conditions	110
Table 9.4. Experimental Conditions in different injection pressures	128
Table 10.1. Engine specifications	137
Table 10.2. Specifications measurement gases by exhaust gas and opacity	138
Table 10.3. Fuel Properties from Various Fuels	139

LIST OF FIGURES

	Page
Figure 1.1. Trans-esterification Reaction of Biodiesel	2
Figure 2.1. The experimental setup of spray by Agarwal A.K et al [21]	9
Figure 2.2. Spray penetration and spray cone angle	9
Figure 2.3. Spray cone angle for diesel fuel compare with Jatropha Blends with different ambient pressure (JB 20- Jatropha Blend 20%, JB100- Jatropha 100%) by Patel C et al [28]	14
Figure 2.4. Spray Figures from different fuels with three different injection pressures (P_{inj}) (0.7 msASOI, 15 kg/m ³ , Biodiesel Palm Oil (BDFp), Biodiesel Cooking Oil (BDFc)) by Wang x, et al [26]	15
Figure 2.5. Image of illustrating the droplets within the spray by Guan L et al [34]	16
Figure 2.6. Sauter Mean Diameter (SMD)in Palm Oil (BDF20-Biodiesel Fuel 20%, BDF50- Biodiesel Fuel 50% and BDF100- Biodiesel Fuel 100%) by Choi S and Oh Y [32]	17
Figure 2.7. Diesel spray combustion [35]	19
Figure 2.8. Improvement of spray atomization and evaporation processes in flash boiling spray [40,41]	20
Figure 2.9. Modeling of flash boiling spray [40, 41]	20
Figure 2.10. Two-phase region formation in multi-component fuel in phase change Process [44,45]	21
Figure 2.11. Two-phase of mixing fuel consisting of liquefied CO ₂ and <i>n</i> -tridecane [46]	23
Figure 2.12. Ignition delay of single component and <i>n</i> -peptane/ <i>n</i> -tridecane mixed fuel [46]	23
Figure 3.1. Physical Structure of two phase and three phase	28
Figure 3.2. (a) Illustration of biodiesel and water in emulsion (enlargement 100x); (b) Illustration of biodiesel and water in emulsion (enlargement 200x) [12]	29
Figure 3.3. Schematic diagram of micro-explosions in water-diesel and biodiesel emulsion [24]	31

Figure 3.4. Illustration of making water-diesel emulsions [24] (a) Preparing water, diesel oil, and emulsions; (b) Mixing between all ingredients and stirred until 15 minutes; (c) After stirring 15 minutes, the water-diesel emulsions were mixed	32
Figure 4.1. Molecular Structure, (a) Diesel Fuel; (b) Biodiesel; (c) Vegetable Oil [3]	37
Figure 4.2. Trans-esterification Triglycerides with Alcohol	38
Figure 4.3. The trans-esterification of vegetable oil with alcohol to ester and glycerol [8]	39
Figure 4.4. The process flow sheet developed in ChemCad 6.3.1 [23]	43
Figure 4.5. Liquid mass fraction in different column; (a) Column 7, (b) Column 18, (c) column 21 [23]	45
Figure 5.1. Density from various blends	49
Figure 5.2. Viscosity from various blends	49
Figure 5.3. Flash point from various blends	50
Figure 5.4. Cetane number from various blends	51
Figure 5.5. Copper strip corrosion from various blends	52
Figure 5.6. Distillation from various blends	52
Figure 5.7. FTIR n-Tridecane	53
Figure 5.8. FTIR JME 25%	54
Figure 5.9. FTIR JME 50%	55
Figure 5.10. FTIR JME 75%	56
Figure 5.11. Density from various fuels	57
Figure 5.12. Kinematic viscosity from various fuels	58
Figure 5.13. Flash point from various fuels	59
Figure 5.14. Cetane index from various fuels	60
Figure 5.15. Caloric value from various fuels	60

Figure 5.16. Distillation ratio from various fuels	61
Figure 5.17. Infrared spectrometry of BD100	62
Figure 5.18. Infrared spectrometry of BD5W10	62
Figure 5.19. Infrared Spectrometry of BD5	63
Figure 5.20. Infrared Spectrometry of BD10	63
Figure 5.21. Density from various Fuels	65
Figure 5.22. Viscosity from various fuels	65
Figure 5.23. Distillation from various fuels	65
Figure 6.1. Pressure-temperature diagram of multi-component fuel	69
Figure 6.2. Schematic diagram of constant volume vessel	70
Figure 6.3. Optical setup for shadowgraph photography	70
Figure 6.4. Optical set up for super high spatial resolution photography	71
Figure 6.5. Shadowgraph images at different time at $P_{inj} = 100$ MPa	73
Figure 6.6. Spray tip penetration in non-evaporating (a) All fuels at $P_{inj} = 100$ MPa; (b) JME100 and tridecane at $P_{inj} = 50$ MPa; (c) JME100 and tridecane at $P_{inj} = 100$ MPa; (d) JME100 and tridecane at $P_{inj} = 150$ MPa	74
Figure 6.7. Parameters of spray characteristics	75
Figure 6.8. Spray cone angle in non-evaporating (a) All fuels at $P_{inj} = 100$ MPa; (b) JME100 and tridecane at $P_{inj} = 50$ MPa; (c) JME100 and tridecane at $P_{inj} = 100$ MPa; (d) JME100 and tridecane at $P_{inj} = 150$ MPa	76
Figure 6.9. (a) Analysis Region; (b) Sauter Mean Diameter (μm) at $T = 293$ K, $P_{inj} = 100$ MPa, $P_a = 1.58$ MPa, $\rho_a = 18.75$ kg/m^3 , $t/t_{inj} = 0.5$	77
Figure 6.10. Droplet number frequency from JME blends at $T = 293$ K, $P_{inj} = 100$ MPa, $P_a = 1.58$ MPa, $\rho_a = 18.75$ kg/m^3 , $t/t_{inj} = 0.5$	78

Figure 6.11. The spray evolution process from different fuels with three different injection pressure ($P_{inj} = 50, 100, 150 \text{ MPa}$, $\rho_a = 18.75 \text{ kg/m}^3$, $T_a = 293 \text{ K}$) at 1.0 ms after start of injection (ASOI)	80
Figure 6.12. Spray tip Penetration and spray angle in non-evaporating condition (a)(b) 50 MPa, (c) (d) 100MPa, and (e) (f) 150 MPa	81
Figure 6.13. SMD with different injection pressure at non-evaporating condition ($P_{inj}=50, 100, 150 \text{ MPa}$)	82
Figure 7.1. Distillation Curves for JME blends	86
Figure 7.2. Spray Image for Evaporating of JME and its Blends ($t/t_{inj}=1.0$, $T_a=573 \text{ K}$, $P_a=1.85 \text{ MPa}$)	86
Figure 7.3. Spray Tip Penetration in Evaporating Condition for Various Fuels	87
Figure 7.4. Spray Angle in Evaporating Condition for Various Fuels	88
Figure 7.5. Fuel Distillation of BDF and BHD	88
Figure 7.6. Spray Evolution Process	89
Figure 7.7 Spray Tip Penetration and Spray Angle in Evaporating Condition for Various Fuels	90
Figure 7.8. Sauter Mean Diameter from Various Fuels ($T_a= 400, 500 \text{ K}$)	91
Figure 7.9. Droplet Number Frequency from Various Fuels ($T_a= 500 \text{ K}$; $P_{inj}= 100 \text{ MPa}$; $P_a= 1.77 \text{ MPa}$)	92
Figure 8.1. The structure of complete and incomplete spray [1]	95
Figure 8.2. Schematic Diagram of Sheet Scattered Photography	97
Figure 8.3. Sheet Scattered Photography Images at Different Time ($P_{inj}=100 \text{ MPa}$)	98
Figure 8.4. Liquid Penetration Length in Various Fuels	99
Figure 8.5. Effect of Physical characteristics in Fuel on Liquid Phase Penetration	100

Figure 8.6. Definition of Spray Angle	100
Figure 8.7. Spray Angle in Liquid Phase for Various Fuels	101
Figure 8.8. Sheet Scattered Photography Images at Different Time ($P_{inj}=100$ MPa)	102
Figure 8.9. Sheet Scattered Photography Images at $t=100$ ms	102
Figure 8.10. Liquid Phase Penetration from Various Fuel at 100 MPa	103
Figure 8.11. Effect of Physical characteristics in Fuel on Liquid Phase Penetration in Various Fuels	103
Figure 8.12. Spray Angle in Liquid Phase for Various Fuels	104
Figure 8.13. Liquid Phase Penetration of BHD in Different Injection Pressures	105
Figure 9.1. Schematic diagram of experiment	111
Figure 9.2. Brake specific fuel consumption from various fuels	113
Figure 9.3. Thermal efficiency from various fuels	113
Figure 9.4. Brake Mean Effective Pressures	115
Figure 9.5. CO Emissions in low and Partial Loads	116
Figure 9.6. NO _x Emissions in Low and Partial Loads	117
Figure 9.7. THC Emissions in Low and Partial Load	118
Figure 9.8. Smoke Emissions in Low and Partial Loads	119
Figure 9.9. Cylinder pressure at low and partial with EGR 0, 10%, 20%	120
Figure 9.10. Heat release at low and partial load with EGR 0, 10%, 20%	121
Figure 9.11. Combustion Phasing CA50 and CA90 versus EGR Rate	122
Figure 9.12. Correlation between CA50 with Viscosity and Density	123
Figure 9.13. Correlation between CA50 with Combustion Period	123
Figure 9.14. Heat Balance without EGR at low and partial load	126

Figure 9.15. Heat Balance with EGR 10 and 20 at Partial Load	127
Figure 9.16. Brake mean effective pressures in different injection pressures	128
Figure 9.17. Thermal efficiency in different injection pressures	129
Figure 9.18. Brake specific fuel consumption in different injection pressures	129
Figure 9.19. Heat Release Rate at $P_{inj} = 100, 125$ and 150 MPa	130
Figure 9.20. Cylinder pressure in different injection pressures	130
Figure 9.21. Emissions from various fuels in different injection pressures	131
Figure 9.22. Correlation between CA50 and CA90 in different injection pressures	132
Figure 9.23. Correlation between combustion period and injection pressures	132
Figure 10.1. Experimental Set Up	137
Figure 10.2. Specific Fuel Consumption from Various Fuels	139
Figure 10.3. Thermal Efficiency from Various Fuels	140
Figure 10.4. CO Emission from Various Fuels	141
Figure 10.5. CO ₂ Emission from Various Fuels	142
Figure 10.6. Smoke Opacity from Various Fuels	143

Chapter 1. Introduction

1.1 Introduction

The vegetable oils and animal fats were investigated as diesel fuels well before the energy crisis in the 1970s and early 1980s. It is also known that Rudolf Diesel (1858-1913), the inventor of the engine that had some interested in biodiesels. Dr. Diesel had an early experiment on vegetable oil fuel with the French Government. He visualized that pure vegetable oils could power early diesel engines for agriculture, where petroleum was not available at the time. Nevertheless, the biodiesel industry was not established in Europe until the late 1980s [1].

World War II and the oil crisis in the 1970s saw a brief interested in using vegetable oils to diesel engines. Unfortunately, the newer diesel engine could not run the biodiesel due to high viscosity compared to diesel fuel. Then, it was a Belgian inventor in 1937 who first investigated the trans-esterification to convert vegetable oils into fatty acid alkyl esters and use them to replace the diesel fuel. The biodiesel was much less viscous and easy to burn in a diesel engine.

During World War II, vegetable oils also used as an emergency fuel and for other purposes. For example, in Brazil, it was prohibited to export the cottonseed oil in order to substitute it for imported diesel fuel. In China, it produced diesel fuel, lubricating oils made from tung and other vegetable oils. The Japanese battleship, *Yamato*, reportedly used edible refined soybean oil as bunker fuel [2]. *Jatropha curcas* has been used since World War II in Madagascar, Cape Verde, and Benin and some of its fuel parameters have met German and Austrian standards [3].

The viscosity of vegetable oils is greater than diesel fuel. High viscosity causes poor atomization of the fuel in the engine's combustion chambers and effects in operational problems such as engine deposits. There are four methods to reduce the high viscosity of vegetable oils to enable their use in common diesel engines: blending with diesel fuel, pyrolysis, the micro-emulsion (co solvent blending), and trans-esterification [2]. Trans-esterification is the most common method and leads to monoalkyl esters of vegetable oils and fats called biodiesel. Methanol is usually used for trans-esterification because in many countries it is the least expensive than alcohol.

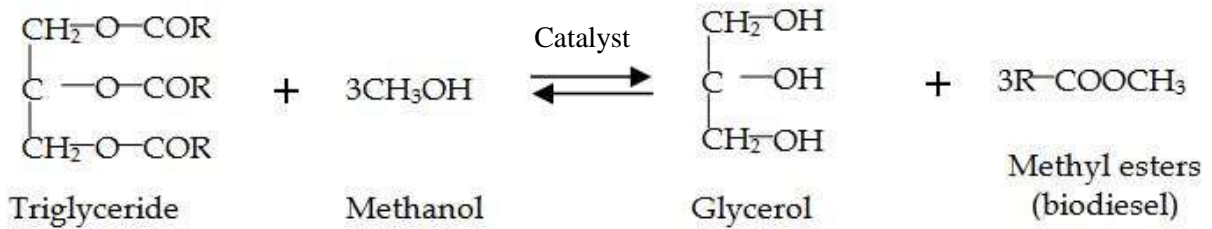


Figure 1.1. Trans-esterification Reaction of Biodiesel

In figure 1.1 shows the trans-esterification reaction of biodiesel. The *triglyceride* known as pure vegetable oil is reacted in the presence of a catalyst (usually KOH/NaOH) with alcohol (usually methanol) to give corresponding of alkyl esters (when using methanol, the methyl ester). While the trans-esterification reaction formally requires a molar ratio of alcohol and oil of 3:1, in practical, a molar ratio of 6:1 needs to be applied in order for the reaction to proceed properly to high yield [2].

Biodiesel has several advantages compared to diesel fuel, such as, produces from renewable resources that can reduce dependence on preserving diesel fuel, reduces most exhaust emissions (except nitrogen oxides/ NO_x) that can improve health impact in the environment, positive economic impacts, can be used in existing diesel engine. Nevertheless, biodiesel has also disadvantages, such as, variation in quality of biodiesel this happened due to each country has differences regulation and standardization in biodiesel and different treatment in making biodiesel can cause the quality of biodiesel different from others, biodiesel is not suitable in the engine at low temperatures, clogging in the engine and slightly increase in Nitrogen Oxide (NO_x) emissions that can caused acid rains.

1.2 Background of the Research

The demand for diesel fuel in the world is rising due to growing number of vehicles and industrialization. The continuous in using diesel fuel would confront the diminished non-renewable world oil resources. However, diesel fuel caused environmental pollution. Therefore, it is urgent to replace the diesel fuel effectively and introduce from land resources as an alternative source. Many researchers have studied the non-edible fuel oil such as *jatropha curcas* [4], *karanja* oil [5] and *carbera odollam* oil [6] and edible fuel such as palm oil [7] and rapeseed oil [8], in order to find the most benefit fuel from biodiesels. However, biodiesel from edible oil would confront the high price of the feedstock and high competition between food and fuel [9]. Nevertheless, non-edible oil would be a good alternative since no

competition between food and fuel. Non-edible oil usually has high fatty acid and it required to have a pretreatment production process [10].

The use of biomass as renewable resources can make carbon become neutral due to its characteristics. "The carbon nutrients" means "plants that are the raw materials of biomass fuels absorb CO₂ in the atmosphere during its growth process and photosynthesize, so if you burn it using biomass fuel as a source of energy, the emitted CO₂ is zero."

The chemical composition of biodiesel is different from diesel fuel and it contains about 10% of oxygen by weight. Compared to diesel fuel, biodiesel has a higher density, viscosity and flashpoint. Nevertheless, biodiesel does not contain any sulfur, aromatic hydrocarbons, metals and residue [11] and can reduce the emissions such as PM, CO₂, CO, SO_x and HC and can reduce the global warming. Therefore, biodiesel has its own standardization. ASTM D is standard for biodiesel standardization usually used in America and part of the Asian countries. JIS K is standard for biodiesel standardization in Japan.

High fatty acid and viscosity in biodiesel can conduce some problems in diesel engines, such as high deposits in engine, poor durability of the fuel injection system and improper spray formation. In order to reduce some problems in the engine, blending between biodiesel and diesel fuel or other fuels are one of the best solutions. Biodiesel can be used by blending with diesel fuel in existing compressed ignition engines without modifications to the engine. In Japan, the regulation of blending biodiesel between diesel fuels is 5%. Further, it is important to study biodiesel blend properties and compared them to biodiesel standardization. Biodiesel blended with diesel fuel would bring many beneficial characteristics to the diesel engine.

Using biodiesel or FAME (Fatty Acid Methyl Ester) can reduce CO₂ and high in O₂. However, FAME has low volatile and high viscosity compared to diesel fuel. These properties may cause burning failure such as poor atomization, poor mixing conditions. Therefore, it is necessary to improve the fuel property in biodiesel fuel by blending hydrocarbon (such as diesel fuel or n-tridecane).

1.3 Objectives of the study

This study focused of biodiesel fuels such as Jatropha Methyl Ester (JME), Jatropha methyl ester blended with n-tridecane in the proportion of blending are 25%, 50% and 75%, waste cooking oil (WCO), bio hydro finned oil (BHD), and biodiesel water emulsion (BDW). In the present study, the fuel properties of biodiesels were analyzed, spray characteristics of biodiesels are studied under non-

evaporating and evaporating conditions with different injection pressures to analyze the effect of physical properties and in spray characteristics. The biodiesels are chosen between blending the jatropha methyl ester with tridecane and biodiesel water emulsion because they have the same micro-explosion phenomena in the fuel during the evaporating process. Recently, emulsions of fuel with other more volatile liquids are being investigated by researchers and are thought to promote micro-explosions during the evaporation process, therefore, it can be improved in the atomization and fuel-air mixing.

The important objectives of the study are listed below:

1. Analyzed the fuel properties from all biodiesel fuels tested.
2. Measurement the macroscopic and microscopic spray characteristics of non-evaporating and evaporating sprays from biodiesel fuels, such as spray tip penetration, spray angle, Sauter mean diameter and droplet size.
3. Measurement of the laser-induced scattering from biodiesel fuels.
4. Analyzed the combustion and emissions characteristics from biodiesel fuels.
5. Analyzed the heat balance in biodiesel fuels.

1.4 Organization of the thesis

The thesis comprises 11 chapters that cover different aspects of spray characteristics study. This study will report the whole process and results of performed research in six chapters as listed below:

Chapter 1 (introduction): Presents an introduction and background of the research and main objectives of this study.

Chapter 2 (literature review): Presents the fundamental study to previous research of spray characteristics of biodiesel in the different blending of fuels and explain the design approach of a new fuel.

Chapter 3 (emulsion and fuel research): Explains in detail of the emulsions, surfactant, micro-emulsions, and micro-explosions for oil mixed the water.

Chapter 4 (biodiesel production): Explains in detail chemical structure in biodiesel and explain in detail about the biodiesel production.

Chapter 5 (fuel analysis): Explains in detail from analysis FTIR (Fourier Transform Infrared Spectroscopy) from all biodiesel oils and fuel properties such as density, viscosity, cetane number, etc

Chapter 6 (non-evaporating characteristics): Explains in detail the non-evaporating characteristics from all biodiesel oils in room temperature conditions.

Chapter 7 (evaporating characteristics): Explains in detail the evaporating characteristics from all biodiesel oils in temperature of 400, 500 and 600 K.

Chapter 8 (laser-induced scattering): Explains in detail using mie-scattering to analyze the heterogeneous structure from all biodiesel oil.

Chapter 9 (performance and emissions analysis): Explains in detail the performance and emissions analysis from all biodiesel oil in the diesel engine.

Chapter 10 (Combustion and emissions in biodiesel water emulsions): Explain in detail the combustion and emissions analysis in biodiesel water emulsions.

Chapter 11 (conclusion): Lists the final achievement and verifies them withdrawn objectives in the first chapter to ensure all of the objectives have been fulfilled.

References

[1] <http://www.biodiesel.com/biodiesel/history/>

[2] Knothe, G., Krahl, J., and Gerper, J. V. 2010. The Biodiesel Handbook, 2nd edition, urbana Illinois (2010).

[3] Foidl, N, Foidl, G., Sanche.z, M, Mittelbach., and M, Hackel S. 1996. Jatropha curcas as source for the production of biofuel in Nicaragua. *Bioresource Technology*, 58, 77-82.

[4] Rattanaphra, D., and Srinophakun, P. 2010). Biodiesel production from crude sunflower oil and crude jatropha oil using immobilized lipase. *Journal of Chemical Engineering of Japan*, 43, 104-108.

[5] Meher, L. C., Kulkarni, M. G, Dalai, A. K., and Nail, S. N. (2006). Transesterification of karanja (Pongamiapinnata oil) by solid basic catalysts. *European Journal of Lipid Science and Technology*, 108, 3898-3978.

[6] Kansedo, J., Lee, K. T., and Bhatia, S. (2009). Cerbera odollam (sea mango) oil as a promising non-edible feedstock for biodiesel production. *Fuel*, 88, 1148-1150.

[7] Nongbe, M. C., Ekou, T., Ekou, L., Yao, K. B., Grogneq, E. L., Felpin, F. X. (2017). Biodiesel production from palm oil using sulfonated graphene catalyst. *Renewable Energy*, 106, 135-141.

[8] Hu, Q., Hua, W., Yin, Y., Zhang, X., Liu, L., Shi, J., Zhao, Y., Qin, Y., Chen, C., and Wang, H. (2017). Rapeseed research and production in China. *The Crop Journal*, 5, 127-135.

- [9] Silitonga, A. S., Masjuki, H. H., Mahlia, T. M. I., Ong, H. C., Chong, W. T., and Boosroh, M. H. (2013). Overview properties of biodiesel diesel blends from edible and non-edible feedstock. *Renewable and sustainable energy reviews*, 22, 346-360.
- [10] Berchmans, H. J., and Hirata, S. (2008). Biodiesel production from crude *Jatropha curcas* L seed oil with a high content of free fatty acids. *Bioresource Technology*, 6, 1716-1721.
- [11] Atabani, A. E., Silitonga, A. S., Badruddin, I. A., Mahlia, T. M. I., Masjuki, H. H., Mekhilef, S. (2012). A comprehensive review on biodiesel as an alternative energy resource and its characteristics. *Renewable and sustainable energy reviews*, 16 (4), 2070-2093.

Chapter 2. Literature Review

2.1. Introduction

Biodiesel is made by organics or natural resources and its low emissions makes it environment friendly can be considered as a future optional fuel for diesel engines [1]. Since petroleum fuel is a non-renewable energy and its availability is limited, the research of alternative fuels is of vital importance. Moreover, petroleum fuels contribute many pollutants. Certainly, biodiesel represents a solution. The use of biodiesel fuel has been investigated by considering the aspects of the spray characteristics behavior: combustion analysis, environmentally acceptable emissions, economic competitiveness and technical feasibility.

Biodiesel Fuel (BDF) derives from the seeds from different plants, such as soybean, *rapeseed*, *jatropha*, palm oil, *pongamia*, etc. Biodiesel can be recycled and it can be easily to process. The common method in processing biodiesel is the trans-esterification. Trans-esterification is the process which leads to monoalkyl esters of vegetable oils and fats. Methanol is usually used for trans-esterification process since it is the less expensive than alcohol.

According to these consideration, biodiesel from *Jatropha* and palm oil are thought to be the potential biodiesel to substitute diesel fuel in Asia, Europe and Africa. *Jatropha curcas* is a non-edible plant that grows in tropical areas [2]. Palm oil (*Elaeisguineensis*) can grow in local area of West Africa and then it can become an agrarian product [3]. The palm oil is a tropical plant that grows in humid areas; it can be easily found in Indonesia. The tree can grow up to 20-30 m height [4]. It is important to study the biodiesel *jatropha* and palm oil behavior during combustion and spray in Diesel Engine in order to compare them with diesel fuels.

Biodiesel fuels may decrease the spread of pollutants and organic wastes [5]. In general, biodiesel has high density, viscosity, weak in oxidation compared with a diesel engine. Biodiesel with high viscosity can make weak in atomization and can make residuals in the engine [6]. The oxygen in biodiesel has 11-15 wt. %, therefore it can reduce some emissions as well as improve the combustion of the diesel engine [7]. BDF in diesel engine can be able to reduce some emissions such as PM, CO₂, CO, SO_x and HC [8]. Despite of that, the weaknesses of BDF such its high viscosity and its low volatility need to be overcome in order to have a good proportional combustion in diesel engines.

The Study on spray characteristics plays an important role in understanding the spray behavior for various biodiesel with different blends percentages. Non-evaporating spray characteristic is the ability of the fuel spray to break up into small particles in the roomtemperature conditions. On diesel fuel (DF) and gasoline, emissions are lowered by improving the characteristics of sprays and by increasing the fuel mixture [9]. Table 1 shows the fuel properties of palm oil and jatropha biodiesel, diesel fuel and its blends. Higher viscosity may affect the spray velocity and the breakup process, whereas lower caloric value requires larger injection duration for biodiesel [10]. Biodiesel from jatropha and palm oil have a higher value of viscosity than the diesel fuel (almost the double); this may decrease the breakup process. It is significant to understand the importance of the implementation of biodiesel in diesel engines. Diesel engines are not designed for biodiesel fuel; a significant modification in the engine composition should be applied, in order to use biodiesels. Therefore, it is necessary to study the fuel atomization in both the biodiesel and the normal fuel, in order to understand the differences of contribution of the combustion and emissions.

The present review tries to consolidate the experimental research finding, reported in the non-evaporating spray characteristics of biodiesel jatropha, palm oil and its blends such as spray tip penetration, spray cone angle and sauter mean diameter.

2.2. Spray Characteristics

It is fundamental to know well the characteristics of spray in biodiesel fuels engine performance. There are two categories for fuel sprays: macroscopic structures and microscopic structures. Spray cone (plume) angle, velocity of spray and spray tip penetration can be identified as the macroscopic structures, while Sauter Mean Diameter (SMD), droplet velocity and droplet size can be identified as microscopic structures [10].

The velocity of spray and spray tip penetration are helpful to explore the probability of liquid spray impingement while a spray cone (plume) angle demonstrates the spread of droplets due to breakup and air entrainment [10]. The experiment of spray structure is recorded and captured by using a high speed camera. The spray structure can be implemented by many methods such as shadowgraph method, mie-scattering method using a rapid video camera such as rapid Schlieren photography. The microscopic characteristics can be calculated by laser diffraction particle analyzer, a phase doppler particle analyzer and a particle image velocimetry [11].

Figure 2.1 represents an experimental setup of spray characteristics by Agarwal A.K et al, 2015. The pressure in nozzle opening was standing up at 1000 bar using a high pneumatic pump. During injection, a high speed camera is captured to take images from fuel spray.

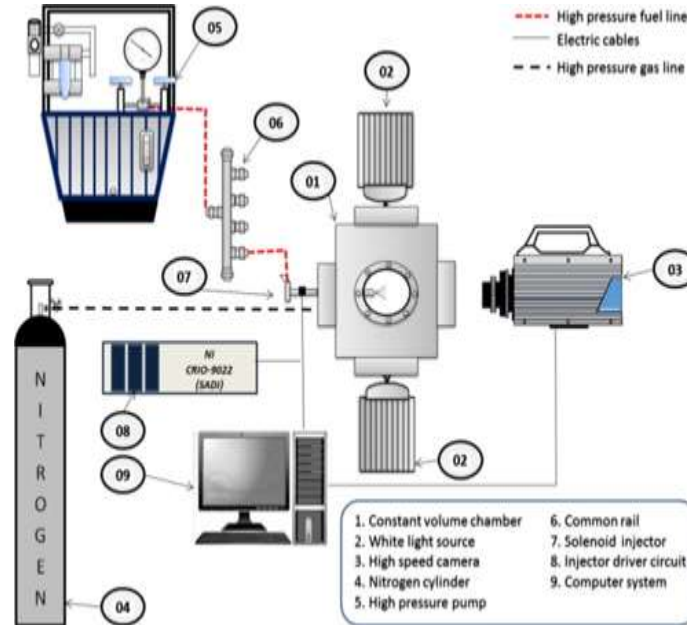


Figure 2.1. The experimental setup of spray by Agarwal A.K et al [12]

2.2.1. Spray Tip Penetration

Spray (tip) penetration is the spray length between the injector exits and the spray tip (S). The cone or plume angle is characterized by the edges between two configurations or lines associating the spout tip [11]. In Figure 2.2, the spray penetration is demonstrated by S . $S/2$ is the separation from the injector tip carried for the cone angle. Some authors choose $S/2$ or $S/3$ [13] and furthermore can be 60% from S [14].

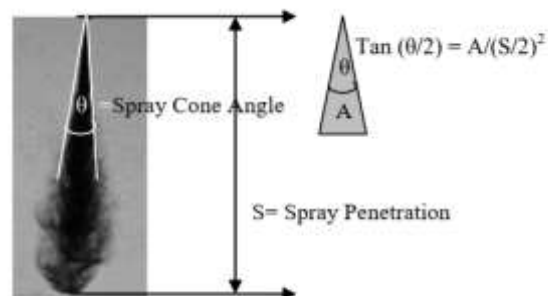


Figure 2.2. Spray penetration and spray cone angle

Spray tip penetration formula can be computed utilizing Hiroyasu-Arai [15] displayed in eqs (1) and (2), these conditions were used by various analysts to ascertain that the spray tip penetration separates for diesel fuels and biodiesel.

$$S = 2.95 \times \left(\frac{\Delta P}{\rho_a}\right)^{0.25} \times (D_n \times t)^{0.5}, \text{for } t > t_b \quad (1)$$

$$S = 0.39 \times \left(2 \times \frac{\Delta P}{\rho_a}\right)^{0.5} \times t, \text{for } t < t_b \quad (2)$$

Where S is the spray tip penetration (m), t_b is separate time (s) and t is the infusion time (s).

The high penetration is helpful for the air entrainment. However, it might prompt divider impingement [16]. The high tip penetration and greater cone edge are interesting for the most extreme air utilization and better ignition in light of the extended of splash territory [17]. Soid S.N, et al also studied the characteristics of spray in a constant volume combustion chamber for palm oil diesel blends with different injection pressures equal to 20 MPa, 30 MPa and 34 MPa by using a pneumatic cylinder. Spray penetration is incremented by expanding the injection pressure [17].

Table 2.1. Fuel Properties of diesel fuel (DF), palm methyl ester (PME), jatropha methyl ester (JME) and its blends

Properties	Kinematic Viscosity (mm ² /s)	Surface Tension (mN/m)	Density (kg/m ³)	Caloric value (kJ/kg)	Ref.
Diesel Fuel (DF)	2.9	26.0	830	44.1	[7],[18],[19]
Palm Methyl Ester (PME)	5.53	26.2	874.4	36.494	[20]
JatrophaMethyl Ester (JME)	5.4	30.7	870	42.8	[21],[22]
Jatropha Pure Oil (JPO)	49.78	34	909	39.8	[22],[23],[24]
JME 5%+PME 5%+DF 90%	2.35±0.01	-	831	45.233	[25]
JME 25%+PME 25%+DF 50%	3.14±0.03	-	843	41.537	[25]
PME 20% + DF 80%	24.55	-	855	42.840	[17]
PME 40%+DF 60%	27.32	-	863	41.558	[17]

Table 2.1 shows some of the fuel properties of various biodiesel fuels. As can be seen that the density of jatropha pure oil (JPO) is 8.7% higher than diesel fuel. The viscosity in JPO is higher than DF. In addition, after the trans-esterification process, JPO becomes to JME. The viscosity and density of JME can be reduced up to 89% and 4.3% than JPO. However, the blending of biodiesel between PME 20% and DF 80% has the viscosity of 2.9% higher than DF; but it has less viscosity 2.21% than BDFP. Nevertheless, the blending between BDFP40% and DF60% has a density 3.8% higher than DF.

Kinematic Viscosity is very important to be understood; a higher viscosity may affect the spray velocity and the breakup process, whereas a lower caloric value may affect the larger injection duration for biodiesel. Therefore, the understanding of the properties and its impacts on the spray behavior before it is applied in the engine application is very important.

Wang x, et al studied that the correlation between diesel fuel and biodiesel fuels in several conditions for the spray penetration. The conditions for injection pressure were varied from 100, 200 and 300 MPa; the ambient densities were 15 kg/m³ and 30 kg/m³. In the condition of density equal to 15 kg/m³, palm oil methyl ester has longer penetrating spray compared to diesel fuel. Diesel fuel and biodiesel palm oil have comparative values of penetrations spray before 0.3 ms [26].

Gao Y et al studied that the increased of the blending ratio of biodiesel in diesel fuel can be affected by the increasing of the spray penetration [27]. The increase of viscosity in the fuel can prevent the breaking of the spray jet. Therefore, the spray droplets would be increased. When the droplet size is large, it creates a large momentum causing less advances in the movement [15].

Suh H.K et al concentrated on the impact of fuel blending ratio and injection pressure, demonstrating that spray development of biodiesel is shorter than diesel fuel. This happens because the injection velocity of biodiesel turn out to be not as much as the one of diesel fuel. The high viscosity and few infused mass of biodiesel cannot overcome the friction between the surface of nozzle hole and the fuel [7].

Patel C, et al researched the spray characteristics under various ambient pressure (0.1; 1 and 2 MPa) with the same injection pressure of 20 MPa. In general, spray tip penetration can be influenced by the ambient pressure. At an ambient pressure of 0.1 MPa, diesel fuel sprays tends to move earlier than biodiesel jatropha and BDFJ20. Then, at an ambient pressure of 1 and 2 MPa, biodiesel jatropha and BDFJ20 tend to increase respect to diesel fuel. This can be explained by the fact that, the fuel properties such as high viscosity in biodiesel can impact in needle's movement. The needle will become slow in biodiesel compare to diesel fuel [27].

Table 2.2. Comparison between spray structure of biodiesel and diesel fuel

Biodiesel	Conditions	Spray Penetration	Spray Cone Angle	References
JME5% (Jatropha 5%)	-	Increased	Decreased	
JME10 (Jatropha 10%)	-	Increased	Decreased	[27]
JME50 (Jatropha 50%)	-	Increased	Decreased	
JME20 (Jatropha 20%)		Decreased	Decreased	
	Pinj= 20 MPa; Pamb=0.1MPa	Decreased	Decreased	
JME100%				
JME20 (Jatropha 20%)		Increased	Decreased	
	Pinj= 20MPa; Pamb= 1MPa	Increased	Decreased	[28]
JME100%				
JME20 (Jatropha 20%)		Increased	Decreased	
	Pinj= 20 MPa; Pamb= 2 MPa	Increased	Decreased	
JME100%				
	$\rho_{amb}=15\text{Kg/m}^3$; Pinj=100 MPa	Increased	Decreased	
	$\rho_{amb}=15\text{Kg/m}^3$; Pinj=200 MPa	Increased	Decreased	
	$\rho_{amb}=15\text{Kg/m}^3$; Pinj=300 MPa	Increased	Decreased	[26]
PME100% Palm Methyl Ester	$\rho_{amb}=30\text{Kg/m}^3$; Pinj=100 MPa	Increased	Decreased	
	$\rho_{amb}=30\text{Kg/m}^3$; Pinj=200 MPa	Increased	Decreased	
PME100% Palm Methyl Ester	$\rho_{amb}=30\text{Kg/m}^3$; Pinj=300 MPa	Increased	Decreased	[26]

As it can be seen in Table 2.2 describing non-evaporating spray characteristics condition, the high value of the density and the surface tension can affect the length of the spray tip penetration. In different injection pressures, biodiesel palm oil has a higher spray penetration than diesel fuel (DF) because the density of palm oil is of 5% higher than diesel fuel and the surface tension of palm oil is 0.76% higher than diesel fuel.

It can be seen in the table 1.1 and 1.2, for non-evaporating spray conditions, that jatropha biodiesel has a higher spray tip penetration compared to diesel fuel due to the density of jatropha oil (4.59% more than diesel fuel) and due also to the higher surface tension of biodiesel jatropha (15.3% more than diesel fuel). From table 1 it shows that the blending proportion of biodiesel jatropha or palm oil with diesel fuel can affect the value of surface tension and density. Therefore, it can be influenced for the length of the spray penetration and also the spray cone angle.

2.2.2. Spray cone angle

Researchers have presented different definitions regarding to the spray cone or plume angle. Mo J, et al established that cone (plume) angle is the angle between two stripes, that can be found between two half infiltration on the nozzle tip and the spray boundary [11].

Figure 2 shows the spray cone angle of dispersion of spray near the injector. The angle is given by

$$\theta = 2 \arctan\left(\frac{A}{\left(\frac{S}{2}\right)^2}\right) \quad (3)$$

Where A is the splash territory (area) and S is a length of the penetration.

Hirayasu and Arai studied amid the main phase of the spray (tip) penetration and the needle opened then the development is transient. For larger phase, the needle is completely open and the infusion is steady. Therefore, the angle is given as follow [21]

$$\theta = 83.5 \left(\frac{L}{D}\right)^{-0.22} \left(\frac{D}{D_s}\right)^{0.15} \left(\frac{\rho_g}{\rho_l}\right)^{0.26} \quad (4)$$

Where θ is the spray cone or plume angle, D_s is the hole diameter of the sac, L is the nozzle hole's length.

The cone angle is affected by the characteristics of the nozzle, the air density, the fuel and the Reynolds number of the fuel. Moreover, the cone angle increases with the increase of the injection pressure and together with the decrease of the working fluid temperature [15].

Table 2.2 shows the spray cone angle conditions with various biodiesel jatropha and biodiesel palm oil with its blends compared to diesel fuel.

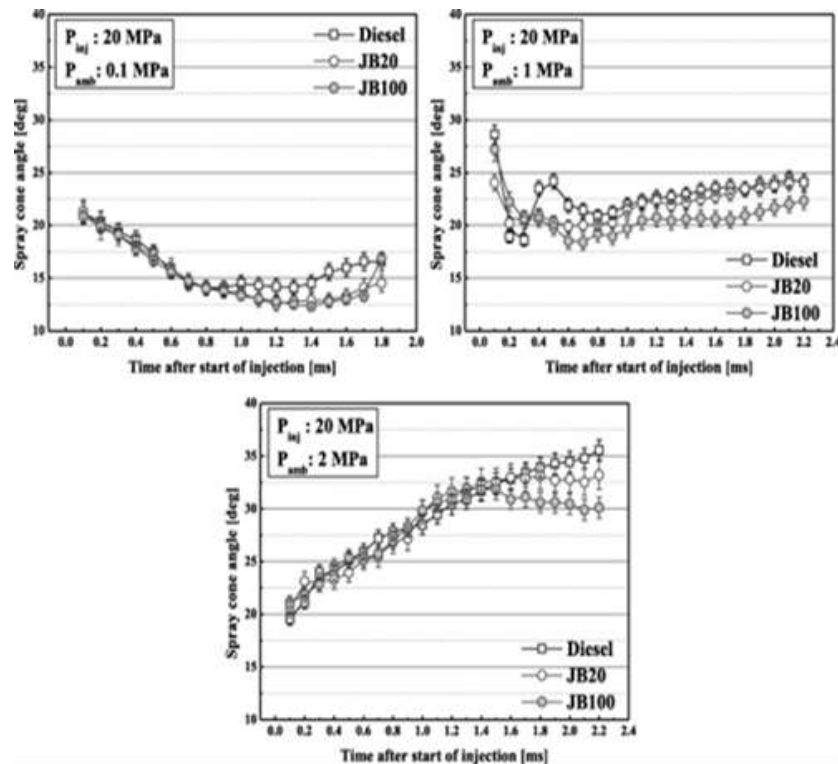


Figure 2.3. Spray cone angle for diesel fuel compare with Jatropha Blends with different ambient pressure (JB 20- Jatropha Blend 20%, JB100- Jatropha 100%) by Patel C et al [28]

Figure 2.3 shows researched by Patel C, et al on the process of spray cone (plume) angle in different ambient pressure equal to 0, 1; 1 and 2Mpa. It illustrated that at a lower ambient pressure (0.1 and 1 MPa), spray cone angle would reduce by increasing the time of injection. Nevertheless, in high ambient pressure (2 MPa) spray cone angle would be increased by increasing the time of injection. At an ambient pressure of 1 MPa, spray cone angle for diesel fuel appears to be higher compared to biodiesel [28]. Lahane S & Subramanian K.A found out that the spray cone or plume- angle for biodiesel fuel and its blends is smaller compared to DF since biodiesel blends has a higher density and viscosity compared to DF[16].

GaoY,et al studied that spray cone (plume) angle decreased when the blend ratio was increased. Since the increase of injector pressure can cause the spray to spread and effecting to the increased of cone angle [27]. Figure 8 shows the spray images from different injection pressures of DF and BDFP. The BDFP gives narrower spray angles than diesel fuel (DF). BDFP presents slightly darker images than diesel fuel; this suggests a weakened light scattering effect [27]. As seen in table 1, biodiesels have high surface tension

and viscosity. Therefore, biodiesels are difficult to atomize. Higher viscosity may affect the spray velocity and the breakup process whereas a lower caloric value requires larger injection duration for biodiesels [10].

It can summarize from Table 2.2 that biodiesel jatropha has a smaller spray cone angle compared to diesel fuel. This condition occurs because biodiesel jatropha has higher in density and surface tension than diesel fuel. It can also concluded from Figure 2.4 that biodiesel palm oil has a smaller cone angle than diesel fuel. The proportion of blending between biodiesel and diesel fuel may affect the spray cone angle. This condition happens because biodiesel palm oil has a higher value in density and surface tension than diesel fuel.

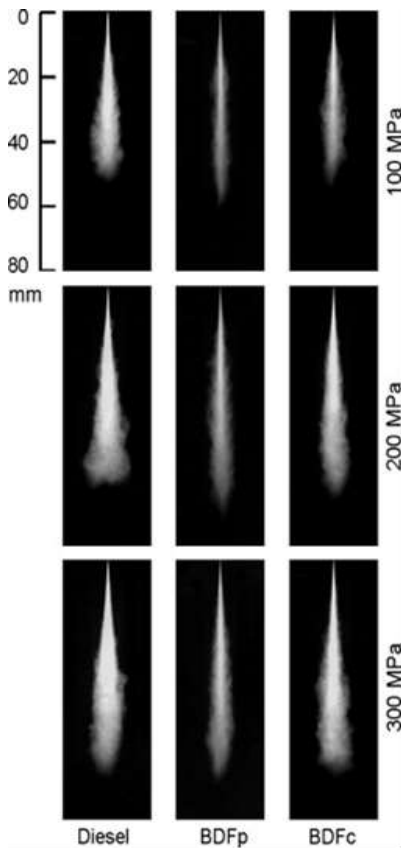


Figure 2.4. Spray Figures from different fuels with three different injection pressures (P_{inj}) (0.7 ms ASOI, 15 kg/m^3 , Biodiesel Palm Oil (BDFp), Biodiesel Cooking Oil (BDFc)) by Wang x, et al [26]

The spray cone angle in the non-evaporating conditions of biodiesel jatropha and palm oil is inversely proportional to the spray tip penetrations [12]. The jatropha and the palm oil biodiesel are higher in spray tip penetration than diesel fuel. Nevertheless, the jatropha and palm oil biodiesel have a smaller

cone angle than diesel fuel. The causes of these differences are the different values of each property among biodiesel jatropha, palm oil and diesel fuel.

2.2.3. Sauter Mean Diameter

In the combustion, the circulations of spray droplets in the Sauter Mean Diameter (SMD) are the parameter to be used in order to investigate the attributes of atomization since they are related to the decrease of the emission and ignition of the fuel [29]. In general, the SMD in the biodiesel spray is observed to be slightly higher compared to diesel fuel [10].

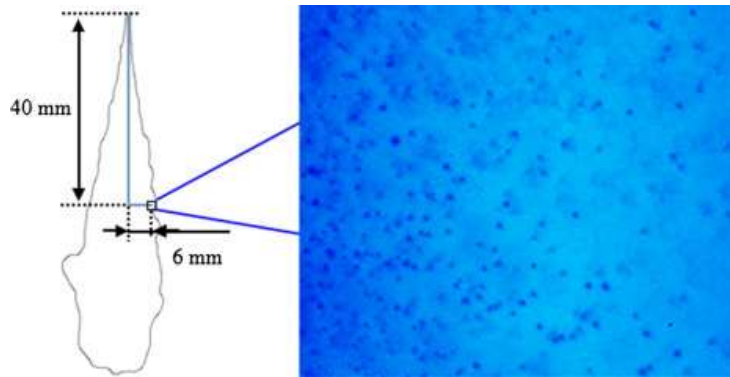


Figure 2.5. Image of illustrating the droplets within the spray by Guan L et al [34]

Figure 2.5 shows the image illustrating droplets within the spray. Droplet size is also determined by SMD, which is characterized by the distance across (diameter) of a droplet that superficies to the proportion of volume are equivalent to the whole shower [30]. The mean diameter d_{10} is given by

$$d_{10} = \frac{\sum_{i=1}^k x_i \Delta n_i}{\sum_{i=1}^k \Delta n_i} \quad (5)$$

Where n is droplet's number and x is the diameter of the droplet.

Lefebvre A.H (1989) calculated the Sauter Mean Diameter (SMD) is given

$$d_{32} \text{ or SMD} = \frac{\sum x_i^3 \Delta n_i}{\sum x_i^2 \Delta n_i} \quad (6)$$

SMD is all droplets within the fuel spray packet are represented by the volume-to-surface area mean diameter. A small fuel droplet diameter is more easily to evaporate than a large droplet, this because the large diameter would consumes a long evaporation times because the volume of a spherical droplet of this size [32]. The fuel droplet size is important to study because it is related to combustion and exhaust characteristics in the engine. In general, biodiesel sprays have higher SMD compared to diesel fuel sprays. Suh H.K et al investigated that droplet diameter for biodiesel blends were higher than diesel fuel sprays [7]. Lee C.S at al also studied that SMD of biodiesel-blended fuel is larger than diesel fuel [31].

In Figure 2.6 Choi.S and Oh.Y investigated to Sauter Mean Diameter for palm oil. The SMD Palm oil blended was higher than Diesel fuel [32]. The SMD decreased when the injection pressure was increased. From the Figure display that the blending ratio of BDF increased can cause the enhanced of SMD. This correlation was happening due to the higher viscosity of biodiesel can gain the friction between the contacting surface of the nozzle and the fuel [33]. Therefore, the injection velocity of biodiesel and biodiesel blends is reduced [33].

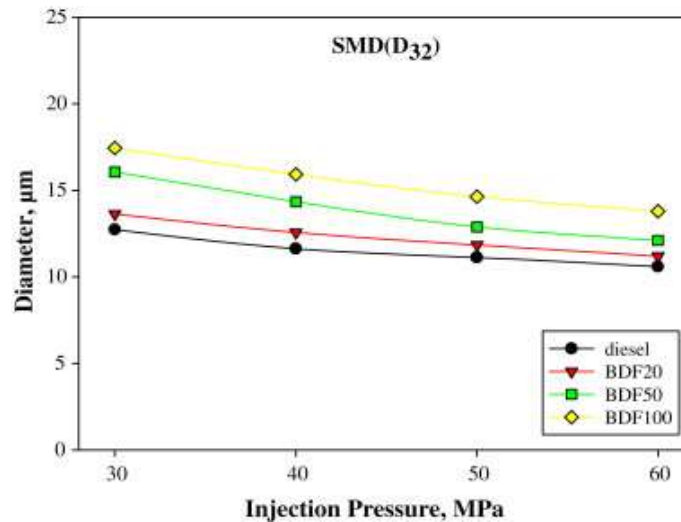


Figure 2.6. Sauter Mean Diameter (SMD)in Palm Oil (BDF20-Biodiesel Fuel 20%, BDF50-Biodiesel Fuel 50% and BDF100- Biodiesel Fuel 100%) by Choi S and Oh Y[32]

Table 2.3. The Comparison of SMD from Biodiesel Palm Oil

Biodiesel	Conditions	SMD	Ref.
Palm Oil 100% (PME100)	$\rho_{amb}=30\text{Kg/m}^3$; $P_{inj}=100\text{ MPa}$	Greater than DF	[26]
	$\rho_{amb}=30\text{Kg/m}^3$; $P_{inj}=200\text{ MPa}$	Greater than DF	
	$\rho_{amb}=30\text{Kg/m}^3$; $P_{inj}=300\text{ MPa}$	Greater than DF	
Palm Oil 20% (PME20)	$P_{inj}=30\text{ MPa}$	Greater than DF; Smaller than BDFP50; Smaller thanBDFP100	[32]
	$P_{inj}=40\text{ MPa}$		
	$P_{inj}=50\text{ MPa}$		
	$P_{inj}=60\text{ MPa}$		
Palm Oil 50% (PME50)	$P_{inj}=30\text{ MPa}$	Greater than DF; Greater than BDFP20; Smaller thanBDFP100	[32]
	$P_{inj}=40\text{ MPa}$		
	$P_{inj}=50\text{ MPa}$		
	$P_{inj}=60\text{ MPa}$		
Palm Oil 100% PME100	$P_{inj}=30\text{ MPa}$	Greatest than DF, BDFP20 and BDFP50	
	$P_{inj}=40\text{ MPa}$		
	$P_{inj}=50\text{ MPa}$		
	$P_{inj}=60\text{ MPa}$		

From Table 2.3 it is evident that the injection pressure on the biodiesel palm oil has a larger diameter droplet size than diesel fuel. This indicated that the larger of surface tension, density and viscosity in biodiesel can affect the diameter droplet size, while higher diameter droplet size can affect the poor of spray characteristics in diesel engine.

2.2.4. Evaporating Spray

In order to achieve the combustion, the fuel droplets have to evaporate and mix with the oxygen. Evaporating spray is conducted in constant volume vessel filled with hot gas in rapid compression machine or in a real engine with optical access to the combustion chamber volume [10]. Parameters can be taken in evaporating sprays are liquid/vapor spray tip penetration, lift-off length, intensity and homogeneity in the fuel.

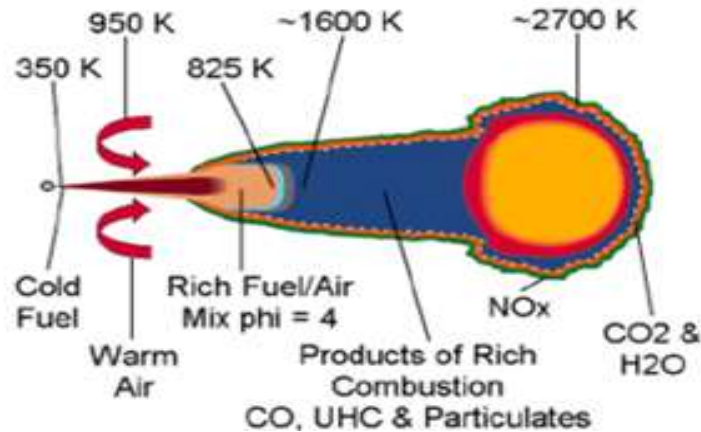


Figure 2.7. Diesel spray combustion [35]

Figure 2.7 shows the illustrated the spray combustion. The combustion process will produce NO_x, CO₂ and H₂O. Usually in the combustion process, the spray tip penetration reaches nearly steady state value after a short period time. NO_x forms on the outer surface of the flame where oxygen and higher temperature exists [36]. Biodiesel sprays are demonstrated to have a longer liquid length due to slower breakup and lower volatility compared to diesel [37]. In general, fuel properties play important role in determining the spray parameters such as liquid length compared to ambient gas properties [10]. Higher cetane number in biodiesel from the fuel oxygen content exhibits a shorter ignition delay and lift off length also shorter than diesel indicating that the air entrainment will be inferior in biodiesel spray combustion.

2.3. Fuel Design approach for Spray Combustion Control

2.3.1. Flash Boiling Process for Single Component

The spray characteristics of flash boiling spray by use of single component such as *n*-pentane or *n*-hexane (components of Gasoline) under the relative low-pressure ambient field for the application of Gasoline port injection. These studies were constructed by the atomization characteristics [38], [39], modelling of the flashing process [40], [41], and the vapor concentration measurement [42].

Figure 2.8 shows the physical process of this flashing spray in pressure-temperature diagram and the typical example images of flashing spray structure for the *n*-pentane spray with a variation of the ambient pressure at room temperature condition. As shown here, flash boiling spray should be occurred when the liquid pressure is depressed below the liquid vapor pressure. The high atomization quality of the spray is required for flashing regime with larger spray dispersion angle and fine droplets diameter in case of lower ambient pressure conditions. For this flash boiling spray, the simple analytical model concerning the spray vaporization process based on cavitation bubble dynamics, considering a bubble nucleation process, bubble growth calculation and fuel film breakup process have been developed as shown in Figure 2.9 [40], [41]. Jiro et al. extended themodeling scheme to the application for the multi-dimensional CFD code of KIVA3V [43].

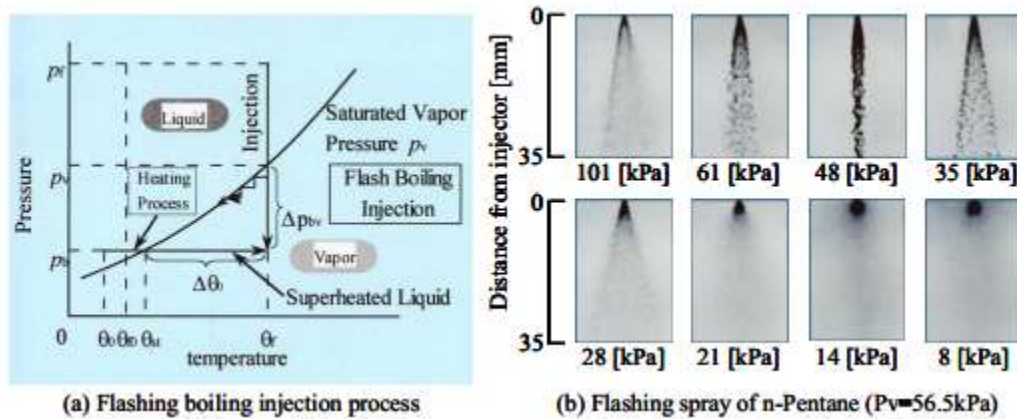


Figure 2.8. Improvement of spray atomization and evaporation processes in flash boiling spray [40,41]

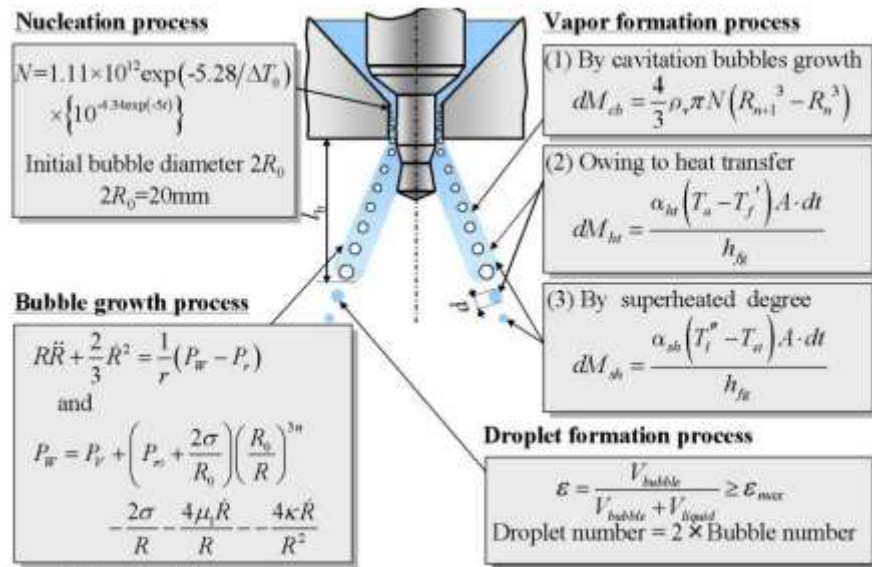


Figure 2.9. Modeling of flash boiling spray [40, 41]

2.3.2. Flash Boiling for Two Component Solution

Analysis of phase change process through liquid-vapor equilibrium based on chemical thermodynamics is required for two component solution [44], [45]. Figure 2.10 shows pressure-temperature diagram of two component solution by two kinds of liquid whose vapor pressures that is corresponding to the boiling point, are different. For the mixing solution, the critical point is depending on the fuels itself and mixing mole fraction. Here, it is peculiar that there appears two phase region where liquid and vapor phases of both components are mixed in. And, it should be noticed that heavier fuel like gas oil is converted into the relatively lighter fuel like gasoline owing to a kind of mutual molecular interaction, as estimated by liquid-vapor equilibrium theory based on chemical thermodynamics. And in the case that the liquid pressure exists in the two-phase region, we could get twophase mixture where the vapor of the lower boiling point component is dominant, and the fuel vaporization is promoted comparing to the pure one of higher boiling point. Therefore, by applying the mixing fuels between lower boiling point fuel and higher boiling point one, we can get this two-phase region, and it is leading to the improvement of evaporation due to the flashing effect or prompt evaporation.

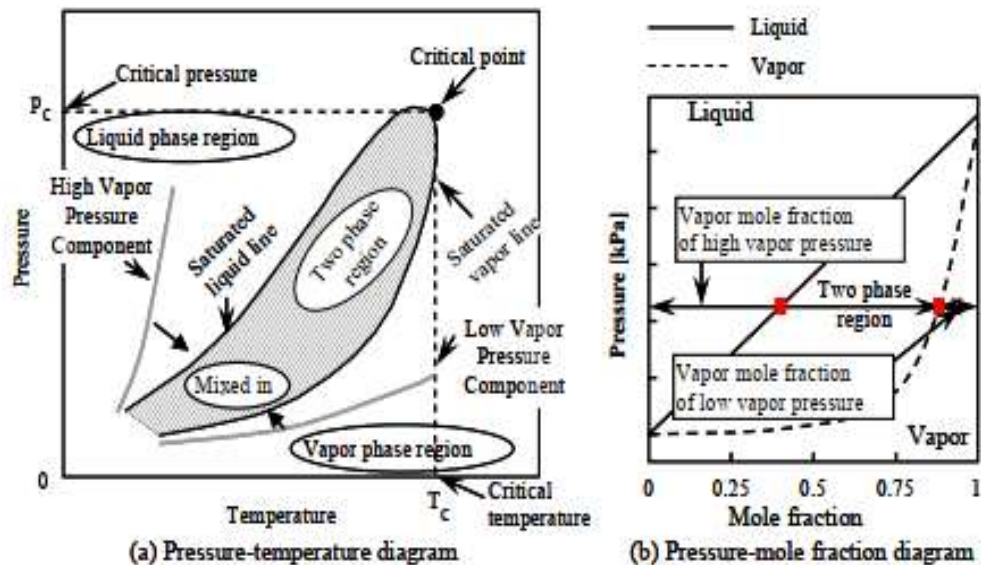


Figure 2.10. Two-phase region formation in multi-component fuel in phase change process [44,45]

2.3.3. The Design of Fuel

Table 2.4 shows the fuel design approach from Senda, J [46]. There are five major issues relating to spray combustion control. The first relates to the physical control of temporal and spatial vapor distribution through the formation of a two-phase region in mixed fuel and realization that the flash boiling spray has a higher atomization quality. Figure 2.11 describes the two-phase region of liquefied CO₂ and *n*-tridecane solutions obtained through the fugacity analysis of the vapor-liquid equilibrium by use of the modified BWR state equation. The graph presents the two-phase region profiles with the CO₂ mole fraction as a parameter. The artificial control of the two-phase region profile in the *P-T* diagram is made possible by changing the CO₂ mixing fraction, effectively enhancing spray evaporation inside the combustion chamber.

Table 2.4. Fuel design approach [46]

<p>(1) Physical control = Capability of time and spatial control on fuel vapor distribution by formation of two phase region in mixing fuel → Formation of flash boiling spray → Improvement of spray evaporation</p>
<p>(2) Chemical control = Capability of control on combustion process → Emission Control – Soot & NO_x → Simultaneous reduction of both Soot and NO_x (CO₂-gas oil mixing fuel) → Ignition Control (Gasoline-gas oil mixing fuel) HC Control (Gasoline-gas oil mixing fuel)</p>
<p>(3) Improving thermal efficiency by lower injection pressure → High spray atomization and evaporation quality with Flashing Process</p>
<p>(4) Control the fuel transportation properties in mixing fuels</p>
<p>(5) Effective liquefaction of gaseous and solid fuels → Conversion of heavy fuels or solid fuels into high quality → Lighter liquid fuels through chemical-thermodynamics</p>

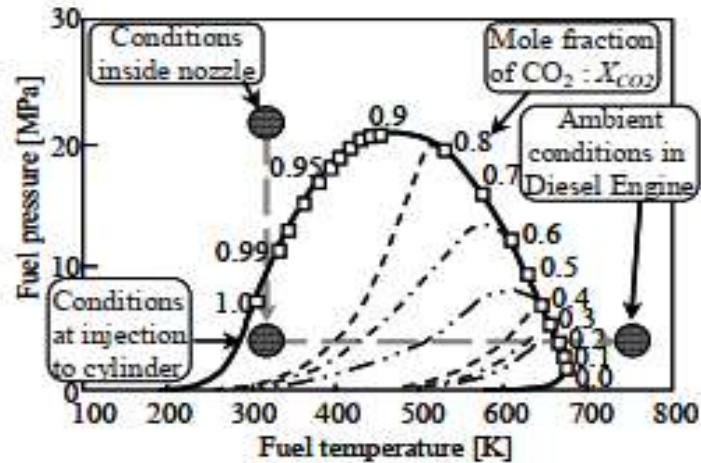


Figure 2.11. Two-phase of mixing fuel consisting of liquefied CO₂ and *n*-tridecane [46].

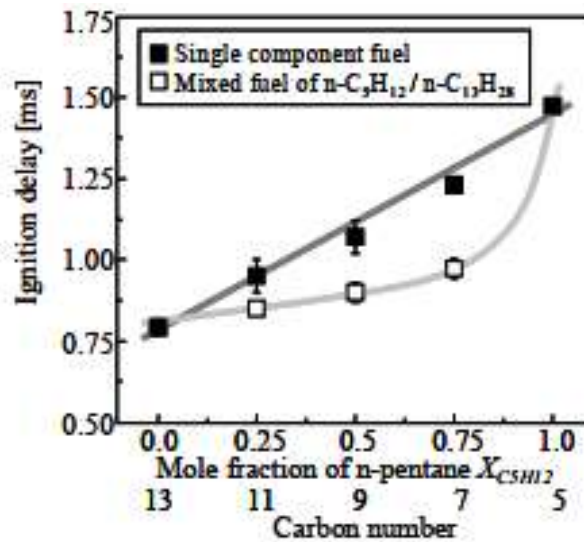


Figure 2.12. Ignition delay of single component and *n*-pentane/*n*-tridecane mixed fuel [46]

The second point relates to the control of chemical processes, including emission formation, spontaneous ignition, and HC oxidation. Here, the principle of the ignition control is explained by showing experimental data acquired using a rapid compression and expansion machine (RCEM) [45]. Figure 2.12 shows the data plots of ignition delay for mixed fuels on *n*-pentane (C=5) and *n*-tridecane (C=13) obtained using the RCEM and having a pancake combustion chamber with a diameter of

100mm. Fuel was injected at a pressure of 15MPa from a single-hole nozzle with a diameter of 0.20mm. The injection timing was set at 5deg. crank angle (CA) before top dead centre (BTDC) where the ambient pressure and temperature were 3.8MPa and 750K respectively [46]. The mole fraction of *n*pentane in the mixed fuel was changed from 0 (C=5) to 1.0 (C=13). The Figure describes the ignition delay of single component fuel lengthens linearly with the decrease in carbon number. Conversely, the ignition delay data for the mixed fuels remain at the same level as that for high-ignitability fuel (*n*tridecane) regardless of the *n*-pentane mole fractions. It was found that the higher ignitability fuel (tridecane) controls the ignition process of mixed fuel sprays. From the above discussion it is concluded that an averaged ignitability value of two fuels does not determine the ignition process of mixed fuel sprays, but the higher ignitability fuel governs the ignition process of the mixed fuel [46].

The third point concerns the important of thermal efficiency of an engine system by the use of relatively low injection pressure because enhanced spray atomization and fast evaporation of the flashing spray does not demand high injection pressures [46].

The fourth and fifth points derive from the fuel design approach. Due to the fact that the properties of mixed fuels, except for volatility and ignitability, have a linear relation for a mixing fraction, the average properties of a mixed fuel can be determined artificially [46]. Furthermore, since, according to chemical thermodynamics, the saturated liquid line of the two-phase region is located in the lower pressure side rather than the saturated vapor pressure curve of the pure gaseous substance, gaseous fuel could be converted effectively into liquid fuel. On the basis of the above discussion, the authors propose a fuel design methodology that takes into account the physical and chemical properties of fuels to be mixed. As mentioned above, when a high boiling point fuel such as gas oil and a low boiling point fuel such as gas fuel or gasoline are mixed, the lower boiling point fuel promotes spray evaporation, while the higher boiling point fuel acts to shorten the ignition delay of a mixed fuel spray [46].

2.4 References:

- [1] Krawczyk, T. 1996. Biodiesel - Alternative fuel makes in roads but hurdles remain. *INFORM* 7, pp. 801-829.
- [2] Chhetri, A. B., Tango, M. S., Budge, S.M., Watts, K.C., and Islam, M.R. 2008. Non-edible plant oil as new sources for biodiesel productions. *Int. J. Mol. Sci*, 9 (2), pp 169-180.
- [3] Basiron, Y. 2007. Palm oil production through sustainable plantation. *Europ. J. of Lipid Sci and Tech*, 109, pp 289-295.

- [4] Lam, M.K., Tan, K.T., Lee, K.T., and Mohamed, A.R. 2009. Malaysian Palm Oil: Surviving the food versus fuel disputes for a sustainable future. *Renewable and Energy Reviews*, 13 (6-7), pp 1456-1464.
- [5] Ikegami, M. 2002. The use of fatty acid methyl ester called biodiesel fuel, Meeting for Investigation into the actual conditions for diesel exhaust gas emissions with alternative fuels, JSAE.
- [6] Alptekin, E., and Canakci, M. 2008. Determination of the density & the viscosities of biodiesel-diesel fuel blends. *Renewable Energy*, Volume 33, pp 2623-2630.
- [7] Suh, H. K ., Roh, G.H., and Lee, C.S. 2008. Spray and combustion characteristics of biodiesel/diesel blended fuel in a direct injection common-rail diesel engine. *Trans ASME Journal of Engineering Gas Turbines and Power*, Volume 130, pp (032807-1) – (032807-9).
- [8] Fang, T., Lin, Y. C., Foong, T M., and Lee C. F. 2009. Biodiesel combustion in an-optical HSDI diesel engine under low premixed combustion conditions. *Fuel*, Volume 88, pp 2154-2162.
- [9] Sankar, S.V.,Maher, K. E., Robart, D. M., and Bachalo WD.1999. Rapid characterization of fuel atomizers using an optical patternator. *Journal Engineering Gas Turbines Power*, Volume 121, pp 409-414.
- [10] Boggavarapu, P., and Ravikrishna, R. V. 2013. A Review on Atomization & Sprays of Biofuels for IC Engine Applications.*Inter. J. of Spray & Combustion Dynamics*, Volume 5, Number 2, pp 85-21.
- [11] Mo, J., Tang, C., Li, J., Guan, L., and Huang, Z. 2016. Experimental Investigation on The Effect of n-butanol Blending on Spray Characteristics of Soybean Biodiesel in Common-rail Fuel Injection System.*Fuel*, Volume 182, pp 391-401.
- [12] Agarwal, A.K., Som, S., Shukla, P.C., Goyal, H., and Longman, D. 2015. In-nozzle flow and spray Characteristics for mineral diesel karanja&jatropha biodiesels. *Applied Energy*. Volume 156. Pp 138-148.
- [13] He, C., Ge, Y., Tan, J., Han, X. 2008. Spray properties of alternatives fuels a comparative analysis of biodiesel & diesel. *Inter. J. of Energy Research*, Volume 32, pp 1329-1338.
- [14] Desantes, J. M., Deng, J., Li, C., Dang, F., Liao, Z., Wu, Z and Li L. 2009. Experimental Study of Biodiesel Blends Effects on Diesel Injection Process. *Energy & Fuels*, Volume 23. Pp 3227-3235.
- [15] Hiroyasu, H., and Arai, M., Structures of fuels spray in diesel engines. *SAE paper* 90045 (1990).
- [16] Lahane S., Subramanian K.A. 2015. Effect of different percentages of biodiesel-blends on injection, spray, combustion, performance & emission characteristics of a diesel engine. *Fuel*, Volume 139, pp 537-545.
- [17] Soid, S. N., Zainal, Z.A., Iqbal, M.A., and Miskam, M. A. 2012. Macroscopic spray characteristics of palm oil-diesel blends in a constant vol combustion chamber. *J of Scientific & Indust Research*, Volume 71, pp 740-747.
- [18] Harun, N. M.d., Najmul, H. S.M., Shamim, A. M. D. 2009. Karanja (pongamiapinnata) biodiesel prod. In Bangladesh, characterization of karanja biodiesel & its effect on diesel emissions. *Fuel Processing Tech*, Volume 90, pp 1080-1086.

- [19] Boggavarapu P., and Ravikrishna R.V. 2012. A Comparison of jatropha methyl ester & diesel non-evaporating sprays. In: ICLASS-2012, 12th Triennial Inter. Conference on Liquid Atomization and Spray Systems. Heidelberg, Germany.
- [20] Wang, X., Huang, Z., Kuti, O.A., Zhang, W., and Nishida, K. 2010. Experimental and analytical study on biodiesel & diesel spray characteristics under ultra-high injection pressure. *Inter. J. of heat fluid flow*, Volume 31. Pp 659-666.
- [21] Raja, A. S., Smart, R.D.S., and Lee, C.L. R. 2011. Biodiesel Production Jatropha Oil and its characterization. *Research Journal of Chemical Sciences*. Volume 1, pp 81-87.
- [22] Hashimoto, N., Nishida, A., and Ozawa Y. 2014. Fundamental Combustion Characteristics of jatropha Oil as Alternative Fuel for Gas Turbines. *Fuel*, Volume 126, pp 194-201
- [23] Deshmukh, D., Madan, M. A., Anand, T.N.C and Ravikrishna, R.V. 2012. Spray characterization of straight vegetable oil at high injection pressures. *Fuel*, Volume 97. Pp 879-883.
- [24] Mohan, A.M., Deshmukh, D., Anand, T.N.C., and Ravikrishna, R. V. 2010. Effervescent spray characterization of jatropha pure plant oil. In: ICLASS Euro. 23rd annual conference on liquid atomization & spray systems.
- [25] Nalgundwar, A., Paul, B., Sharma, K. S. 2016. Comparison of performance and emissions characteristics of DI CI engine fueled with dual biodiesel blends of palm and jatropha, Volume 173, pp 172-179.
- [26] Wang, X., Huang, Z., Kuti, O A., Zhang, W., and Nishida K. 2011. An experimental investigation on spray, ignition & combustion characteristics of biodiesels. *Proceeding of the Combustion Institute*, Volume 33 (2), pp 2071-2077.
- [27] Gao, Y., Deng, J., Li, C., Dang, F., Liao, Z., Wu Z., and Li, L. 2009. Experimental study of the spray characteristics of Biodiesel Based on inedible oil. *Biotechnology Advances*, Volume 27. Pp 616-624.
- [28] Patel, C., Lee, S., Tiwari, N., Agarwal, A. K., Lee, C. S., and Park, S. 2016. Spray characterization, combustion, noise and vibrations investigations of jatropha biodiesel fueled genset engine. *Fuel*, Volume 185, pp 410-420.
- [29] Suh, H.K., and Lee, C. S. 2016. A review on atomization and exhaust emissions of a biodiesel-fueled compression ignition engine. *Renew & Sustainable Energy Reviews*, Volume 58, pp 1601-1620.
- [30] Lefebvre, A. H. 1989. Atomization and sprays. Taylor & Francis, New York, ISBN 0-891116-603-3.
- [31] Lee, C.S., Park, S.W., and Kwon, S. I. 2005. An experimental study on the atomization and combustion characteristics of biodiesel-blended fuels. *Energy Fuels*, Volume 19, pp 2201-2208.
- [32] Choi, S., and Oh, Y., 2012. The spray characteristics of unrefined biodiesel. *Renewable Energy*, Volume 42, pp 136-139.
- [33] Park, S.H., Cha, J.P., and Lee, C. S. 2011. Spray & engine performance characteristics of biodiesel and its blends with diesel and ethanol Fuels. *Combustion Science Technology*, Volume 183, pp 802-822.

- [34] Guan, L., Tang, C., Yang, K., Mo, J., and Huang, Z. 2015. Effect of di-n-butyl ether blending with soybean-biodiesel on spray & atomization characteristics in a common-rail fuel injection system. *Fuel*, Volume 140, Pp 116-125.
- [35] Flynn, F.P., Durrett, R.P., Hunter, G.L., ZurLoye, A.O., Akinyemi, O.C., Dec, J.E., and Westbrook, C. K. 1999. Diesel Combustion: An Integrated View Combining Laser Diagnostics, Chemical Kinetics, and Empirical Validation, *SAE Technical Paper* No: 1999-01-0509.
- [36] Baumgarten.C., Mixture formation in internal combustion engines. Springer (2006)
- [37] Itani, L. M., Bruneaux, G., Leella, A. D., and Schulz, C. 2015. Two tracer LIF imaging of preferential evaporation of multi-component gasoline fuel sprays under engine conditions. *Proceedings of the combustion institute*, Volume 35, pp 2915-2922.
- [38] Senda, J., Yamaguchi, M., Wakashiro, T., Tsukamoto, T., Hojyo, Y., and Fujimoto H. 1991. Spray Characteristics of Pintle Type Injector under Low-Pressure Field. *Proc. the 5th International Conference on Liquid Atomization and Spray Systems*, (Gaithersburg) : pp.857-864.
- [39] Senda, J., Nishikiori, T., Tsukamoto, T., and Fujimoto, H. 1992. Atomization of Spray under Low Pressure Field from Pintle Type Gasoline Injector. *SAE Technical Paper* : No.920382.
- [40] Senda, J., Hojyo, Y., and Fujimoto, H. 1994. Modeling of Atomization Process in Flash Boiling Spray. *SAE Technical Paper* : No.941925.
- [41] Senda, J., Yamaguchi, M., Tsukamoto, T., and Fujimoto, H. 1994. Characteristics of Spray Injection from Gasoline Injector. *JSME International Journal, Series B*, Vol.37, No.4, pp.931-936.
- [42] Adachi, M., McDonell, V. G., Tanaka, D., Senda, J., and Fujimoto, H. 1997. Characterization of Fuel Vapor Concentration Inside a Flash Boiling Spray. *SAE Technical Paper* : No.970871.
- [43] Kawano, D., Goto, Y., Okada, M., and Senda, J. 2004. Modeling Atomization and Vaporization Processes of Flash-Boiling Spray. *SAE Technical Paper* : No.2004-01-0534.
- [44] Senda J, Ikeda M, Yamamoto M, Kawaguchi B and Fujimoto H. 1999. Low Emission Diesel Combustion System by Use of Reformulated Fuel with Liquefied CO₂ and n-Tridecane. *SAE Technical Paper* : No.1999-01-1136 : pp.1-15
- [45] Senda J, Kawano D, Hotta I, Kawakami K and Fujimoto H. 2000. Fuel Design Concept for Low Emission in Engine System. *SAE Technical Paper* : No.2000-01-1258 : pp.1-13.
- [46] Senda, J. 2010. Fuel design approach for spray combustion control by use of multi-component mixing fuel related to flash boiling spray. *THIESEL*. Conference on Thermo- and Fluid Dynamic Processes in Diesel Engines.

Chapter 3. Emulsion Fuel Research

3.1. Introduction

Diesel engines play important role in mass transportation, power generation and agriculture. Although HC and CO emissions in diesel engines are very low than gasoline engine, however, the level of NO_x and smoke are higher than gasoline engine. Therefore, modifying the fuels is one of the ways to control the emissions as many researchers have already reported for the performance improvement and reduction in emissions o diesel engines.

Water in diesel emulsions is fuels which combine between water and fuels. The emulsion fuel can be explained as an emulsion of water in diesel fuel with specific surfactants or additives to make stabile in the system [1]. There are two types of emulsions; two and three phase types. The two-phase of emulsions depend on the capacity of the isolated, type of mixing, type of surfactant [2]. The Emulsions are classified as water-in-oil (W/O) emulsions and oil-in-water (O/W) emulsions.

According to inner and outer phases, the three-phase of emulsions are divided into two types. There are oil in-water-in-oil (O/W/O) and water-in-oil-in water (W/O/W) emulsions. Physical structure of two phase and three phase of emulsions can be seen in Figure 3.1. O/W/O emulsions are suitable for engines and W/O/W emulsions are usually used in applications such as make up, food and medical product [3,4].The three phase emulsions give low NO_x and CO compared to other types of emulsions [5,6]. The viscosity of the three-phase emulsions found higher than two-phase emulsions. Nevertheless, the higher viscosity is not a problem of the formulation as a fuel [3,4]. The physical structure of three phases and two phases can be shown in the figure below.

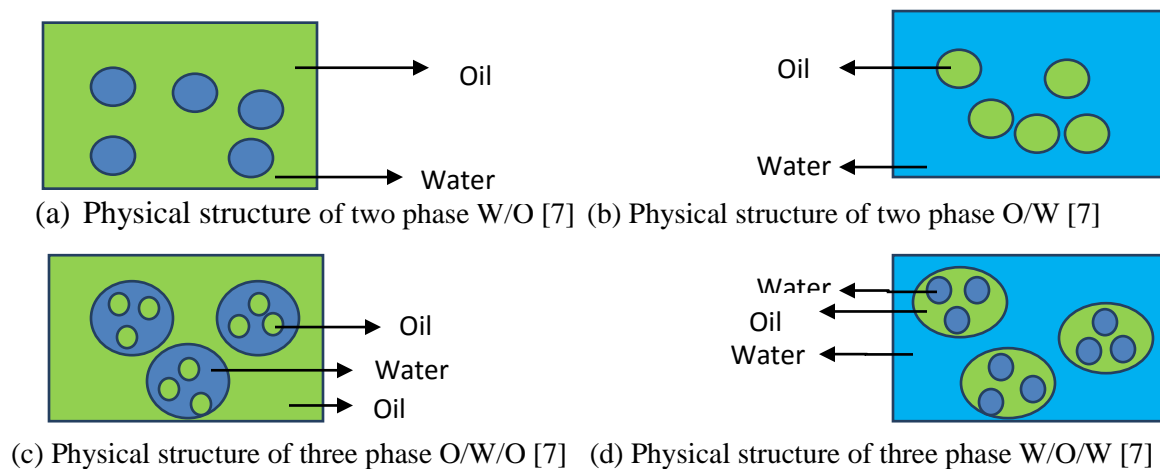


Figure 3.1. Physical Structure of two phase and three phase

The characteristics of emulsions are unstable and will split up into the stable states of the dispersed and continuous phase materials [8]. Function of surfactants is to maintain the stability of emulsions. The criteria depend on the hydrophilic-lipophilic balance (HLB). There are three types of HLB family and it depends on the type of emulsions- O/W or W/O; 1) from 4-8, stabilized W/O emulsions; 2) from 8-10, stabilized bi-continuous emulsions; 3) From 10 to 18, stabilized O/W emulsions. Surfactants should burn completely without removing other gas emissions or affecting property from fuel [1]. The surfactants can be used such as span 80 (*sorbitan monooleate*) and Tween 80 (*ethoxylated sorbitan monooleate*) but others researchers used PuriNOx and *Aquazole* [9-11]. The fuels can be visualized in a 100x to 200x magnification as shown in Figure 3.2.

The advantages of water in diesel oil or biodiesel oil emulsion can reduce the emissions such as nitrogen oxides (NOx) and particulate matters. However, there is possible in increasing in carbon monoxide and hydrocarbon. Another advantage, water in diesel emulsions can increase the combustion efficiency. This is caused by the micro explosions that can make atomization in the fuel.

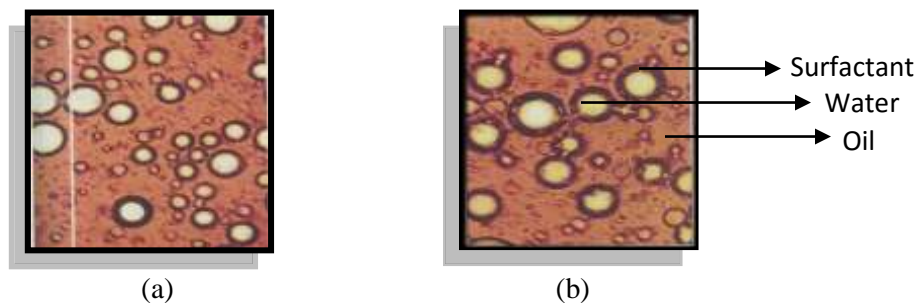


Figure 3.2. (a) Illustration of biodiesel and water in emulsion (enlargement 100x);
(b) Illustration of biodiesel and water in emulsion (enlargement 200x) [12]

3.2. Water-diesel emulsions

The water-diesel emulsions obtain from water in the form of micrometer-sized droplets gives some positive effects on the combustion of the fuel. The study has already found by theory [13] and experimentally [14] more than 40 years ago. Use diesel emulsions have been shown to give several positive effects, such as reduced nitrogen oxides (NOx), lower emissions and particulate matter in exhaust, and improved combustion efficiency.

Water diesel emulsions have been studied from many researchers. Tadashi et al. [15] studied that the effect of the ratio up to 0.8 by mass in water-diesel emulsions can reduce NOx emission up to 60% and smoke about 50-70% at a given load (BMEP of 5.31 kg/cm²). Nevertheless, at low load, BSFC was

slightly increase compared to diesel oil due to overcooling and over mixing of the charge. Sheng et al. [16] investigated that the combustion of water-diesel emulsion spray in a combustion bomb and simulated road-load conditions. Their results show that smoke can decrease up to 30% and NO_x emission can be decreased. Abu zaid [17] conducted the effect of water-diesel emulsion with different ratio of 0, 5, 10, 15, and 20 on the performance in diesel engine. His result showed that brake thermal efficiency was increased to 3.5% for 20% water-diesel emulsions.

The water –diesel emulsion along with other techniques such as EGR and different injection timing can give beneficial results to overcome the emissions. Nazha et al. [18] studied that with 16.7% hot EGR can reduce 20% smoke and 55% NO_x emission can be down. Subramanian et al. [18] studied that 5% of hydrogen peroxide in water-diesel emulsion could improve the overall performance and emissions of a diesel engine. They reported that NO_x, CO, HC, and smoke emissions can decrease drastically compared to plain diesel-water emulsion.

3.3 Water-biodiesel emulsions

Over the past few years, there have been studies about water emulsions in biodiesel oil. Qi et al. [20] studied that the ethanol-biodiesel soybean-water emulsions (0.5, 1 ml water and 80 ml biodiesel). They reported that BSFC (Brake specific fuel consumption) of biodiesel water emulsions was higher than biodiesel oil. CO, HC emissions were higher than biodiesel oil at low and medium engine load. NO_x emission was reduced from biodiesel oil from all engine loads. Masjuki et al. [21] investigated the palm oil emulsion. It was found that water-biodiesel emulsions containing 15% of water can effect in reduction of NO_x and smoke emissions than pure biodiesel palm oil. They also reported that the engine performance, fuel consumption and wear resistance of palm oil emulsion were equal to diesel oil. Awang and May [22] carried on an experimental investigation on single cylinder diesel engine with emulsions from palm oil water emulsions. They found that polymeric surfactant was the most suitable emulsifier for palm oil biodiesel. The experimental results show that the reduction in NO_x, moreover, the increase of water in emulsified fuel can cause lower in the caloric value.

3.4. Micro-explosions

Figure 3.3 shows the schematic diagram from water-diesel and biodiesel emulsions. Water inside the oil in the form of micrometer-sized droplets has a good effect on the combustion in the engine. Water is covered by oil droplet resulting in micro-explosion diesel that surrounded by water particle. The micro-explosion appears if the low boiling point of liquid or water is surrounded by the high boiling point of liquid like biodiesel oil or diesel oil. The low boiling point liquid as water is becoming unstable when the heat transfer occurs in the diesel during the compression stroke in the engine. This condition may lead to micro-explosion that would better in the fuel mixing with air. Therefore, NO and PM emissions would decrease and water- in-diesel oil or biodiesel oil emulsion can run in the engine without making any modification [23]. Another reason is that the existence of water and the existence of oil-water interface in low interfacial tension occurs a better atomization in oil during the injection in the engine [1].

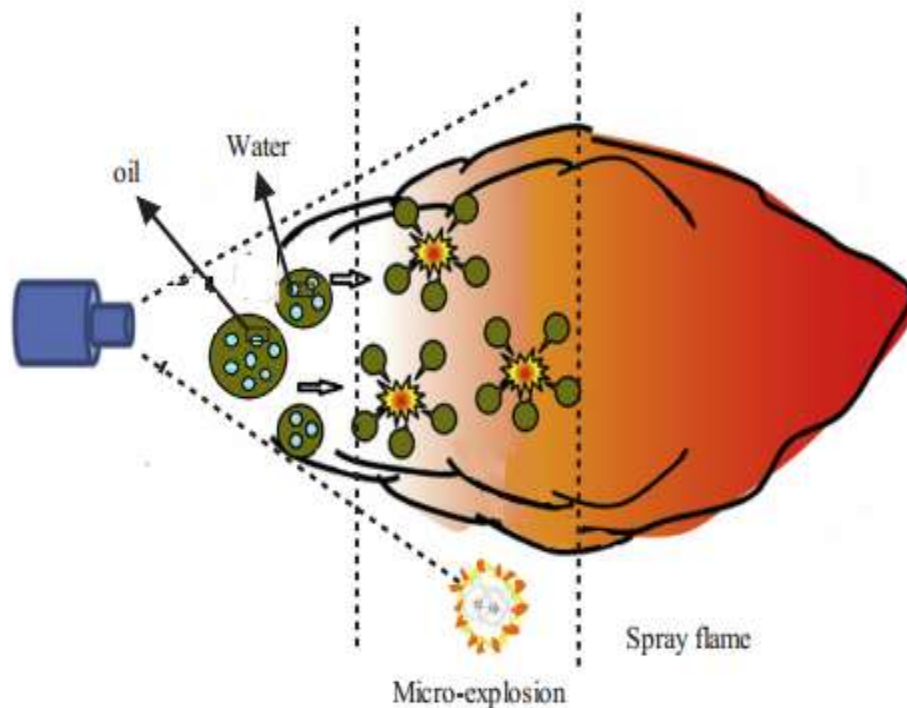


Figure 3.3. Schematic diagram of micro-explosions in water-diesel and biodiesel emulsion [24].

3.5. Case studies in water-diesel emulsions

A case study in water-diesel emulsion has been studied in 2011 by the author [25]. The composition of making water-diesel emulsions are percentages by volume: 77% diesel oil, 15 % water, and 8% emulsifier. The making of water-diesel emulsions can be shown in Figure 3.4. In Figure 3.4 shows that diesel oil mixed with the emulsions and water was added then stirred until 15 minutes. After 15 minutes it can be showed that between water and diesel oil was mixed perfectly by the emulsions.



(a)



(b)



(c)

Figure 3.4. Illustration of making water-diesel emulsions [25] (a) Preparing water, diesel oil, and emulsions; (b) Mixing between all ingredients and stirred until 15 minutes; (c) After stirring 15 minutes, the water-diesel emulsions were mixed.

3.5.1. Experimental conditions

The experimental was conducted in one hour for performance tested and 17 hours for endurance tested. The fuels were diesel oil and water-diesel emulsion. The engine used for performance tested was a single cylinder, 4 stroke (branded name Tian Li, made in China) and the speed was constant at 2000 rpm. The load was electricity generators, one phase, with load idle, 20%, 40%, 60%, and 80%. The engine used for endurance tested was Mitsubishi 3300 cc, the power was 30 kW, IDI diesel engine with load the same as performance tested.

3.5.2. Results

The results show that after the endurance test, at 60% load, water-diesel emulsion has 11% efficient than diesel oil. However, in minimum loads (idle, 20%, and 40%), before and after endurance tested diesel oil has more efficient compared to diesel-water emulsion.

The results for emissions show that after endurance test, at all loads, water-diesel emulsion can reduce NO_x emission and opacity to 3.2% (20% load). In maximum load (80%), water-diesel emulsion can reduce emissions from NO_x and CO up to 42% to 23.7%, as compared to diesel oil.

Moreover, the results for fuel consumption after 17 hour running engine test showed that from one to 9 hour endurance test, water-diesel emulsion has no advantages in fuel consumption compared to diesel oil. However, after 11 hour endurance test showed that water-diesel emulsion was more efficient 5% than diesel oil. In 17 hours running engine, water-diesel emulsion is the highest efficiency up to 15.85% as compared to diesel oil.

3.5.3. Conclusions

Water in diesel emulsions is fuels which combine between water and fuels. The advantages in using water diesel emulsions that it can reduce the NO_x emission and opacity. In other cases, after 11 hour running the engine, the water diesel emulsions can rise the thermal efficiency up to 5% than diesel oil. Moreover, 17 hours of running engine can give best thermal efficiency due to rise to 15.85% comparing to diesel fuel.

In water diesel emulsions, the micro-explosion appears if the low boiling point of liquid or water is surrounded by the high boiling point of liquid like biodiesel oil or diesel oil. The low boiling point liquid as water is becoming unstable when the heat transfer occurs in the diesel during the compression stroke in the engine. This condition may lead to micro-explosion that would better in the fuel mixing with air. Therefore, the micro-explosions can lead better combustion and reduced the emissions.

3.6. References

- [1] Lif, A., and Holmberg, K. 2006. Water-in-diesel emulsions and related systems. *Advances in Colloid and Interface Science*, 123-126, 231-239.
- [2] Hasannuddin, A. K., Aiman, A. B., Aizam, S. A., Ahmad, M. I., Zahari, M., Mohd, S. S., and Wira, J. Y. 2014. Stability studies of water-in-diesel fuel emulsion. *Appl Mech Mater*, 663:54–57.
- [3] Lin, C.Y., and Wang, K. H. 2003. Diesel engine performance and emission characteristics using three phase emulsions as fuel. *Fuel*, 83:537–545.
- [4] Lin, C.Y., and Wang, K. H. 2003. The fuel properties of three-phase emulsions as an alternative fuel for diesel engines. *Fuel*, 82:1367–1375.
- [5] Lin, C.Y., and Wang, K. H. 2004. Effects of a combustion improver on diesel engine performance and emission characteristics when using three-phase emulsions as an alternative fuel. *Energy Fuel*, 18:477–484.
- [6] Lin, C. Y., and Wang, K. H. 2004. Effects of an oxygenated additive on the emulsification characteristics of two- and three-phase diesel emulsions. *Fuel*, 83:507–515.
- [7] Ftwi, Y. H., Rashid, A. A. A, and Isa, M. T. 2011. Water-in-diesel emulsion and its micro-explosion phenomenon-review. *IEEE*, 12:314–318.
- [8] Ahmad, M. I., Hirofumi, N., Hasannuddin, A. K., and Wira, J. 2014. An overview of utilizing water-in-diesel emulsion fuel in diesel engine and its potential research study. *J Energy Inst*, 87:273–288.
- [9] Barnaud, F., Schmelzle, P., and Schulz, P. 2000. An original emulsified water–diesel fuel for heavy-duty applications. *SAE Paper No. 2000-01-1861*.
- [10] Brown, K.F., Chadderton, J., Daly, D. T., Langer, D. A., and Duncan, D. 2000. Opportunity for diesel emission reductions using advanced catalysts and water blend fuel. *SAE Paper No. 2000-010182*.
- [11] Schmelzle, P., and Chandes, K. 2004. The challenge facing Aquazole: compatibility with new engine and DPF technologies. *SAE Paper No. 2004-01-1885*.
- [12] Bhikuning, A. 2008. Nano Technology for new alternative energy. *National Seminar Industrial Engineering*. Trisakti University. Jakarta
- [13] Ballester, J. M., Fueyo, N., and Dopazo, C. 1996. Combustion characteristics of heavy oil-water emulsions, *Fuel*, 75 (6), 695-705.

-
- [14] Cook, D. H., and Law, C. K. 1978. A preliminary study on the utilization of water-in-oil emulsion in diesel engines, *Combustion Science Technology*, 18(5), 217-221.
- [15] Tadashi, M., Minoru, T., Yaushi, M., and Noboru, M. 1978. Experimental reduction in NO_x, smoke and BSFC in a diesel engine using uniquely produced water (0-80%) to fuel emulsion. *SAE Paper No.* 780224.
- [16] Sheng, H. Z., Chen, L., Zhang, Z.P., An, C., and Cheng, C. Q. 1994. The droplet group micro explosions in water-in-oil emulsion sprays and their effects on diesel engine combustion. *In: Twenty fifth symposiums (international on combustion the combustion institute):* p. 175-181.
- [17] Abu, Z. M. 2004. Performance of single cylinder direct injection diesel engine using water emulsions. *Energy Convers Manage*, 45: 697-705.
- [18] Nazha, M. A. A., Rajakaruna, H., and Wagstaff, S. A. 2001. The use of emulsion, water induction and EGR for controlling diesel engine emissions. Society of Automotive Engineers. *SAE paper no.* 2001-01-1941.
- [19] Subramanian, K, A., and Ramesh, A. 2008. Use of hydrogen peroxide to improve the performance and reduce emissions of a CI engine fuelled with water diesel emulsion. Society of Automotive Engineers. *SAE paper no.* 2008-01-0653.
- [20] Qi, D.H., Chen, H., and Mathews, R.D. 2010. Combustion and emission characteristics of ethanol–biodiesel–water micro-emulsions used in a direct injection compression ignition engine. *Fuel*. 89 (5): 958–964.
- [21] Masjuki, H., Abdulmuin, M. Z., Sii, H. S., Chua, L. H., and Seow, K. S. 1994. Palm oil diesel emulsion as a fuel for diesel engine performance and wear characteristics. *Journal for Energy Heat Mass Transfer*, 16: 295-304.
- [22] Awang, R., and May, C.Y. Water-in-oil emulsion of palm biodiesel. *Journal of oil palm Research*. 20: 571-576.
- [23] Ravikumar, T.S., Basar, P.D., and Attfield, M. J. 2001. Emulsified diesel-an immediate and effective solution for diesel exhaust emission reduction. Society of automotive engineers. *SAE paper no.* 2001-28-0037.
- [24] Jiaqiang, E., Zhiqing, Z., Jingwei, C.P., Minh, H, P., Xiaohuan, Z., Qingguo, P., Bin, Z., and Zibin, Y. 2018. Performance and emission evaluation of a marine diesel engine fueled by water biodiesel-diesel emulsion blends with a fuel additive of a cerium oxide nano particle. *Energy Conversion and Management*, 169, 194-205.
- [25] Bhikuning, A., and Hafnan, M. 2011. The effect of diesel fuel mixed water in engine performance and emission. *International Journal of Mechanical & Mechatronics Engineering*, 11 (4), 18-23.

Chapter 4. Biodiesel Production

4.1. Introduction

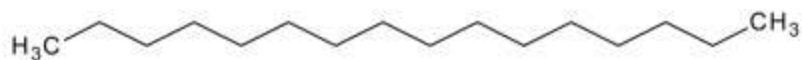
Nowadays, the use in biodiesel has becoming big trends. The decrease of petroleum oil makes researchers try to find the substitute oil in the future. Biodiesel is one of the potential resources to replace the petroleum oil. Biodiesel is an alternative fuel made from renewable sources such as vegetable oils and animal fats. It is biodegradable and nontoxic, has low emission and environmentally friendly [1].

Natural vegetable oils and animal fats are pressed or extracted to obtain crude oil or fat. These oils used to be free fatty acids, phospholipids, sterols, water, odorants and other impurities. Even refined oils and fats contain small amounts of free fatty acids and water. The free fatty acid and water contents have significant effects on the trans-esterification of glycerides with alcohol using catalyst and then the separation of fatty acid and glycerol [2]. There are four main biodiesel production have been research. In this chapter, explanation in biodiesel production will be explained further.

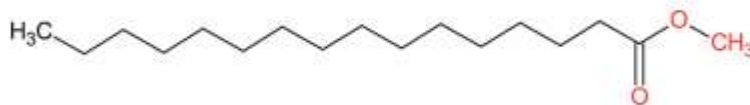
4.2. Chemical Structure

Diesel fuel is obtained from the fractional distillation of crude oil. Diesel fuel contains of hydrocarbon molecules that range in size from 8 to 21 carbon atoms. An ordinary diesel fuel containing 16 carbon atoms is presented in Figure 4.1 (a). Diesel fuel molecule is composed of a pure hydrocarbon, that is, a molecule containing only hydrogen and carbon, with no oxygen molecules. Thus, after proper burning in atmospheric air, only CO₂ and H₂O are released from this molecule. Sometimes, hydrogen sulfide (H₂S) is also produced because of the presence of sulfur (S) in diesel [3].

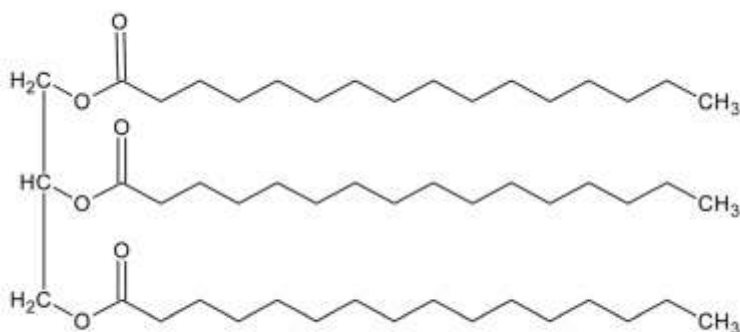
Biodiesels contain long chain carbon molecules with hydrogen atoms, similar to petro diesel, with an additional ester functional group (–COOR). Biodiesel with 17 or 16 carbons withan ester group is illustrated in Figure 4.1 (b). Vegetable oil also typically contains long rows of carbon and hydrogen atoms with ester functional groups. The molecules in vegetable oils are almost three times larger than normal diesel molecules. This largesized structure is known as a triglyceride. The atomic size and structure of vegetable oil make it gel in cold weather, which means its direct use in engines is difficult. The ordinary atomic structure of vegetable oil is shown in Figure 4.1 (c). Triglycerides are initially reduced to *diglycerides*, which are then reduced to *monoglycerides*. *Monoglycerides* are reduced to fatty acid esters. The gradual reaction mechanism producing the *monoglycerides* from triglycerides¹⁰ or vegetable oils is shown in Figure 4. 2, where R represents an alkyl group; R₁ , R₂ , and R₃ are the fatty acid chains; and k₁, k₂, k₃, k₄, k₅, and k₆ represent the catalysts [3].



Diesel Fuel (a)



Biodiesel (b)



Vegetable oil or Triglyceride (c)

Figure 4.1. Molecular Structure, (a) Diesel Fuel; (b) Biodiesel; (c) Vegetable Oil [3].

4.3. The Production of Biodiesel

4.3.1. Blending Oil

Blending oil is blending between oil (pure biodiesel oil) to diesel oil. In 1982, the diesel fleet was empowered with filtered and used frying pan oil [4]. The oils are 100% used cooking oil and 95% used cooking oil blending with 5% diesel fuel. Mixing or preheating is used as needed to compensate for cooler ambient temperatures. The problem occurred was the contamination of lubricating oil because the increase of viscosity due to polymerization of polyunsaturated vegetable oil.

Some disadvantages in using vegetable oil into diesel engine are high viscosity, lower volatility, the reactivity of unsaturated hydrocarbon chain [5]. The problems could appear in the diesel engine in

longer period of time, such as, carbon deposits, thickening and forming of lubricating oil gel as a result of contamination by vegetable oils, the formation of coke and trumpet on the injector so that the trigger of atomization does not occur properly [2]. However, using vegetable oil have some advantages such as readability, renewability, liquid- nature portability [2].

Many researchers conducted direct blending oil into the engine. In 1986, Schautman et al. [6] conducted a long-term performance test using fuel blend of 75% unrefined mechanically expelled soybean oil and 25% diesel fuel. The fuel blend was burned in a direct injection diesel engine for 159 h before the test was terminated because a constant load could not be held on the engine. A test failure occurred after 90 h into the screening test due to a 670% increase in the lubricating oil viscosity. Schlick et al. [7] conducted the performance of a direct injection 2.59 L, 3 cylinder 2600 series Ford diesel engine operating on unrefined soybean oil and sun flower oil blended with number 2 diesel fuel on a 25:75 v/v basis. The power remained constant throughout 200 hour of operation. Surplus of carbon deposits on all combustion chamber parts precludes the use of these fuel blends at least in this engine.

Direct used of blending vegetable oil into the engine has been generally considered but the problems are occurred such as high viscosity, acid composition, free fatty acid contents, carbon deposits and lubricating oil thickening [2]. Therefore, direct blending of vegetable oil are not recommended to conduct into the diesel engine.

4.3.2. Trans-esterification

Trans-esterification is the reaction of a fat or oil with an alcohol or methanol to form esters and glycerol [2]. In trans-esterification, a catalyst is used to improve the reaction rate or yield. Due to the reversible reaction, surplus of alcohol is needed to shift the equilibrium to the products side. Methanol is needed in reaction with triglycerides and KOH/NaOH can make easily dissolved. The reaction of trans-esterifications can be shown in Figure 4.2.

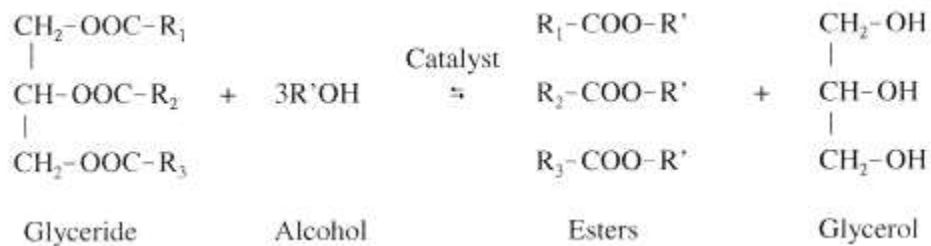


Figure 4.2. Trans-esterification Triglycerides with Alcohol.

After trans-esterification of triglycerides, the products are a mixture of esters, glycerol, alcohol, catalyst and tri-, di- and monoglycerides. Obtaining pure esters was not easy, since there were impurities in the esters, such as di- and monoglycerides[8]. The monoglycerides caused turbidity (crystals) in the mixture of esters. This problem occurred for trans-esterification from animal fat specially beef tallow. The impurities raised the cloud and pour points. Moreover, the saturated fatty acid esters in beef tallow esters is large almost 50% w/w. This makes higher in cloud and pour points than vegetable oil.

Trans-esterification consists of a number of consecutive, reversible reactions [9]. The triglyceride is converted stepwise to diglyceride, monoglyceride and finally glycerol as can be seen in Figure 4.3.

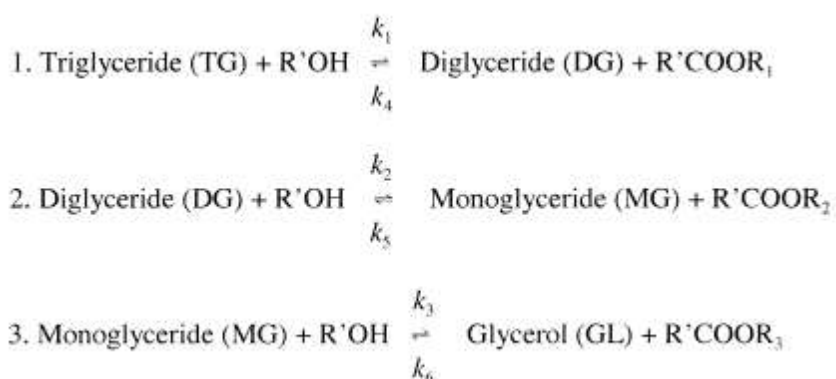


Figure 4.3.The Trans-esterification of Vegetable Oil with Alcohol to Ester and Glycerol [8].

Catalysts are classified as alkali, acid, or enzyme. Alkali-catalyzed trans-esterification is much faster than acid-catalyzed [10]. However if a glyceride has a higher free fatty acid content and more water, acid-catalyzed trans-esterification is suitable [9]. The acids could be sulfuric acid, phosphoric acid, hydrochloric acid or organic sulfonic acid. Alkalies includesodium hydroxide, sodium methoxide, potassium hydroxide, potassium methoxide, sodium amide, sodium hydride,potassium amide and potassium hydride [11].

Many researchers conducted the trans-esterification process in making a biodiesel. Recently, many research content the trans-esterification of biodiesel in using new methods. Encinar et al. [12] studied the trans-esterification process of rapeseed oil using ultra sound. The rapeseed oil fatty acid and properties can be seen in Table 4.1. Ultra sound power and catalyst concentration had a positive effect in the yield and the reaction rate. The methanol: oil molar ratio also increased the yield of the reaction, but negatively influenced the process rate.the use of ultrasound irradiation did not require any additional heating, which could represent an energy savings for biodiesel manufacture. Keera et al. [13] studied the production of biodiesel fromvegetable oils, soybean and cottonseed oils using sodium hydroxide as

alkaline catalyst. The variables affecting the yield and characteristics of the biodiesel produced. The variables investigated were reaction time (1–3 h), catalyst concentration (0.5–1.5 w/wt%), and oil-to-methanol molar ratio (1:3–1:9). The results, the best yield percentage was obtained using a methanol/oil molar ratio of 6:1, sodium hydroxide as catalyst (1%) and 60 ± 1 °C temperature for 1 h. Sarno and Iuliano [14] obtained the biodiesel production from waste cooking oil using *Thermomyces lanuginosus* (TL) lipase (E.C.3.1.1.3) anchored on Fe₃O₄/Au nanoparticles through physical interactions. A remarkable biodiesel yield of ~90% was obtained without any pre-treatment and at a lipase concentration of 20%, 45°C reaction temperature, 1:6 oil/methanol molar ratio, after 24 h. The immobilized enzyme showed fast kinetic (the biodiesel yield was already of 34.6% after only 3 h) and activity slightly dependent on the length of the acid chains.

Trans-esterification process can be one of the considerations in making biodiesel. The new method is still growing to have better results in the properties in biodiesel.

Table 4.2. Rapeseed Fatty Acid Oil Profile and Properties [12].

Fatty Acid	Percentage (%)
C16:0 Palmitic	3.5
C18:0 Stearic	0.9
C18:1 Oleic	64.4
C18:2 Linoleic	22.3
C18:3 Linolenic	8.2
Others acids	0.7
Properties	
Density at 15°C (kg/m ³)	906.2
Viscosity at 40 °C (cSt)	36.3
Water content (wt, %)	0.8
Acidity index (mgKOH·g ⁻¹)	2.7
Iodine value(gI ₂ ·100 g ⁻¹)	113.5
Saponification value (mgKOH·g ⁻¹)	194.7

4.3.3. Micro-emulsions

To solve the problem of the high viscosity of vegetable oils, micro-emulsions with solvents such as methanol, ethanol and 1-butanol have been studied. A micro-emulsion is defined as a colloidal equilibrium dispersion of optically isotropic fluid microstructures with dimensions generally in the 1 ± 150 nm range formed spontaneously from two normally immiscible liquids and one or more ionic or non-ionic amphiphiles [15]. The advantage in micro-emulsions is that can improve the spray characteristics by explosive vaporization [16]

Many studies are carried with micro-emulsions in making a biodiesel. Goering et al [17] conducted a short term performances of both ionic and non-ionic micro-emulsions of aqueous ethanol in soybean oil were nearly as good as that of No. 2 diesel, in spite of the lower cetane number and energy content but the durabilities were not determined. Recently, diesel and biodiesel water emulsions are investigated. Liang et al [18] conducted a research in water diesel emulsion with neat diesel and distilled water mixed with surfactant. The method of Hydrophilic Lipophilic balance (HLB) is used to help find stable emulsion. The oxygen enrich was added 21-24 % in volume. The water content was 0%, 10%, 20%, and 30%. The results show that lower BSFC, higher cylinder pressure, shorter ignition delay, reducing the emissions (PM and NOx) were observed when oxygen enriches in combustion were applied. Attia and Kulchiski [19] investigated the performance from water diesel emulsions in three cylinder diesel. Based on membrane emulsification, two different membranes of pore sizes of 0.2 μ m and 0.45 μ m has been individually used to change the emulsion structure while keeping the same water fuel emulsion volumetric content (at 17% water volumetric content and 0.5% mixing emulsifier content). The Results showed that emulsions with large size of water droplets resulted in greater reduction in NOx emissions up to 25%. While, emulsions with finer droplets not only gave reductions in engine smoke and unburned hydrocarbons of values greater than 80% and 35% respectively, but also resulted in an increase of the engine effective efficiency up to 20%.

Micro-emulsions theory seems have a good prospect in the future. Micro-emulsions in the fuel can support the fuel to have good spray characteristics. Therefore, the combustion can be improved and the emissions can be reduced.

4.3.4. Pyrolysis

Pyrolysis is defined as the conversion of one substance into another by means of heat or by heat with the aid of a catalyst [20]. It involves heating in the absence of air or oxygen and of chemical bonds to yield small molecules [20, 21]. The pyrolyzed material can be vegetable oils, animal fats, natural fatty acids and methyl esters of fatty acids [2].

Pioch et al. [22] investigated the catalytic cracking of vegetable oils to produce biofuels. Copra oil and palm oil stearin were cracked over a standard petroleum catalyst $\text{SiO}_2/\text{Al}_2\text{O}_3$ at 450°C to produce gases, liquids and solids with lower molecular weights. The condensed organic phase was fractionated to produce biogasoline and biodiesel fuels. The chemical compositions (heavy hydrocarbons) of the diesel fractions were similar to fossil fuel.

Pyrolytic chemistry is difficult to characterize because of the variety of reaction paths and the variety of reaction products that may be obtained from the reactions that occur [2].

4.4. Simulation of Biodiesel Production

The simulation of biodiesel production has been made by Chlev and Simeonov [23] by using ChemCad version 6.3.1. The simulation illustrates the production of biodiesel from pure vegetable oil with using an alkaline catalyst. The main areas are trans-esterification, methanol separation, water washing, FAME purification, catalyst neutralization and glycerol purification. The equipment used includes in particular reactors, distillation and extraction columns and components splitters. As a result of the simulation, 100 kg/h vegetable oil, 10 sodium alkali, 120 methanol, 900 kg/h biodiesel with the two final target products - biodiesel and glycerol, are obtained with purity 98 % and 99 % [23].

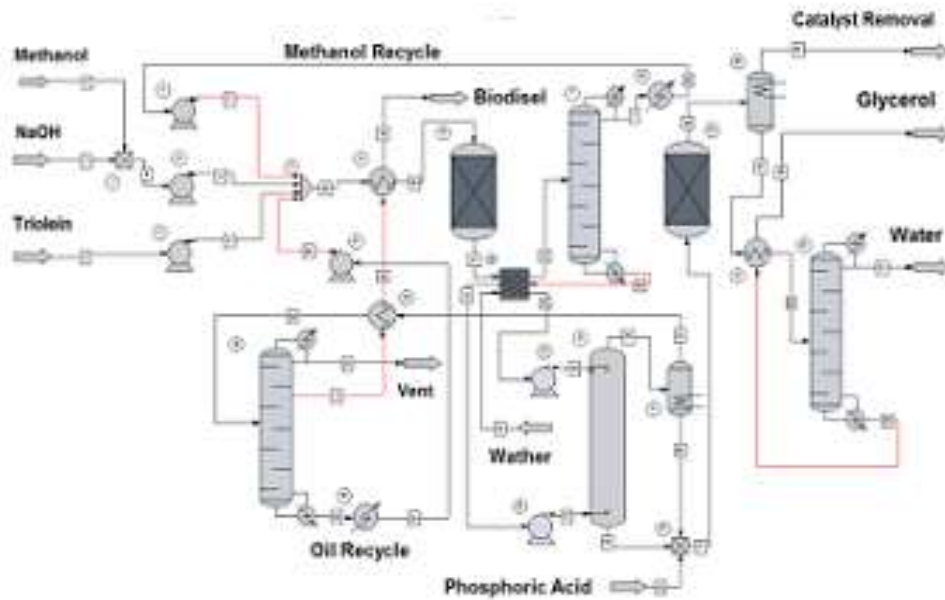
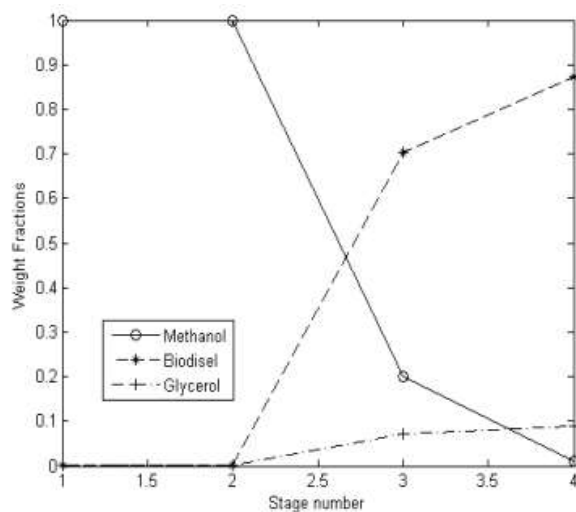


Figure 4.4. The Process Flow Sheet Developed in ChemCad 6.3.1 [23].

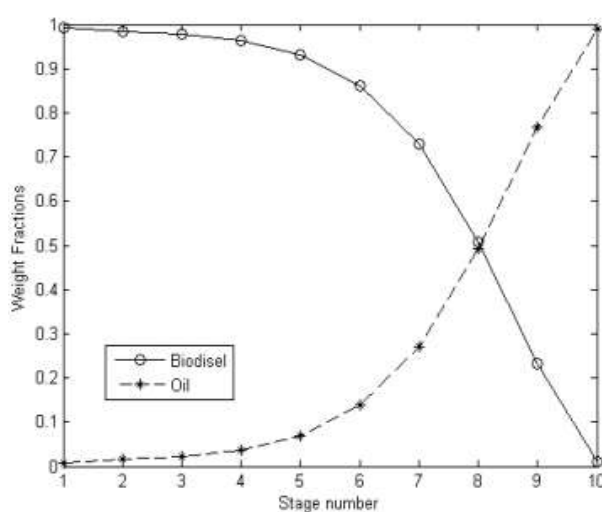
The development of the process model for simulations involves defining the chemical components, selecting appropriate thermodynamic models, proper unit operations and operating conditions such as temperature, pressure, and flow rate [23].

Table 4.3. Physical Properties [23].

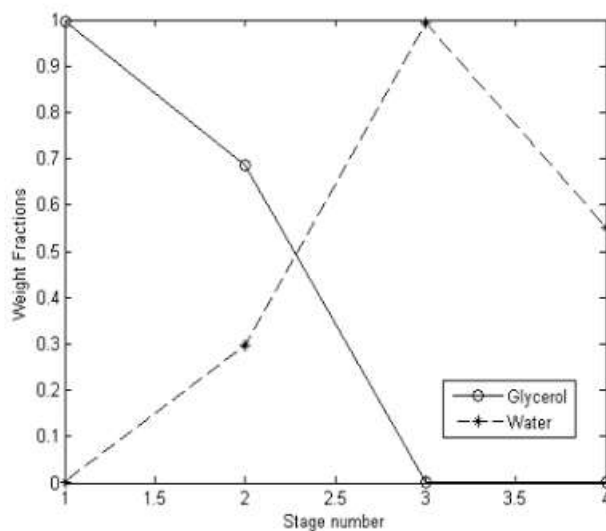
Molecular mass	885.4321
Critical temperature	1366.85 C
Critical pressure	470.0018 kPa
Critical volume	3.090007 m ³ /kmol
Melting point	5.000007 C
Normal boiling point	846.85 C
IG Gibbs of formation	19459.5 kJ/kg
Acentric factor	1.599314
Solubility parameter	17140.54 (J/m ³) ^{**0.5}
Dipole moment	1.050002e-029 C.m
Heat of vaporization	326.2352 kJ/kg
Liquid volume constant	153.4908 cc/mol
UNIQUAC area parameter	31.764
INOQUAC volume parameter	39.17798
Watson factor	13.9026
API gravity	24.22796
Specific gravity 60 F	0.9155723



(a)



(b)



(c)

Figure 4.5. Liquid Mass Fraction in Different Column; (a) Column 7, (b) Column 18, (c) column 21 [23]

Fuel properties in this simulation are shown in Table 4.3 [23]. Table 4.5 shows the liquid mass fraction in different column. Table 4.5 (a) in column 7 shows that the oil is intended for separating the methanol. Table 4.5 (b) in column 18 shows the concentration changed and the unreacted oil. Table 4.5 (c) shows the completely purified glycerol and water in distillation column [23].

4.5. Conclusions

Biodiesels contain long chain carbon molecules with hydrogen atoms, similar to diesel fuel, with an additional ester functional group ($-\text{COOR}$). Biodiesel has O2 in molecular structure and diesel fuel has no O2 content. The oxygen content in biodiesel can improve the combustion and reduced the emissions in the diesel engine.

There are four methods in making biodiesel fuel. There are blending fuels, trans-esterification, micro-emulsion and pyrolysis. The purpose of the biodiesel process is to make lower the viscosity of the oil or fat. Although blending of oils and other solvents and micro-emulsions of vegetable oils lowers the viscosity, engine performance problems, such as carbon deposit and lubricating oil contamination, still exist. Pyrolysis produces more biogasoline than biodiesel fuel. Trans-esterification is basically a

sequential reaction. Triglycerides are first reduced to diglycerides. The diglycerides are subsequently reduced to monoglycerides. The monoglycerides are finally reduced to fatty acid esters.

Biodiesel production can be calculated in simulation by using ChemCad. The simulation is useful to understand the reaction of making biodiesel and to understand the completely purified between glycerol and water in distillation column.

Recently, the biodiesel production is still growing and lots of researches have been made to make the good properties in biodiesel nearly to diesel engine. The challenge is to make biodiesel that can make in long time period without or minimalize any soot deposits and friendly for the emissions.

4.6. References

- [1] Krawczyk, T., 1996. Biodiesel - alternative fuel makes inroads but hurdles remain. *INFORM* 7, 801-829.
- [2] Ma, F., and Hanna M. A. 1999. Biodiesel production: a review. *Bioresource technology*. 70, 1-15.
- [3] Ruhul, A. M., Kalam, M. A., Masjuki, H. H., Fattah, I. M. R., Reham, S.S., and Rashed, M. M. 2015. State of the art biodiesel production process: a review of the heterogeneous catalyst. *RSC Adv*, 5, 101023.
- [4] Anon., 1982. Filtered used frying fat powers diesel fleet. *JAOCs*, 59, 780A-781A.
- [5] Pryde, E.H., 1983. Vegetable oil as diesel fuel: Overview. *JAOCs*, 60, 1557-1558.
- [6] Schlautman, N.J., Schinstock, J.L., Hanna, M.A., 1986. Unrefined expeller soybean oil performance in a diesel engine. *Trans. ASAE*, 29 (1), 70-73.
- [7] Schlick, M.L., Hanna, M.A., and Schinstock, J.L., 1988. Soybean and sunflower oil performance in a diesel engine. *Trans. ASAE*, 31 (5), 1345-1349.
- [8] Ma, F., Clements, L.D., Hanna, M.A., 1998. The effects of catalyst, free fatty acids and water on transesterification of beef tallow. *Trans. ASAE*, 41, 1261-1264.
- [9] Freedman, B., Butterfield, R.O., Pryde, E.H., 1986. Transesterification kinetics of soybean oil. *JAOCs* 63, 1375-1380.
- [10] Freedman, B., Pryde, E.H., Mounts, T.L., 1984. Variables affecting the yields of fatty esters from transesterified vegetable oils. *JAOCs* 61, 1638±1643.
- [11] Sprules, F.J., Price, D., 1950. Production of fatty esters. US Patent 2, 366-494.

- [12] Encinar, J. M., Pardal, A., Sanchez, N., and Nogales, S. 2018. Biodiesel by transesterification of rapeseed oil using ultrasound a kinetic study of base-catalysed reactions. *Energies*, 11,2229.
- [13] Keera, S.T., Sabagh, S.M., and Taman, A. R. 2011. Transesterification of vegetable oil to biodiesel fuel using alkaline catalyst. *Fuel*, 90 (1), 42-47.
- [14] Sarno, M., and Luliano, M. 2019. Biodiesel production from waste cooking oil. *Green Processing and Synthesis* 8(1), 828-836.
- [15] Schwab, A.W., Bagby, M.O., and Freedman, B., 1987. Preparation and properties of diesel fuels from vegetable oils. *Fuel*, 66, 1372-1378.
- [16] Pryde, E.H., 1984. Vegetable oils as fuel alternatives – symposium overview. *JAOC* 61, 1609-1610.
- [17] Goering, C.E., Campion, R.N., Schwab, A.W., and Pryde, E.H., 1982. In vegetable oil fuels, proceedings of the international conference on plant and vegetable oils as fuels, Fargo, North Dakota. *American Society of Agricultural Engineers*, St Joseph, MI 4, 279-286
- [18] Liang, Y., Shu, G., Wei, H., and Zhang, W. 2013. Effect of oxygen enriched combustion and water-diesel emulsions on the performance and emissions of turbocharged diesel engine. *Energy Conversion and management*, 73,69-77.
- [19] Attia, A. M. A., and Kulchitskiy, A. R. 2014. Influence of the structure of water-in-fuel emulsion on diesel engine performance. *Fuel*, 116, 703-708.
- [20] Sonntag, N.O.V. 1979. Reactions of fats and fatty acids. *Bailey's industrial oil and fat products*, vol. 1, 4th edition, ed. Swern, D., John Wiley & Sons, New York, p. 99.
- [21] Weisz, P.B., Haag, W.O., and Rodewald, P.G., 1979. Catalytic production of high-grade fuel (gasoline) from biomass compounds by shape-selective catalysis. *Science*, 206, 57-58.
- [22] Pioch, D., Lozano, P., Rasoanantoandro, M.C., Graille, J., Geneste, P., and Guida, A., 1993. Biofuels from catalytic cracking of tropical vegetable oils. *Oleagineux*, 48, 289-291.
- [23] Chilev, C., and Simeonov, E. 2014. Simulation of biodiesel production by trans-esterification of vegetable oils. *Journal of Chemical Technology and Metallurgy*, 49(5), 479-486.

Chapter 5. Fuel Analysis

5.1. Introduction

In this chapter, the fuel properties and FTIR of all biodiesel fuels were analyzed and discussed. The fuels are blending oil between jatropha methyl ester (JME) with n-Tridecane, biodiesel fuel (BDF), bio hydro-fined diesel oil (BHD), and biodiesel water emulsion.

5.2. Fuel Preparation for JME Blending with n-Tridecane

The JatrophaMethyl Ester (JME) was purchased from Revo International, Japan. The n-tridecane was purchased from Nakalai tesque, Japan. JME was blended with n tridecane under three percentages by volume ; JME 25% blends with n-tridecane 75% (JME25); JME 50% blends with n-tridecane 50% (JME50); and JME 75% blends with n-tridecane 25% (JME 75).

5.2.1. Fuel Properties

The fuel parameter properties were analyzed in Shimadzu Kyoto-Japan used Japan International standard - JIS K based on the method. The density (15°) was determined according to JIS K official method 2249. The kinematic viscosity (40°) was determined under JIS K 2283. The flash point (PMCC) was analyzed based on JIS K 2265. The Cetane number was analyzed on JIS K 2280. The copper strip corrosion was determined under JIS K 2513. The distillation was analyzed based on JIS K 2254. Nevertheless, n-tridecane chemical properties were taken from PubChem data based [6]. The fuel parameter analysis also compared to the ASTM D standard which based on the American and part of Asian biodiesel standardization.

5.2.2. Density

The density in the fuel parameteris important to determine. Density is a chemical property to figure the exact volume of fuel to provide satisfactory combustion [7]. Density can also impact the efficiency of the combustion system and fuel atomization in the engine [8]. Biodiesel usually has a high density compared to diesel fuel. In case, the density is high. It can be influenced by engine output power due to distinctive fuel mass injection [9]. Figure 5.1 shows that the density in jatropha blending with n-tridecane has low values compared to standard JIS K 2249. Nevertheless, the value JME 75 has met the requirements of ASTM D 1298 biodiesel standardization.

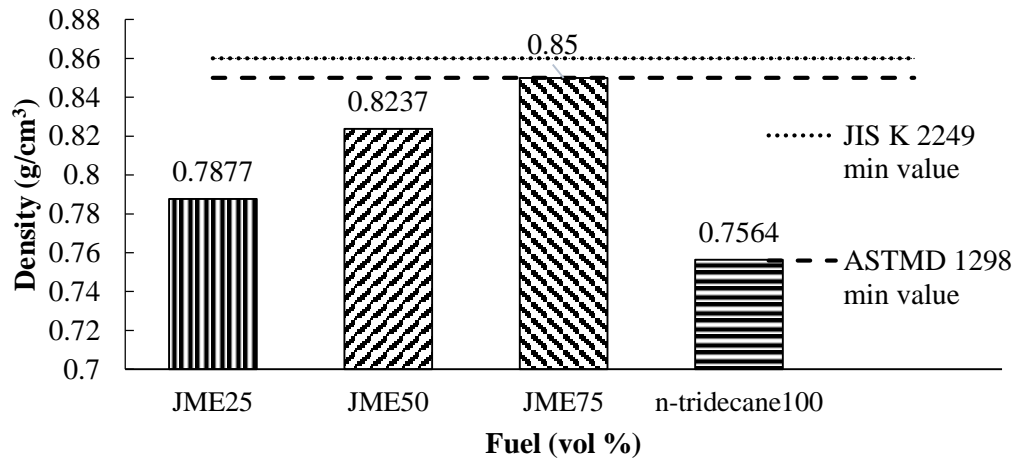


Figure 5.1. Density from various blends

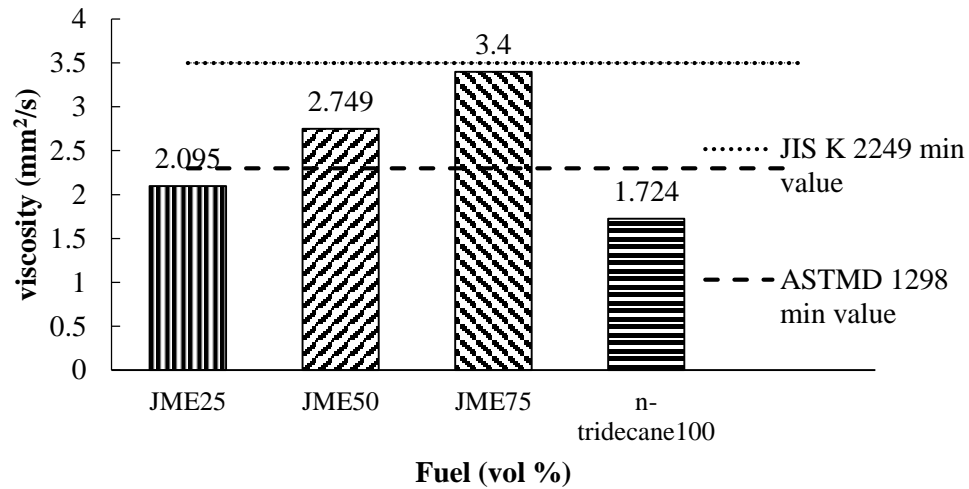


Figure 5.2. Viscosity from various blends

5.2.3. Viscosity

The kinematic viscosity in biodiesel has high value compared to diesel fuel, this condition caused by high fattyacid in biodiesel. High in kinematic viscosity can cause poor in the spray automation and can produce deposits in the engine and it can upgrade the energy to pump the fuel [8]. On the contrary, lower in kinematic viscosity would easier the fuel to pump and attain droplets to injector [10]. Demirbas[10]

studied that diesel fuel has a similar viscosity with biodiesel. Trans-esterification process would decrease the viscosity level than pure biodiesel.

From Figure 5.2, the viscosity value of JME25, JME50, and JME75 have met the requirement for ASTM D 1298. Nevertheless, JME25, JME50, and JME75 have under value for JIS K 2249 standardization. However, n-tridecane 100 has not met all the standardization for JIS K 2249 nor ASTM D 1298.

5.2.4. Flash Point

The fuel flammability condition is pointed by its flash point. The estimation of flash point diverse and conversely corresponding to the instability of the fuel [11]. The Flash point value of diesel fuel is around 55-66 °C. While biodiesel is around 110-180 °C. Biodiesel has its minimum temperature of flash point. The JIS K 2265 has a minimum standard of a flash point that is 120 °C. Otherwise, ASTM D 93 has a lower standard of a minimum flash point that is 100°C.

Figure 5.3 shows that all fuels have met the biodiesel standard of ASTM D 93. Nevertheless, all fuels have not met the standard of JIS K 2265.

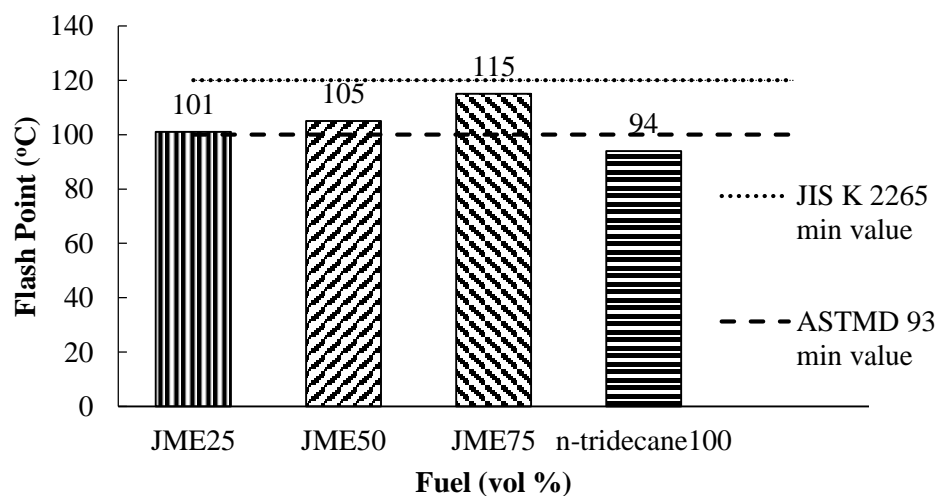


Figure 5.3. Flash point from various blends

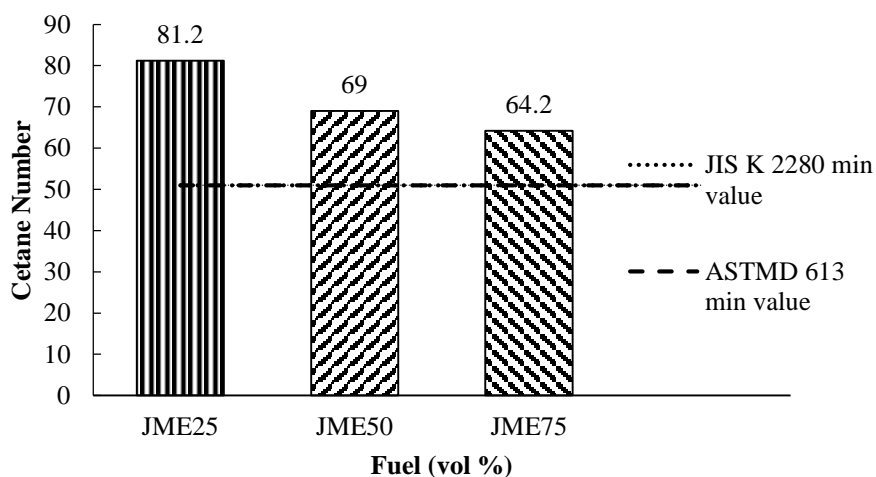


Figure 5.4. Cetanenumberfromvariousblends

5.2.5. CetaneNumber

Figure 5.4 displays the cetane number of various blends. It shows that all the Fuels have met the requirement for cetane number standards. Cetane number is a value that indicates how the fuel will burn completely in the combustion chamber. High cetane number in fuels have several advantages such as the complete combustion will occur in the engine, reduce the knocking and noise in the engine, reduce the warm-up time engine and lower emission during combustion in a safer environment [12].

5.2.6. Copper Strip Corrosion

Copper strip test is to measure the corrosive of sulfur compounds in the fuel. The ASTM D 130 and JIS K 2513 consist of dipping a strip of copper into the fuel for a specified time and define temperature and observing the corrosive action of the fuel [13].

Figure 5.5 shows that JME25, JME50, and JME75 have met the standard requirement of JIS K 213 and ASTM D 130. These indicated that JME 25, JME50, and JME75 are safe from the compound of corrosive sulfur.

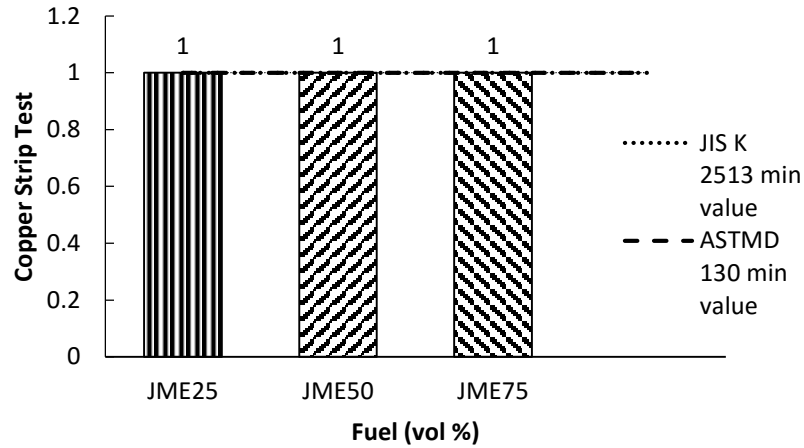


Figure 5.5. Copper strip corrosion from various blends

5.2.7. Distillation

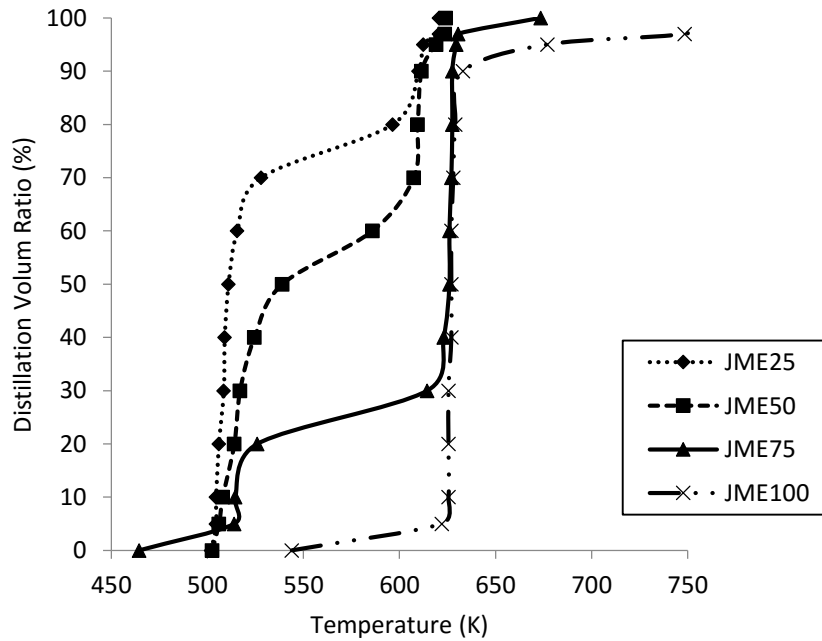


Figure 5.6. Distillation from various blends

The distillation curves can be seen in Figure 5.6. It shows that JME 75% has higher distillation and less volatile than JME 50% and JME 25%. This indicated that JME 75% has poor in spray characteristics (bigger droplets) than JME 50% and JME 25%.

5.2.8. FTIR Analysis

The FTIR (Fourier Transform Infrared Spectroscopy) spectra data were taken using Shimadzu, Irtaffinity-1, and FTIR 8400 spectrometer, in the range of 4000-400 cm^{-1} . Presently, FTIR has been characterized to discover the methyl peak positions from the reaction of trans-esterification of Biodiesel [14]. FTIR spectrometry is a worth equipment to predict wave numbers in biodiesel samples [15].

5.2.9. Tridecane

Tridecane is a combustible fuel. The fuel characteristics from n-tridecane are different from diesel fuel and biodiesel fuel.

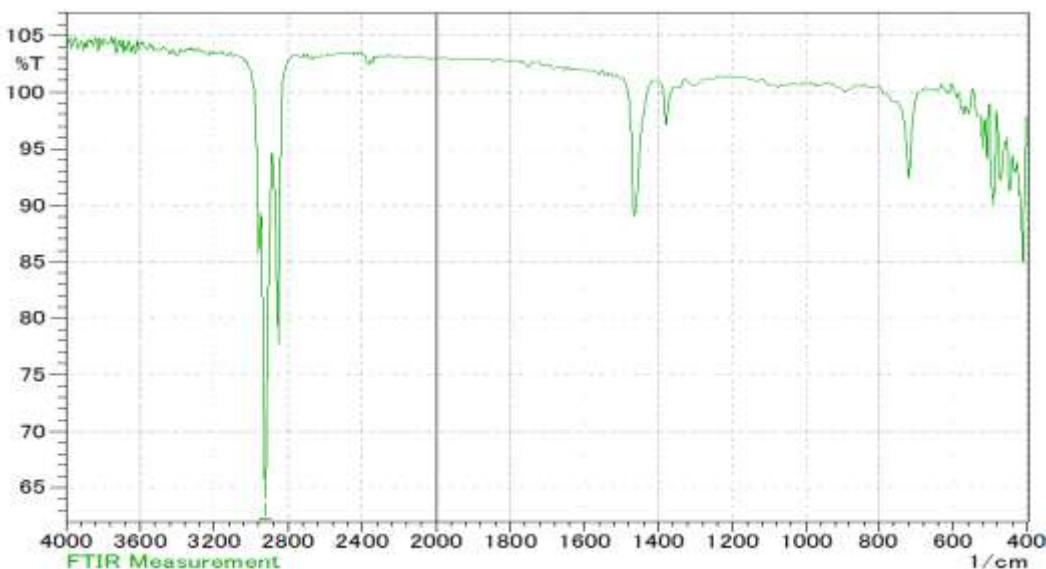


Figure 5.7. FTIR n-Tridecane

The FTIR analysis of n-tridecane is shown in Figure 5.7. In the figure shows there are only three peaks which strong in the FTIR figure. The alkane strong C-H vibration at 2920,23 cm^{-1} , the alkane bending -C-H vibration at 1470 cm^{-1} and the strong alkyl halide C-Cl 720 cm^{-1} . This indicated that n-tridecane is not from vegetable oil since no carbonyl peak between 1740-1750 cm^{-1} [16]. Furthermore, there is no spectral region between 1300-1060 cm^{-1} , which is indicated as methyl ester.

5.2.10. JME 25% (JatrophaMethyl Ester 25% and n-Tridecane 75%)

The result of FTIR analysis of JME 25% is shown in Figure 5.8. In the figure, there are four peaks from FTIR result. It shows strong band in C-H alkane wave number at $2854.65\text{--}2920.23\text{ cm}^{-1}$. The stretch ether C=O vibration at 1760 cm^{-1} . The alkane bending --C-H vibration at 1460 cm^{-1} . The strong alkyl halide C-Cl vibration at 720 cm^{-1} .

JME25% is pointed that the fuel is made from vegetable oil or methyl ester since the C=O peak at 1760 has appeared although the wave number is not strong. However, it is correlated that the blend between n-tridecane and jatropha methyl ester can be approved from FTIR graph. The strong or weak of wave number have corresponded between the percentage amount of blending between fuel and methyl ester.

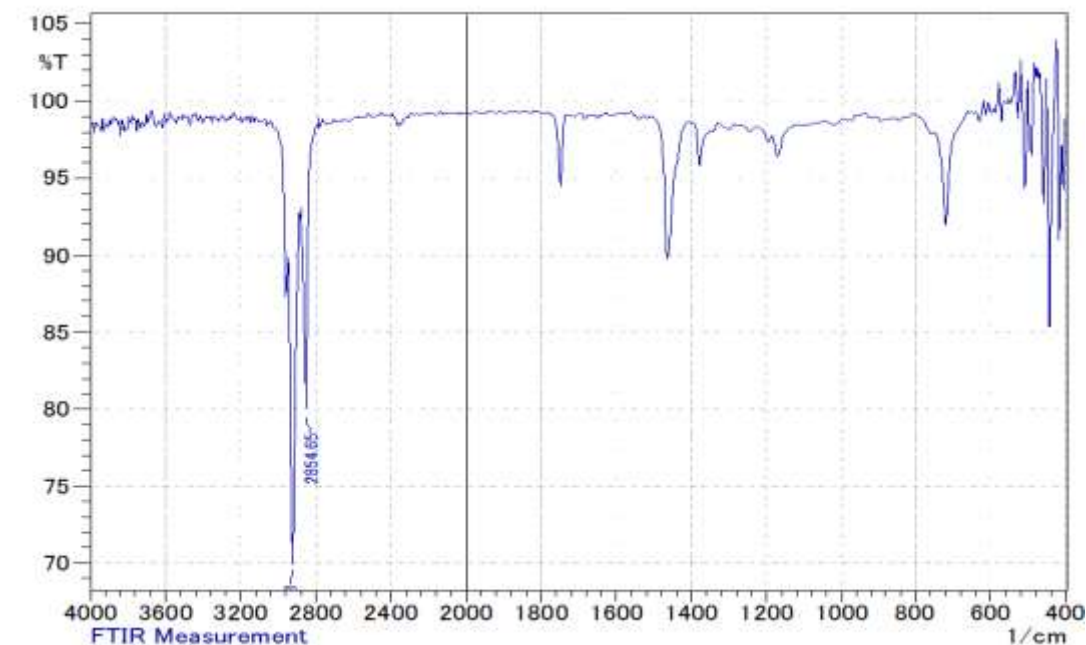


Figure 5.8. FTIR JME 25%

5.2.11. JME 50% (JatrophaMethyl Ester 50% and n-Tridecane 50%)

From the figure 5.9 indicates the FTIR result from JME 50%. From the figure there are five peaks which is strong in FTIR analysis.

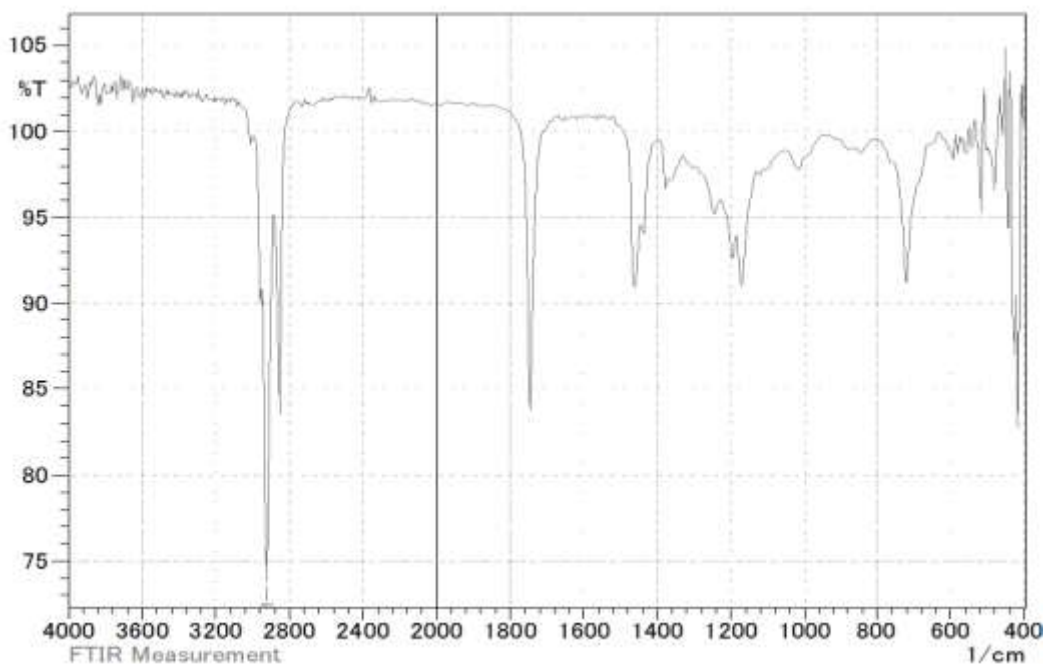


Figure 5.9. FTIR JME 50%

The alkane stretch C-H vibration between 2870 – 2920. 23 cm^{-1} . The strong stretch ether C=O and the wave number is at 1750 cm^{-1} . The alkane bending –C-H vibration at 1470 cm^{-1} , The ether stretch C-O wave number at 1170 cm^{-1} and the strong alkyl halide vibration at 723 cm^{-1} .

JME 50% shows that the carbonyl peak is in 1750 which is longer than JME 25%. The methyl ester peak is at 1170. This pointed that JME 50% is contained of methyl ester from jatropha, which blended with the higher composition of JME 25% and n-tridecane.

5.2.12. JME 75% (Jatropha Methyl Ester 75% and n-Tridecane 25%)

As shown in Figure 5.10, the FTIR analysis of JME 75% is analyzed. There are five peaks which is strong in the FTIR figure. The alkane stretch C-H vibration at $2870 - 2920.23 \text{ cm}^{-1}$, the ether C=O strong stretch at a wave number of 1750 cm^{-1} , The alkane bending -C-H vibration at 1470 cm^{-1} , the ether stretch C-O at a wave number of 1170 cm^{-1} and the strong alkyl halide C-Cl at a wave number of 723 cm^{-1} .

The figure shows that JME 75% has indicated from vegetable oil or methyl ester since it has strong carbonyl peak (1750 cm^{-1}) and strong ester C-O (1168.86). Those lines are longer than JME 25% and JME 50%. This proved that JME 75% is contained large blending proportions between jatropha methyl ester and n-tridecane. As this proved that JME 75% is contained of Jatropha methyl ester 75% and n-tridecane 25%.

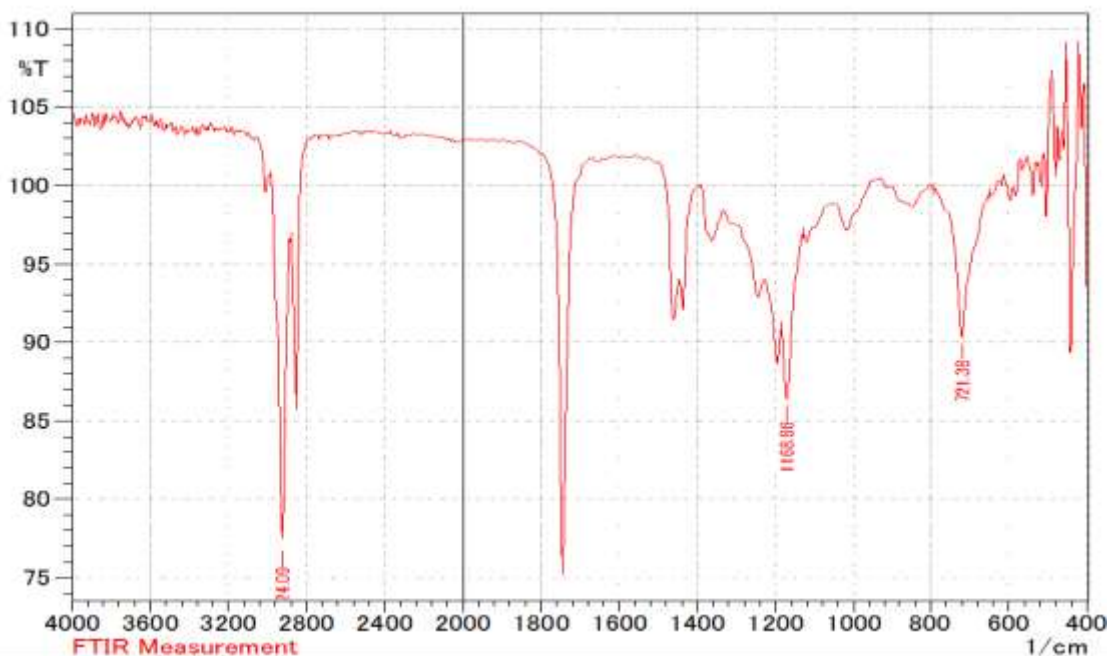


Figure 5.10. FTIR JME 75%

5.3. Chemical Analysis of Biodiesel-Water Emulsions

5.3.1 Fuel Preparation

Biodiesel cooking oil was purchased from PT. Bali Hijau Biodiesel Company and the emulsions were obtained from Mechanical engineering Department Trisakti University Jakarta. In this study, there are four fuels were considered, biodiesel waste cooking oil 100% (BD100), biodiesel cooking oil blended with diesel oil 5% (BD5), biodiesel cooking oil blended with diesel oil 10% (BD10), and biodiesel water emulsions (water 10%, biodiesel 5%, and emulsions 18.7%) blended with diesel oil (BD5W10).

5.3.2. Density

The density is one of the important property in biodiesel. The results are by the ASTM D 1298 method. From Figure 5.11 shows that biodiesel-water emulsions has higher density than BD5 and BD10. From the result shows that the pure biodiesel of waste cooking oil (BD100) has the highest density (881.6 kg/m³), BD5 reached at 825.4 kg/m³, BD10 reached at 833.6 kg/m³ and BD5W10 reached at 842.9 kg/m³.

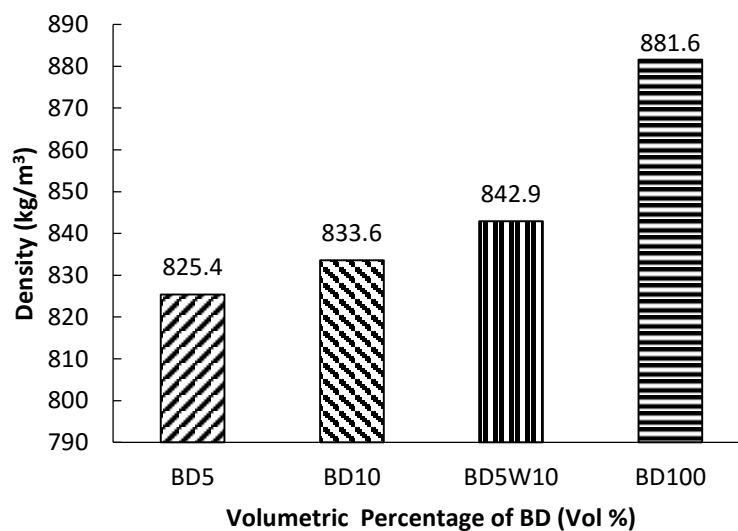


Figure 5.11. Density from various fuels

5.3.3. Kinematic Viscosity

Kinematic viscosity in the fuel is the most important to understand. In this study, the kinematic viscosity was examined by using ASTM D 445. The results can be shown in Figure 5.12. BD5W10 is the highest viscosity than other fuels. High viscosity in the fuel can lead the fuel difficult to atomize and can affect to combustion deterioration [17]. Fuel atomization and volatility are affected by viscosity. The viscosity of pure biodiesel oil is higher than the blends. By blending between pure biodiesel oil and diesel oil can decrease the value of viscosity. Figure 5.12 shown that the increased of emulsions in water-diesel can affect higher in viscosity.

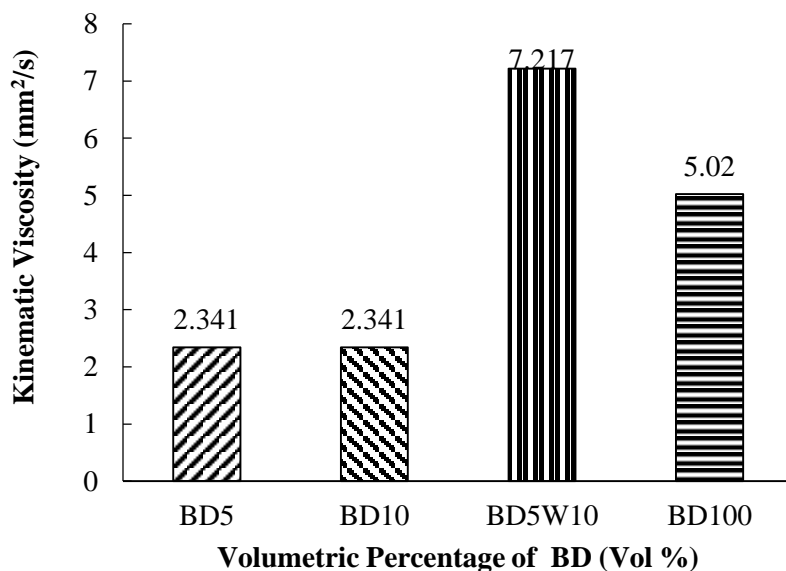


Figure 5.12. Kinematic viscosity from various fuels

5.3.4. Flash Point

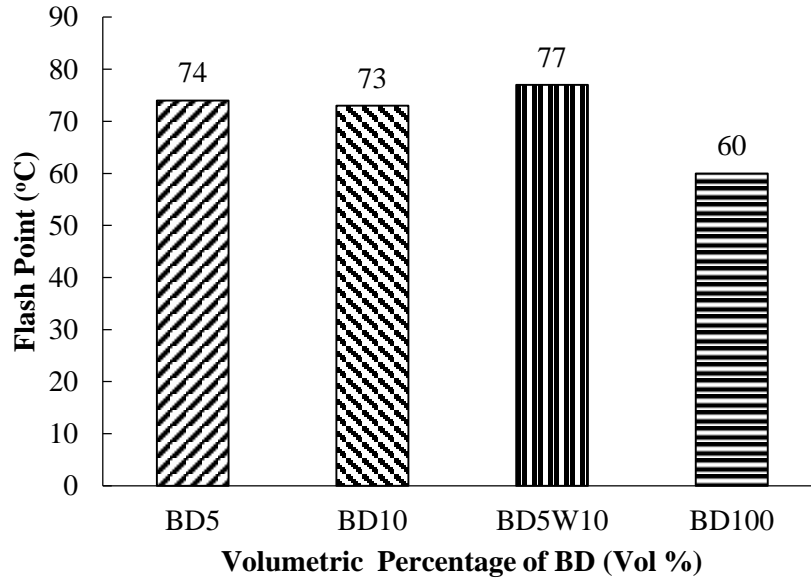


Figure 5.13. Flash point from various fuels

From Figure 5.13 shows that the percentages of biodiesel blending can affect the number of flash point. The biodiesel-water emulsion has the highest flash point than other fuels. The flash point of BD5W10 is pointed 77°C which is higher than BDW5 that has 74°C, and BD10 with 73 °C for a flash point.

5.3.5. Cetane Index

Figure 5.14 shows the cetane index from various fuels. Cetane index is calculated based on the density and the volatility from the fuel [18]. The ignition quality of diesel oil can be described in the cetane number. The value of cetane number should not be too high and too low. The incomplete combustion and smoke can appear if the cetane number is too high because the combustion can occur before the fuel and air are properly mixed. The incomplete combustion can also occur if the cetane number is too low because the engine warms up is to be slow, the engine roughness, higher air temperature and misfiring [19].

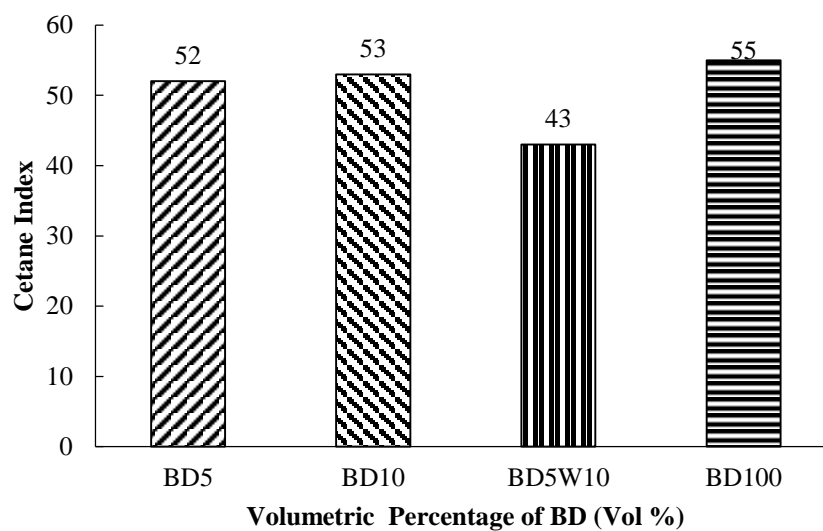


Figure 5.14. Cetane index from various fuels

5.3.6. Caloric Value

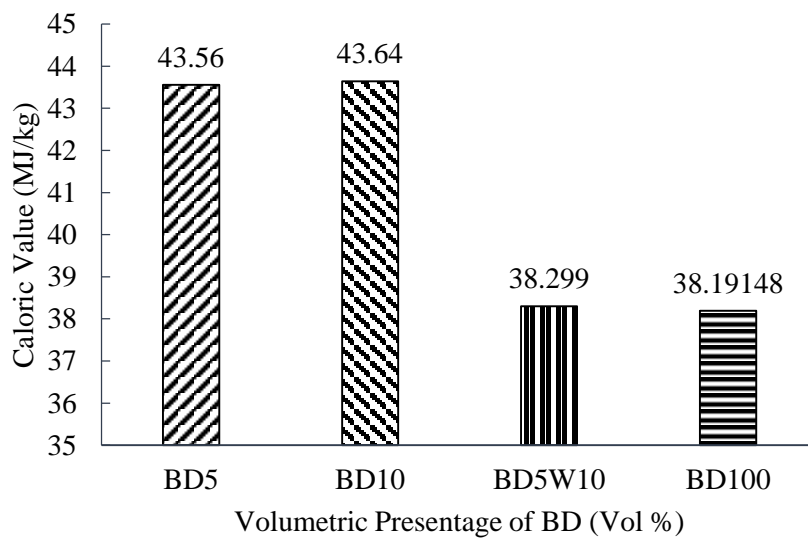


Figure 5.15. Caloric value from various fuels

Figure 5.15 shows the caloric values from various fuels. From Figure 5.15 shows that biodiesel water emulsion of BD5W10 has lower in a caloric value. By adding water in biodiesel and additives (BW18.7) can be affected by a decrease of 12.077% in caloric value as compared to BD5. The caloric value of BD5W10 is nearly as same as BD100. Low caloric value in biodiesel and biodiesel water emulsion are due to its high oxygen content. Nevertheless, the combustion efficiency of biodiesel and biodiesel water emulsion will be high because of the oxygen content in the fuel.

5.3.7. Distillation

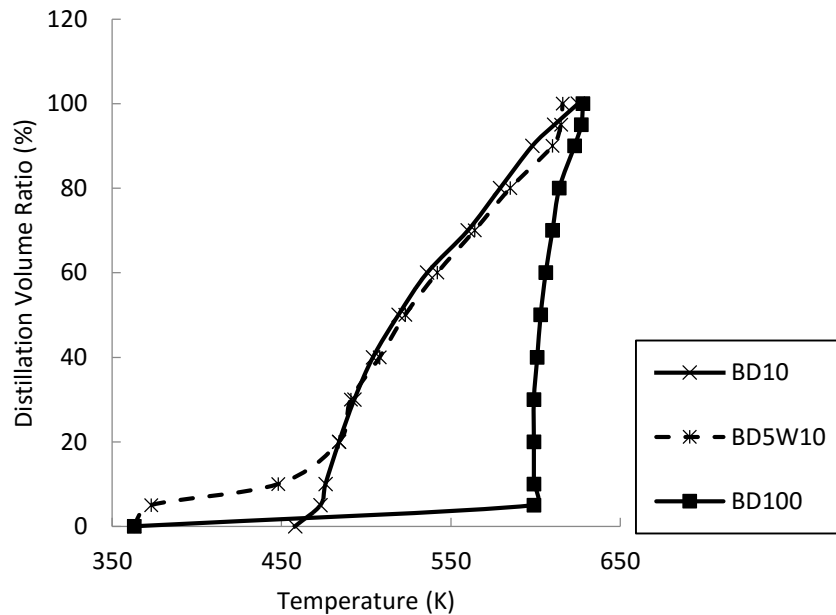


Figure 5.16. Distillation ratio from various fuels

The distillation was calculated by method of ASTM D 86-17. The distillation curves are shown in Figure 5.16. Figure shows that BD100 has less volatility and high distillation than other fuels. This can be indicated that BD100 has poor spray characteristics as compared to other fuels. As seen in Figure 5.16, the distillation of BD5W10 is nearly the same as BD10. This can be indicated that BDW18.7 has better in spray characteristics than BD100.

5.3.8. FTIR Analysis

FTIR is Fourier transform Infrared Spectrometry. FTIR spectrometry can be able to predict the wave number in biodiesels and also can discover the methyl peak positions of trans-esterification in biodiesel [14].

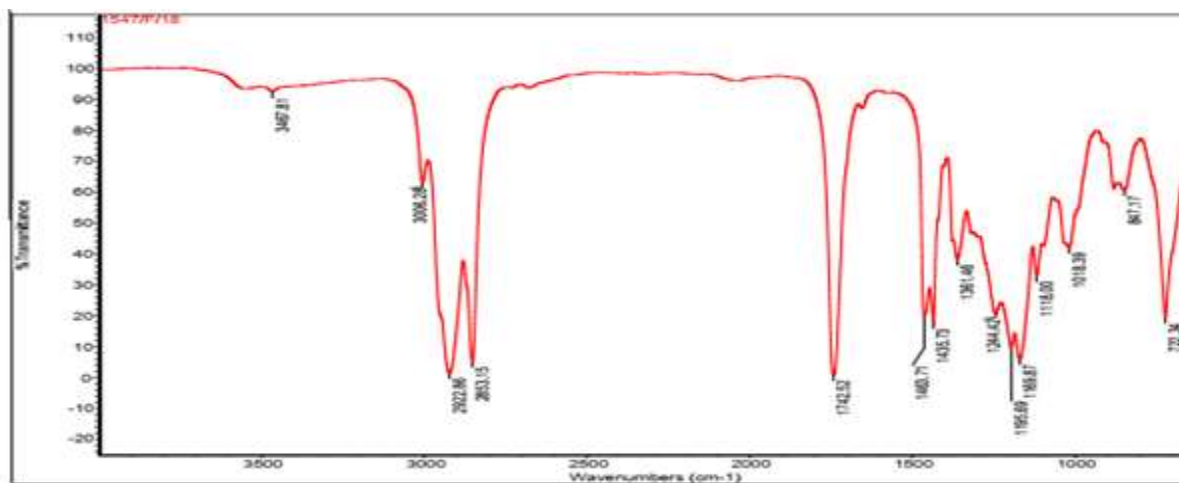


Figure 5.17. Infrared spectrometry of BD100

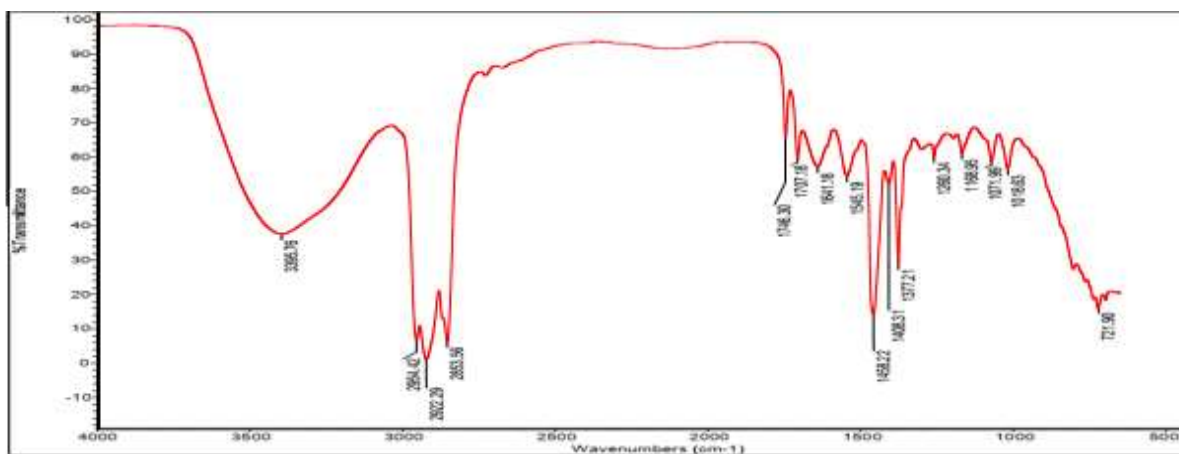


Figure 5.18. Infrared spectrometry of BD5W10

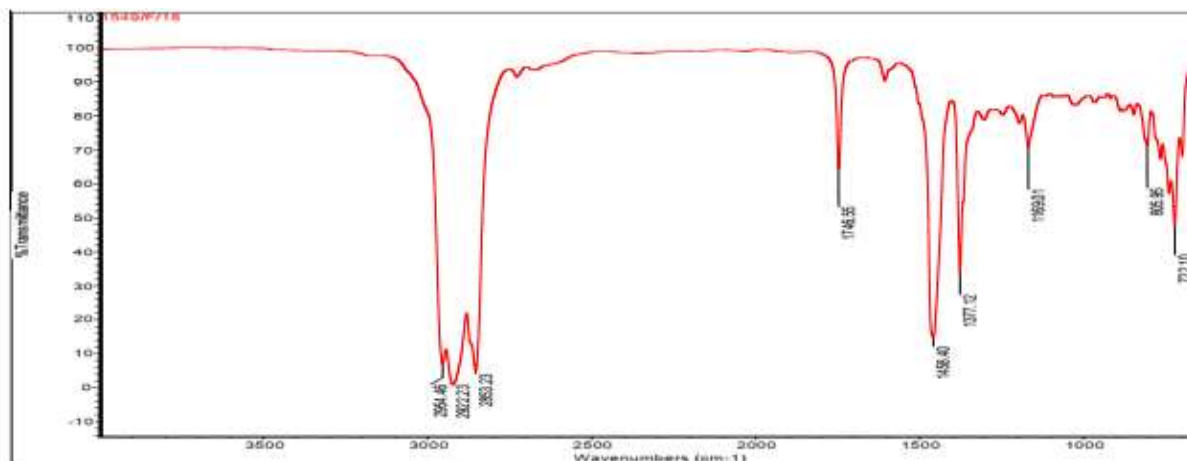


Figure 5.19. Infrared Spectrometry of BD5

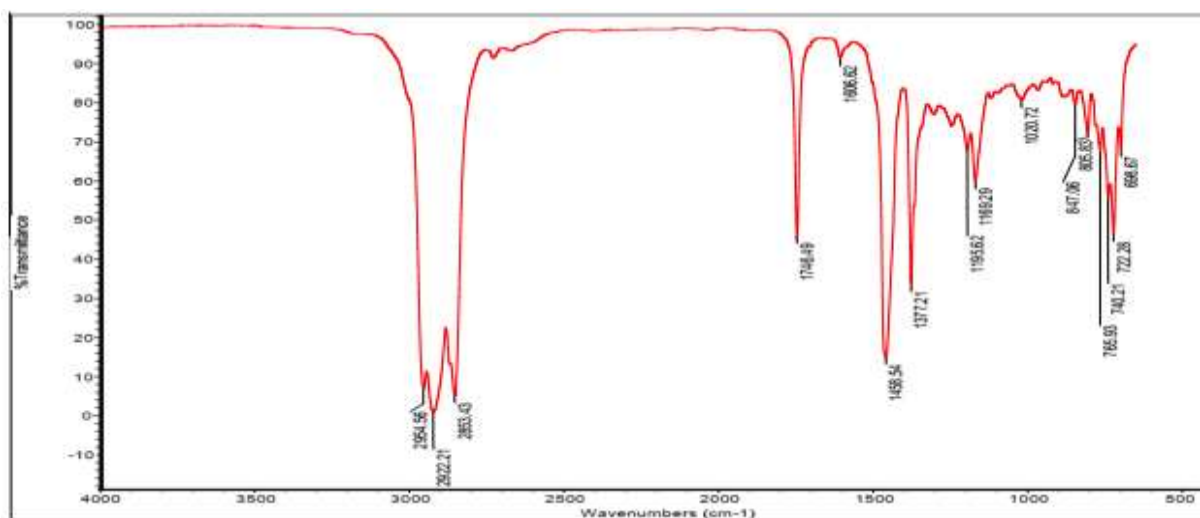


Figure 5.20. Infrared Spectrometry of BD10

From Figure 5.17 until 5.20 show the FTIR result from BD100, BD5W10, BD5, and BD10. In the region from $1800\text{--}1700\text{ cm}^{-1}$, it can be seen that the peaks occur can be signal to the ester $\text{C}=\text{O}$ stretch and these are common as FAME. Another important feature in the figures that BD100, and BD5W10 have different spectrum in the region of $3550\text{--}3200\text{ cm}^{-1}$. This spectrum can be defined as the O-H stretch of the hydrogen bonding [20]. The FTIR analyses below are referred from infrared spectroscopy absorptions table [20,21].

Figure 5.17 shows the FTIR of BD100. From the figure shows the stretch N-H at 3467.81 cm^{-1} , this stretch O-H at 3006.28 cm^{-1} , the alkane stretch C-H vibration at $2853.16\text{--}2922.86\text{ cm}^{-1}$, the ether $\text{C}=\text{O}$ strong stretch at 1742.52 cm^{-1} , the medium O-H bending at 1435.73 cm^{-1} , the strong S=O stretch at 1169.87 cm^{-1} and strong bend of C-H at 722.34 cm^{-1} .

Figure 5.18 shows the infrared spectroscopy of BD5W10. From the figure describes that the strong O-H stretch alcohol at 3395.76 cm^{-1} , the medium C-H stretch at 2853.56 , 2922.29 and 2954.42 , the strong C=O stretch at 1746.30 cm^{-1} and 1707.18 cm^{-1} , the medium C=N stretch at 1641.18 cm^{-1} , the strong N-O stretch at 1545.19 cm^{-1} , the CH₂ bending at 1458.22 cm^{-1} , the medium C-H bending alkane (methyl group) at 1377.21 cm^{-1} and 1408.31 cm^{-1} , the strong S=O stretch (sulphonamide) at 1168.95 cm^{-1} , the strong C-H bending at 721.90 cm^{-1} .

Figure 5.19 indicates the infrared spectroscopy of BD5. The picture displays that the medium C-H stretch alkane at 2853.23 cm^{-1} , 2922.23 cm^{-1} and 2954.46 cm^{-1} , the strong C=O stretch at 1746.55 cm^{-1} , the CH₂ bending at 1458.40 cm^{-1} , the medium C-H bending at 1377.12 cm^{-1} , the strong S=O stretch (sulphonamide) at 1169.01 cm^{-1} , the strong C-H bending at 805.95 cm^{-1} and 722.10 cm^{-1} .

Figure 5.20 represents the FTIR of BD10. From the picture describes that medium C-H stretch alkane at 2853.43 cm^{-1} , $2922,21\text{ cm}^{-1}$ and 2954.56 cm^{-1} , the strong C=O stretch at 1746.49 cm^{-1} , the medium C=C stretch (conjugated alkene) at 1606.62 cm^{-1} , the CH₂ bending at 1458.54 cm^{-1} , the medium C-H bending at 1377.21 cm^{-1} , the strong S=O stretch (sulphonamide) at 1169.29 cm^{-1} , the strong C-H bending at 756.93 cm^{-1} , the strong C=C bending at 740.21 cm^{-1} and the strong C-H bending at 722.28 cm^{-1} .

From figures 5.17 until 5.20 describe the different compositions of fuels can affect the infrared spectroscopy. BD5, BD10, and BD5W10 were blended with diesel oil, therefore the strong S=O stretch can be found in the FTIR figures. BD5W10 is included water additives in the fuels, therefore O-H hydrogen bonding could be found in the infrared spectroscopy figures.

5.4 Chemical Analysis of Bio Hydro-Fined Diesel Oil (BHD) and Biodiesel Fuel (BDF)

5.4.1. Fuel Preparation

In this study, biodiesel fuel (BDF) and bio hydro fined diesel oil (BHD) were collected from Revo International, Kyoto-Japan. BDF is the first generation oil and BHD is the second generation oil. BDF is made from trans-esterification process using KOH as a catalyst; hence, BHD is made from waste cooking oil and processed by bio hydro-finishing. Hydrogenation in second generation oil is the process that vegetable oils are decompressed down to a molecular weight that similar to components in diesel oil and saturated hydrocarbons are converted to saturated hydrocarbon in vegetable oils [22].

5.4.2. Density

Figure 5.21 shows the value of density from BHD and BDF. As seen in Figure 5.21 that density of BHD is lower 55.6% than BDF. BDF has a density of 885 kg/cm³) and BHD has 835.8 kg/cm³. This shows that using bio hydro finning process in biodiesel can decrease the value of density.

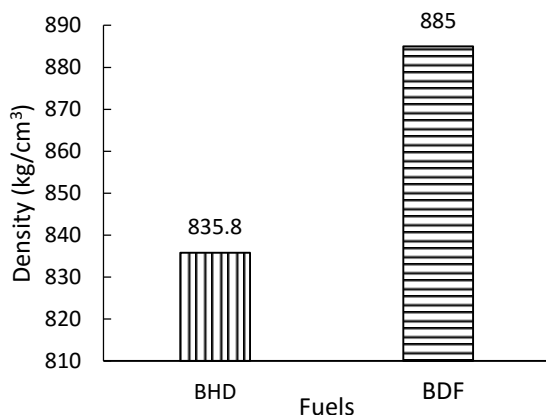


Figure 5.21. Density from various Fuels

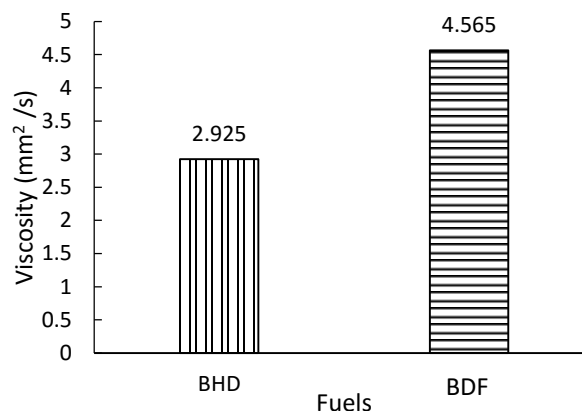


Figure 5.22. Viscosity from various fuels

5.4.3. Viscosity

Figure 5.22 shows the value of viscosity from BHD and BDF. It can be shown that viscosity of BHD can be decreased by 35.92% from BDF. This shows that using bio hydro finning process can make viscosity in the fuel better than trans-esterification process. BDF that using trans-esterification process has higher viscosity than BHD. The viscosity of BDF is 4.565 mm²/s, hence, BHD is 2.925 mm²/s.

5.4.4. Distillation

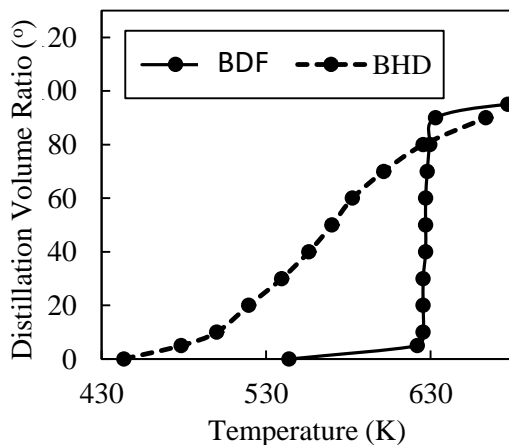


Figure 5.23. Distillation from various fuels

Figure 5.23 shows distillation from BHD and BDF. As seen that BHD is higher volatility than BDF. This can be indicated that BHD has good spray characteristics than BDF.

5.5. Conclusions

The fuel properties of biodiesel have several disadvantages such as high viscosity, high density and high boiling point. Therefore, pure vegetable oil or biodiesel oil is not recommended to conduct in the diesel engine in long term due to the deposits will appear in the engine and some troubles may appear in the engine.

In order to improve the biodiesel, the blending fuel is recommended. Another options is blending between low boiling point fuels with high boiling point, therefore, the fuel properties in biodiesel can be improved. The improved in fuel properties can be effected the improved of combustion and good atomization appears in the diesel engine.

5.6. Reference

- [1] Nongbe, M. C., Ekou, T., Ekou, L., Yao, K. B, Grogneq, E. L, and Felpin, F. X. 2017. Biodiesel Production from palm oil using sulfonatedgraphene catalyst. *Renewable Energy*. 106,135-141.
- [2] Hu, Q., Hua,W.,Yin, Y., Zhang, X., Liu, L., Shi, J., Zhao, Y., Qin, L., Chen, C., and Wang, H. 2017. Rapeseed research and production in China. *The Crop Journal*. 5, 127-135.
- [3] Rattanaphra, D.,andSrinophakun, P. 2010. Biodiesel production from crude sunflower oil and crude jatropa oil using immobilized lipase. *Journal of Chemical Engineering of Japan*. 43, 104-108.
- [4] Meher, L. C., Kulkarni, M. G., Dalai, A. K., Naik, S. N. 2006. Transesterication of karanja (Pongamiapinnata oil by solid basic catalysts. *European Journal of Lipid Science and Technology*. 108, 3898-3978.
- [5] Ikegami, M. 2002. The use of fatty acid methyl ester called biodiesel fuel. Meeting for investigation into the actual conditions for diesel exhaust gas emission with alternative fuels. JSAE.
- [6] <https://pubchem.ncbi.nlm.nih.gov/compound/Tridecane>
- [7] Ramirez, V., and Luis, F.2013. Density and viscosity of biodiesel as a function of temperature: empirical models. *Renewable and Sustainable Energy Reviews*. 19, 652-665.

-
- [8] Xua, J., Grift, T. E., and Hansen, A. C. 2011. Effect of biodiesel on engine performances and emissions. *Renewable Energy Reviews*. 15, 1098-1116.
- [9] Alptekin, E., and Canaksi, M. 2008. Determination of the density and the viscosities of biodiesel-diesel fuel blends. *Renewable Energy*. 33, 2623-2630.
- [10] Demirbas, A. 2009. Progress and recent trends in biodiesel fuels. *Energy Conversion and Management*. 50, 14-34.
- [11] Silitonga, A. S., Masjuki, H. H., Mahlia, T. M. I., Ong, H. C., Chong, W. T., and Boosroh, M. H. 2013. Overview properties of biodiesel diesel blends from edible and non-edible feedstock. *Renewable and Sustainable Energy Reviews*. 22, 346-360.
- [12] <http://farmweeknow.com/blogs-benefits-high-cetane-diesel-fuel-3681>.
- [13] Knothe, G. 2006. Analyzing biodiesel: standards and other methods. *JAOCs*. 83, 823-833.
- [14] Barone, J. R. 2007. 233rd ACS National meeting. *Paper AGRO-153*. Chicago. 25-29.
- [15] Cunha, C. L., Luna, A. S., Oliveira, R. C. G., Xavier, G. M., Paredes, M. L. L., Torres, A. R. 2017. Predicting the properties of biodiesel and its blends using mid-FTIR spectrometry and first-order multivariate calibration. *Fuel*. 204, 185-194.
- [16] Zhang, W. B. 2016. Review on analysis of biodiesel with infrared spectroscopy. *Renewable and Sustainable Energy Reviews*. 16, 6048-6058.
- [17] Xue, J., Grift, T. E., and Hansen, A. C. 2011. Effect of biodiesel on engine performances and emissions: *Renewable and Sustainable Energy Reviews*, 15, 1098-1111.
- [18] Anggono, W., Noor, M.M., Suprianto, F.D., Lesmana, L.A., Gotama, G.J., and Setiyawan, A. 2018. Effect of cerberamanghas biodiesel in diesel engine performance. *International Journal of Automotive and Mechanical Engineering*, 15 (3), 5667-5682.
- [19] Knothe, G., Matheus, A.C., and Ryan III, T.W. 2003. Cetane numbers of branched and straight-chain fatty esters determined in an ignition quality tester. *Fuel*, 82, 971-97.
- [20] Coates, J. 2000. Interpretation of infrared spectra, a practical approach. *Encyclopedia of analytical chemistry*, 12, 10815-10837.
- [21] Rabelo, S.N., Ferraz, V.P., Oliveira, L.S., and Franca, A.S. 2015. FTIR analysis for quantification of fatty acid methyl esters in biodiesel produced by microwave-assisted transesterification. *International Journal of Environmental Science and Development*, 6(12), 964-969.

[22] Loganathan, S. 2011. Biohydro-fined Diesel (BHD) and Biodiesel (BOD) Production Process and Property Review. Innovations in Fuel Economy and Sustainable Road Transport, Pune, India, Institution of Mechanical Engineers (IMEchE), *Woodhead Publishing Limited*, 97-107.

Chapter 6. Non-Evaporating Spray Characteristics

6.1. Introduction

This chapter discusses the non-evaporating spray characteristics using the shadowgraph technique. The fuels tested are from jatropha methyl ester (JME25, JME50, and JME75), bio-hydro fined diesel oil (BHD) and biodiesel fuel (BDF).

6.2. Fuel Design Method

Study on properties from two components of fuel is very important to solve the needs of chemical thermodynamics due to one component can dissolve in another component under the molecular level [1].

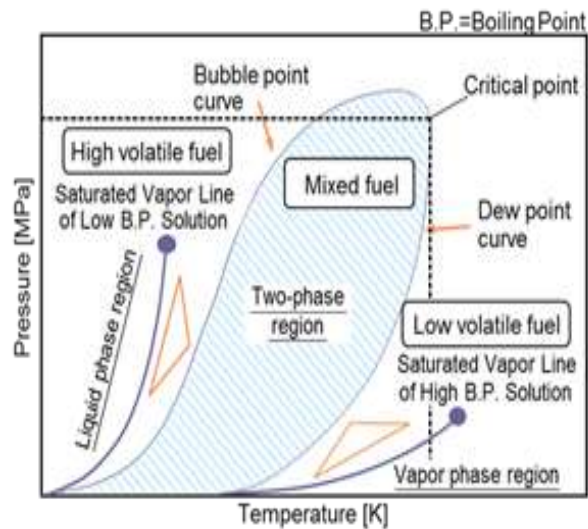


Figure 6.1. Pressure-temperature Diagram of Multi-component Fuel

Figure 6.1 shows the schematic of pressure-temperature diagram from pure substance and mixed fuel. It can be seen in the figure 1 that the pure substance, the vapor region and the liquid region are separated accurately by the saturated vapor pressure line. Then, the vapor pressure line of each component pull each other and shows the resultant of two phase region phase of liquid phase and vapor phase are mixed. Saturated liquid line is at the upper boundary between two phase region and liquid phase. Saturated vapor line is at the lower from the diagram. Both saturated liquid line and saturated vapor line reach at the critical point. In the two phase region, vapor and liquid phase are mixed together. In the case that the liquid pressure exists in the two phase region, therefore, two phase mixture where the vapor of the lower boiling point component is dominant and the fuel vaporization is promoted comparing

to the pure one of higher boiling point [2]. Furthermore, the flash boiling phenomena will never occurs when the pressure drop of the fuel does not reach the two phase region. Therefore, the valuation of vapor-liquid phase and the two phase region is necessary based on the thermodynamic approach so the evaporation process of multi component can be simulate [2]. In this study, this concept is applied to jatropa methyl ester (JME) as a high-boiling point fuel and n-tridecane as a low-boiling point fuel to improve the properties in JME.

6.3. Experimental Method

The experimental setup was designed to conduct this study. The non-evaporating characteristics include parameters such as spray-tip penetration, spray cone angle, and droplet size distribution. The design of visualize and fuel spray characteristics in of constant volume vessel is shown in Figure 6.2. The experiments were conducted by using constant volume vessel that emulates as combustion in diesel engine conditions. The experimental was similar to Kamimoto et al. [3] and Sieber [4]. The combustion chamber contains nitrogen (N_2), oxygen (O_2) and acetylene (C_2H_2). The volume of the combustion chamber is 1000 cc. All data were collected into the computer that connected to the constant volume vessel.

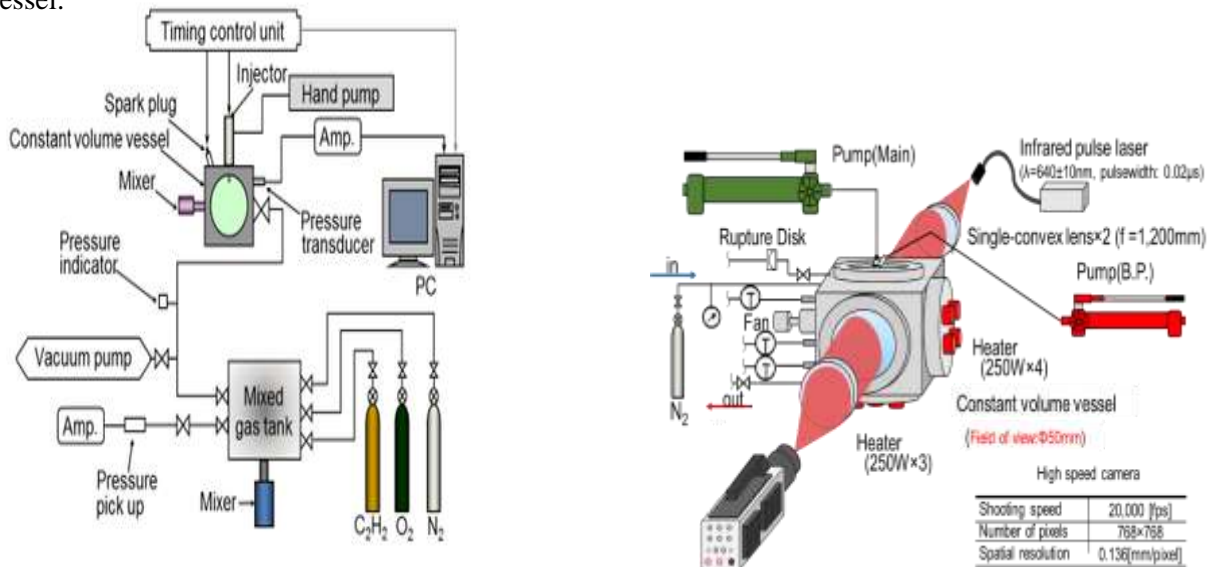


Figure 6.2. Schematic diagram of constant volume vessel. **Figure 6.3.** Optical setup for shadowgraph photography.

Figure 6.3 illustrates a schematic of the spray shadowgraph photography. The image of spray was captured during the injection time and using high-speed camera video phantom with speed 20,000 frames per seconds (fps) and the number of pixels is 768 x768. To create the larger image of spray, the double convex lens ($f = 1.200$ mm) was used and a metal halide lamp was used to compile the visualization of

spray. All images were further modified by using MATLAB code to measure the spray tip penetration, and spray angle.

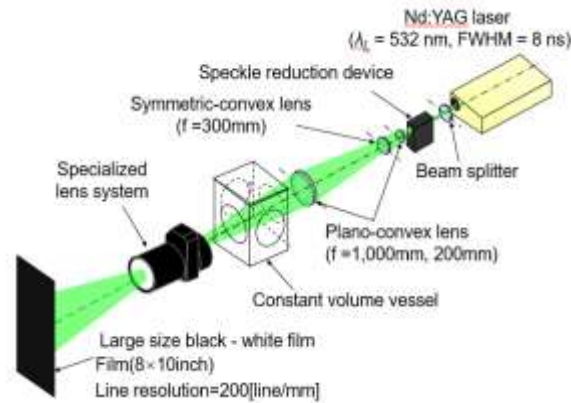


Figure 6.4. Optical set up for super high spatial resolution photography.

Figure 6.4 illustrates of optical set up for super high spatial resolution photography (SHSRP). SHSRP can be used to take a sauter mean diameter (SMD) experiment. The light sources are coming from the YAG laser (Spectra-Physics: PIV400), that is, the wavelength of 532 nm, of which the half-width is 8 ns. Two sheets of the plano-convex lens were used to apply focus to the optical system, and collimate the distorted ray of light. The camera was used to capture the pictures and all the pictures were captured by large size black film (Kodak: TMAX100) with a size of 8 x 10 inch, and with the line resolution from 63 to 200 line/mm.

6.4. Non-evaporating Spray from *Jatropha Methyl Ester (JME)* and its blends

6.4.1. Fuel Properties

The fuel properties of jatropha methyl ester and its blends with n-tridecane are already discussed clearly in chapter 5. Therefore, the summary of fuel property is given in the table 6.1.

Table 6.1. The fuel properties

Mixing Rate (JME : n-tridecane)		25:75	50:50	75:25	100:0
Density (15°C)	[kg/m ³]	788	824	850	876 [5]
Kinematic viscosity (40°)	[mm ² /s]	2.10	2.75	3.40	4.8 [5]
Flash Point	[°C]	101	105	115	170 [5]
Surface tension	[mN/m]	25.5	26.5	28.0	31.1 [6]
Cetane number	[-]	81.2	69.0	64.2	-

As can be seen in Table 6.1, JME 100 has the highest in density, kinematic viscosity, flash point and surface tension. Therefore, to improve the fuel properties in JME100, blending between n-tridecane 25%, 50%, and 75% can make better results in fuel properties as can be seen in Table 6.1.

6.4.2. Experimental Conditions

In this study, the experimental conditions can be shown in Table 6.2.

Table 6.2. The experimental conditions in non-evaporating spray

Test Fuel	n-tridecane, JME100	JME25, JME50, JME75
Ambient Gas	N ₂	
Ambient Temperature [K]	Room temperature	
Ambient Pressure Pa[MPa]	1.50	
Ambient Density ρ_a [kg/m ³]	18.75	
Injection Pressure P _{inj} [MPa]	50, 100, 150	100
Injection Amount M _{inj} [mg]	5.7	
Nozzle Type	G3P (Single hole)	
Hole Diameter d _h [mm]	0.123	

In this study, the chosen of injection pressures of 50, 100, and 150 MPa because the fuel injection pressure usually in the ranged of 20 to 170 MPa and it depends on the engine size and type of combustion system employed [10]. Therefore, the injection pressure of 50, 100 and 150 MPa are in the between the ranged of the injection pressure typically used.

6.4.3 Results and discussions

Figure 6.5 demonstrates the spray image for each fuel taken by shadowgraph photography. As can be seen in the figure, the spray of JME 100 region spread extensively. As the mixing ratio of n-tridecane increases, the region seems to be diluted and the dispersion of spray increases. From the pictures, it can be understandable that the vapors are diluted in the downstream region of the mixed spray. This happens due to mix with low boiling point (tridecane), thus can make advanced in the atomization and the evaporation of the spray.

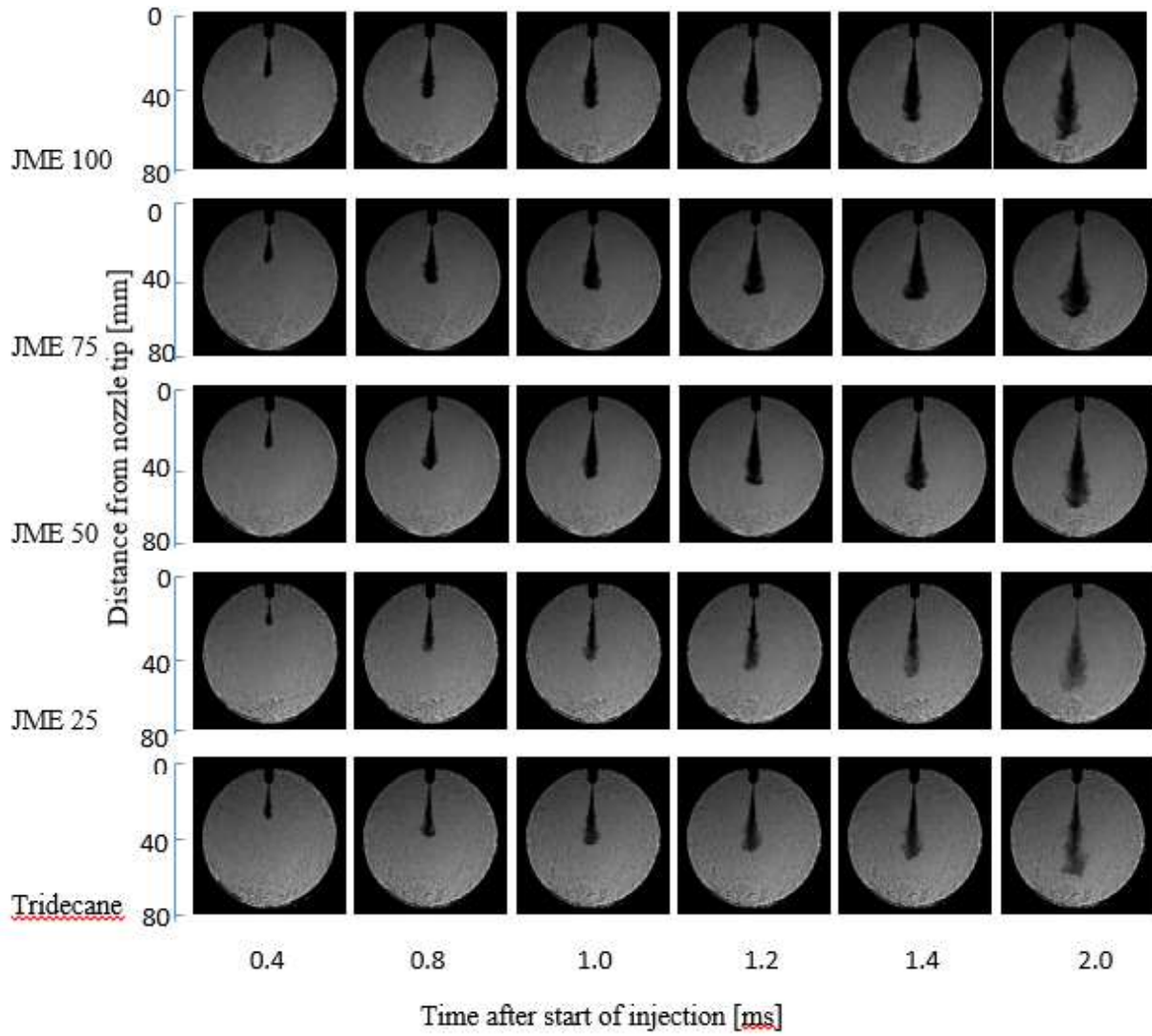


Figure 6.5. Shadowgraph images at different time at $P_{inj} = 100$ MPa

6.4.3.1. Spray Tip Penetration

The prediction and correlations of spray penetration (S) have been studied from many years. The formula developed by Dent [18] as follow:

$$S = 3.07 \left(\frac{\Delta p}{\rho a} \right)^{1/4} (t d_n)^{1/2} \left(\frac{294}{T_g} \right)^{1/4} \quad (1)$$

Where Δp is the pressure drop across the nozzle, t is time after the start of injection and d_n is the nozzle diameter.

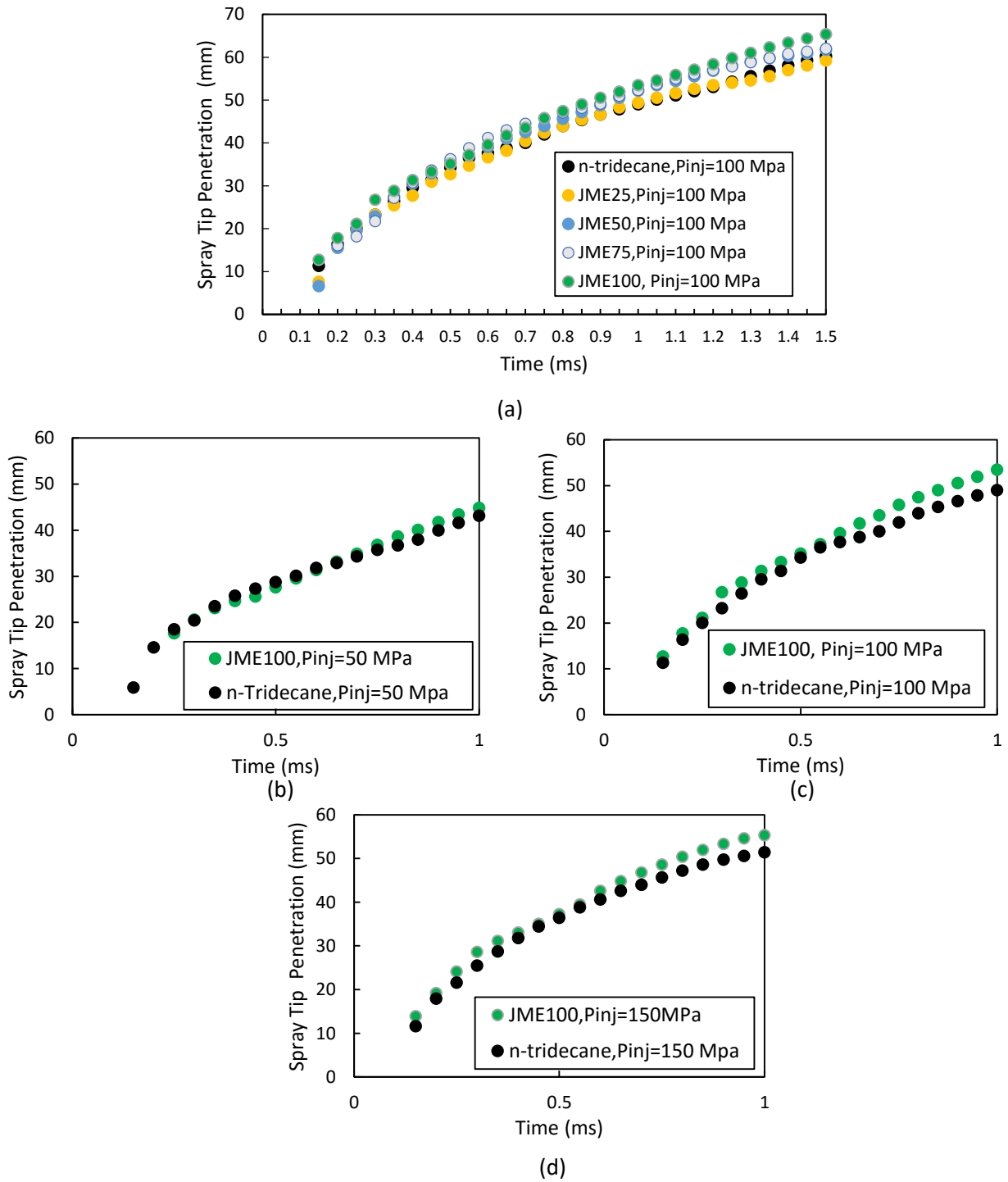


Figure 6.6 Spray Tip Penetration in Non-evaporating (a) All fuels at $P_{inj} = 100$ MPa; (b) JME100 and tridecane at $P_{inj} = 50$ MPa; (c) JME100 and tridecane at $P_{inj} = 100$ MPa; (d) JME100 and tridecane at $P_{inj} = 150$ MPa.

Spray tip penetration for JME25, JME50, JME100, and tridecane with injection pressure at 100 MPa are shown in Figure 6.6 (a) – (d). From Figure 6.5 (a) it can be confirmed that with the percentage of n-tridecane increasing, the spray tip penetration decreased. This is because the spray tip penetration is influenced by fuel density, viscosity, and surface tension. JME100 has higher viscosity, density and surface tension, hence, spray tip penetration is the highest as compared to other fuels. Spray tip penetration of JME75 is higher than JME50 and JME25. This is because that JME75 has higher density, viscosity, and surface tension as compared to JME50 and JME25. Figure 6.6 (b) – (d) show the spray tip penetration by JME100 and n-tridecane with different injection pressure at 50, 100, and 150 MPa. As can be seen that with the increased of injection pressure, the spray tip penetration increased.

The speed and extent to which the fuel spray penetrates across the combustion chamber has an important influence on air utilization and fuel-air mixing rates. Some engine design, where the walls are hot and high air swirl is present, fuel impingement wall is desired. Nevertheless, in multi spray DI diesel combustion system, over penetration gives impingement of liquid fuel on cool surfaces which usually with little or no air swirl, lowers mixing rates and increases unburned emissions [10].

6.4.3.2. Spray Angle

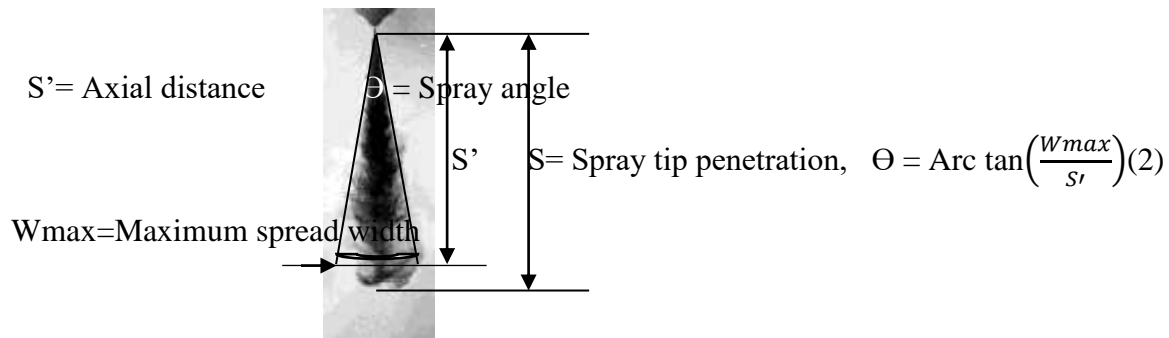
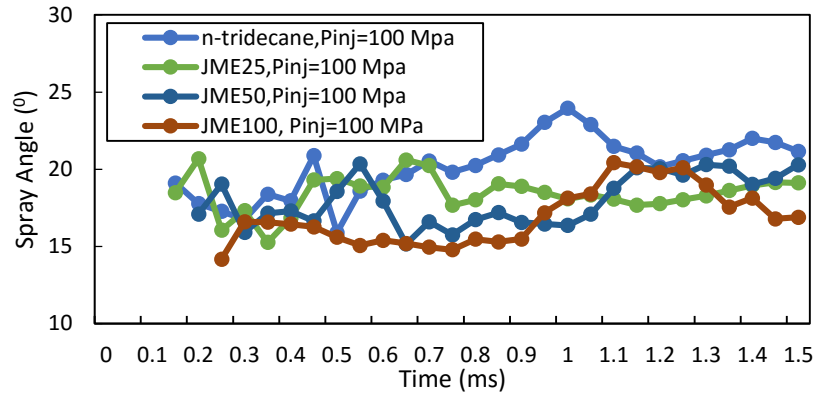
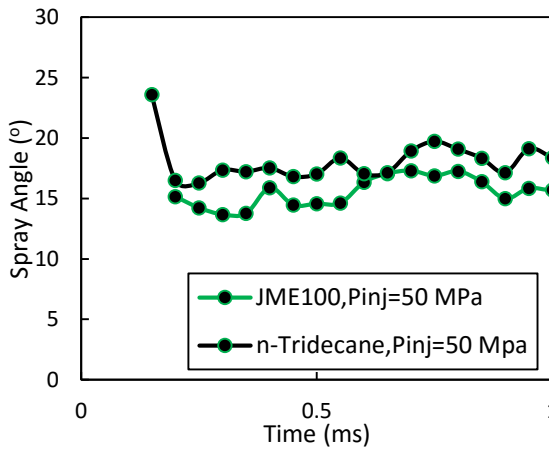


Figure 6.7 .Parameters of spray characteristics

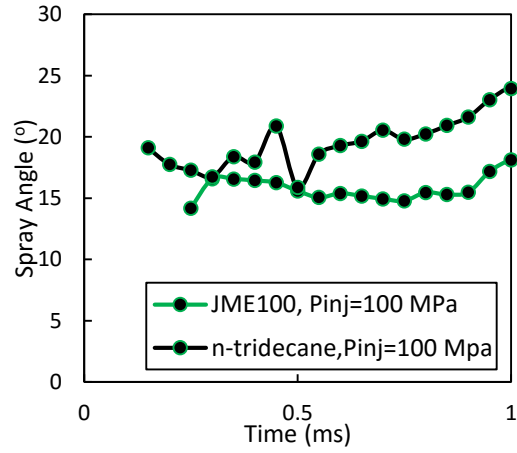
Figure 6.7 shows the figure of spray tip penetration and spray cone angle. Spray tip penetration is the length between the exits of the injector and the spray tip [7]. Spray angle is the angle between two lines connects the ejected tip that related to large scale vortex structure at the spray peripheral region [8].



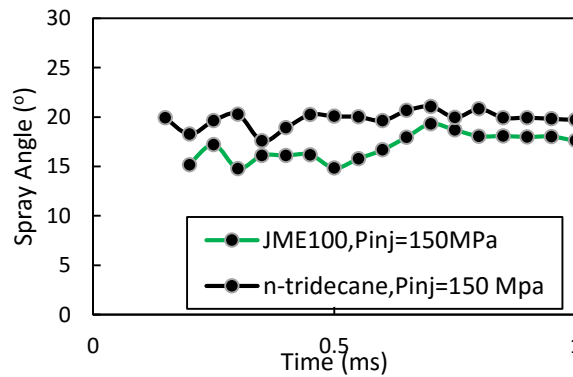
(a)



(b)



(c)



(d)

Figure 6.8. Spray Cone Angle in Non-evaporating (a) All fuels at $P_{inj} = 100$ MPa; (b) JME100 and tridecane at $P_{inj} = 50$ MPa; (c) JME100 and tridecane at $P_{inj} = 100$ MPa; (d) JME100 and tridecane at $P_{inj} = 150$ MPa.

Figure 6.8 shows the spray angle of JME is smaller than n-tridecane. The viscosity of JME100 is higher than n-tridecane, thus it was more difficult to atomize the blends. Therefore, the extension in the horizontal direction was hampered, causing a decrease in the spray angle.

6.4.3.3. Sauter Mean Diameter (SMD)

The Sauter Mean Diameter is explained as the diameter of the sphere which has the same volume and surface area ratio from the small particle [9]. In the combustion process, the distribution of fuel via spray throughout the combustion chamber is important, atomization of the liquid fuel spray depends on injection parameter, air and fuel properties [10]. SMD can be represented the quality of the spray atomization and it related to affect the emission and fuel ignition in the engine [11]. In the case of spray combustion or fuel evaporation, a small fuel droplet is more easily to evaporate as compared with a large droplet. A large droplet takes more time to evaporate because the volume of sphere droplet is greater than a small droplet [11]. Hence, the mean diameter droplets can be indicated as diameter, the number of droplets, and surface of the spray droplets [12]. The measuring of the droplet size can be given as follow [12],

$$\text{SMD} (d_{32}) = \frac{\sum x_i^3 \Delta n_i}{\sum x_i^2 \Delta n_i} \quad (3)$$

Where x_i is the droplet diameter and n_i is the number of droplets in a parcel. The Sauter mean diameter is the diameter of the droplet that has the same surface/volume ratio as that of the total spray.

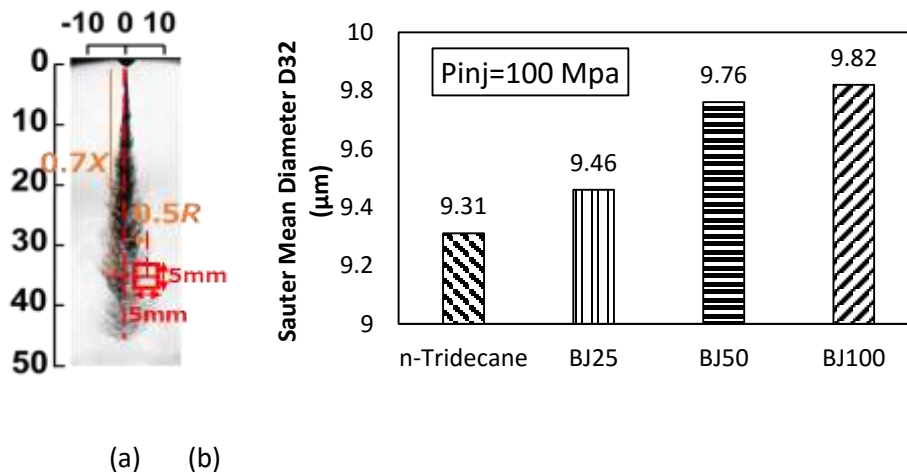


Figure 6.9. (a) Analysis Region; (b) Sauter Mean Diameter (µm) at T= 293 K, Pinj = 100 MPa, Pa = 1.58 MPa, $\rho_a = 18.75 \text{ kg/m}^3$, $t/t_{inj} = 0.5$

Figure 6.9 (a) shows the analysis region for SMD. The analysis area was analyzed with a representative area of 5 mm on a side centered at 0.7 times the spray tip arrival distance X and 0.5 times the radial length R in the spray radial direction. From Figure 6.9 (b), it can be seen that the average particle diameter of SMD increased with the higher percentage of JME. This because of higher percentage of JME makes higher viscosity, density and surface tension. Higher viscosity in the fuel makes difficult to atomize, hence, the SMD is larger than lower percentage of JME.

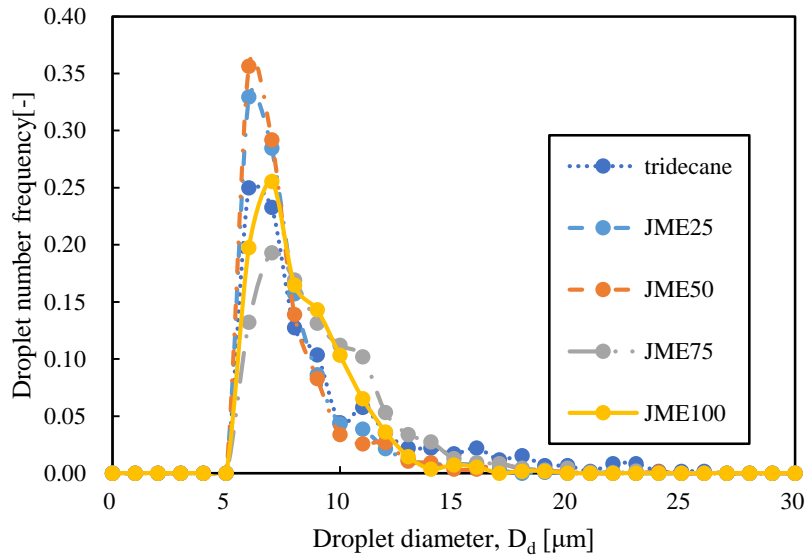


Figure 6.10. Droplet number frequency from JME blends at $T= 293$ K, $P_{inj} = 100$ MPa, $P_a = 1.58$ MPa, $\rho_a = 18.75$ kg/m³, $t/t_{inj} = 0.5$.

During the injection period, the injection conditions such as injection pressure, orifice area, and injection rate may vary. Consequently, the droplet size distribution at a given location in the spray may also change with time during the injection period [10]. In addition, since the details of the atomization process are different in the spray core and at the spray edge, and the trajectories of individual drops depend on their size, initial velocity, and location within the spray, the drop size distribution will vary with position within the spray. Non of these variations has yet been adequately quantified [10].

Figure 6.10 shows droplet frequency from JME blends in non-evaporating condition. From Figure 6.10 shows that JME50 has a higher number of frequency for small droplet diameter. JME100 and JME75 have higher droplet diameter ranged 10-11 μm than JME25, JME50, and tridecane. Moreover, the droplet number frequency of tridecane and JME25 are relatively lower than JME50. This because the position within the spray. Moreover, the size and the velocity may affect the droplet size distribution.

6.5 Non-evaporating Spray from Bio-hydro Fined Diesel Oil (BHD) and Biodiesel Fuel (BDF)

6.5.1. Fuel Properties

The fuel properties of bio-hydro fined diesel oil (BHD) and biodiesel fuel (BDF) are already discussed clearly in chapter 5. Therefore, the summary of fuel property is given in the table 6.5.

Table 6.3. Fuel Properties

	Method	BDF	BHD	n-tridecane [14]
Density (15°C) g/cm^3	JIS K 2249	0.8849	0.8358	0.752
Viscosity (40°) mm^2/s	JIS K 2283	4.565	2.925	2.148
Distillation (T50) K	JIS K 2254	627	570	508

As seen in Table 6.3. BDF has higher density, viscosity and distillation than BHD and tridecane. BHD has better fuel properties compared to BDF. This because BHD is second generation oil that use hydro fined process and not using trans-esterification process. BHD properties like the same as diesel oil and have a potential in reduction emission because it is based from waste cooking oil and contain oxygen in the fuel. The oxygen content in the fuel can make better in combustion and emissions.

6.5.2. Experimental Conditions

In this study, the experimental conditions can be shown in Table 6.6.

Table 6.4. The Experimental Conditions

	Non-evaporating
Test fuel	BDF, BHD, and n-tridecane ($\text{C}_{13}\text{H}_{28}$)
Ambient Gas	N_2
Ambient Temperature T_a [K]	293
Ambient Pressure P_a [MPa]	1.58
Ambient density ρ_a [kg/m^3]	18.75
Pressure Injection P_{inj} [MPa]	50, 100, 150
Injection amount Q_{inj} [mg]	5.7
Nozzle type	G3P (Single hole)
Hole diameter d_h [mm]	0.123

6.5.3. Results and Discussions

In this study, the experiment in non-evaporating was conducted in room temperature. Figure 6.11 shows the spray images at non-evaporating in room temperature from different injection pressure of $C_{13}H_{28}$, BHD, and BDF. From figure shows that BHD and BDF give narrower spray angle than $C_{13}H_{28}$ (tridecane), this happened since the increase of injection pressure can affect the spray to expand and can cause the spray angle increased [15].

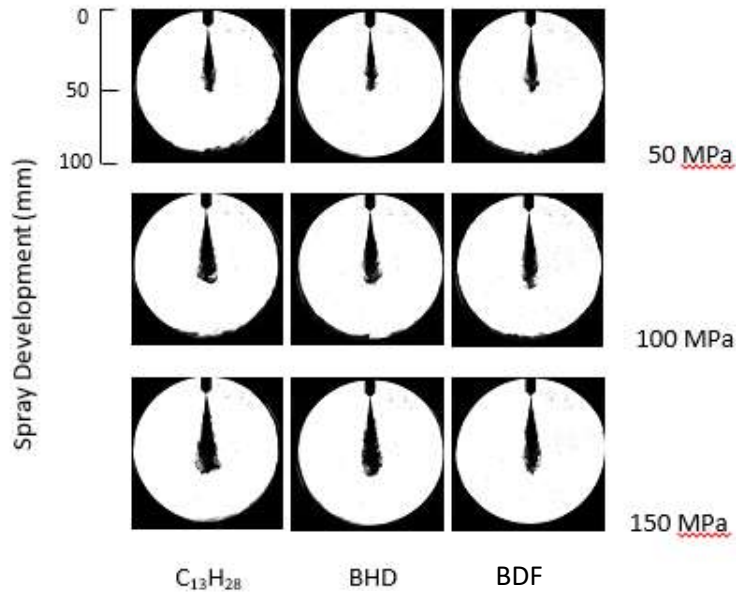


Figure 6.11. The spray evolution process from different fuels with three different injection pressure ($P_{inj} = 50, 100, 150$ MPa, $\rho_a = 18.75$ kg/m³, $T_a = 293$ K) at 1.0 ms after start of injection (ASOI)

6.5.3.1. Spray Characteristics

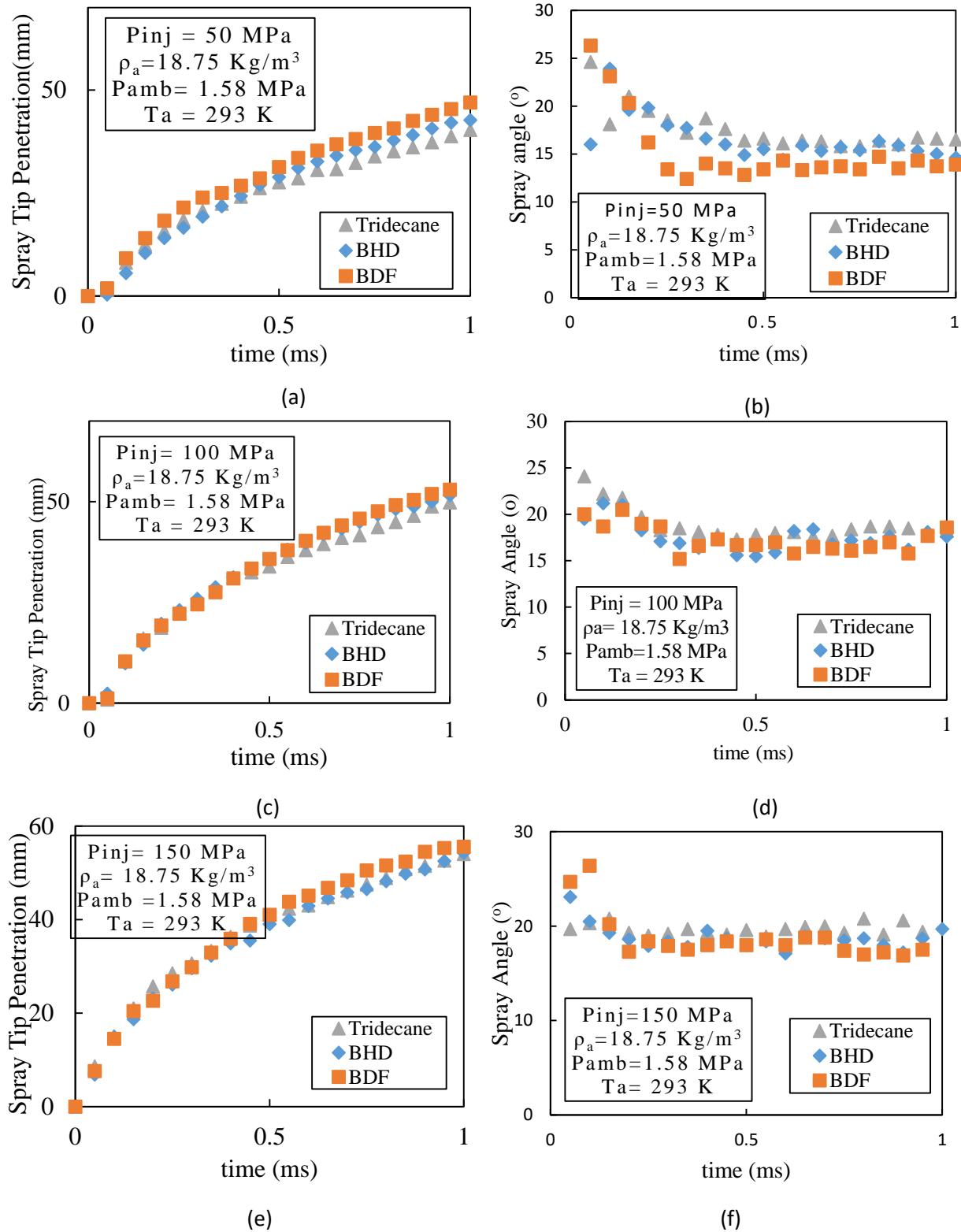


Figure 6.12. Spray tip Penetration and spray angle in non-evaporating condition (a)(b) 50 MPa, (c) (d) 100 MPa, and (e) (f) 150 MPa.

The spray tip penetration from the non-evaporating condition can be seen in Figure. 6.12 (a), (c), and (e). As shown in Figure 6.12 (a), (c), and (e), in general, the spray tip penetration of BDF are slightly larger than BHD and tridecane due to the distillation properties, poor atomization and less momentum exchange between the fuel spray and air [16]. However, it can be seen from Figure 6.12(c) at the condition of $t = 1.0$ ms, and $P_{inj}=100$ MPa, spray tip penetration of WCO is higher 2.64 to 6.03% than BHD and tridecane. The higher viscosity and density in BDF as compared to BHD and tridecane can make difficult for the spray momentum to flow. The spray tip penetration from all fuels is changed by different pressure injections. The increase in pressure injections, the tip penetration of fuels are more likely to increase. This happened probably due to decreasing in the fuel rate caused by higher viscosity [16].

From Figure 6.12 (b), (d), (f) show the spray angle from all fuels in different conditions. As can be seen in Figure 6.12 (b), (d), and (f) that spray angle of BDF have narrower spray angle than BHD and $C_{13}H_{28}$. This happened due to BDF has higher in density, viscosity, and droplet size than BHD and $C_{13}H_{28}$. Higher in density, droplet size, and viscosity can occurs the large momentum, therefore, can cause less in the movement [17].

6.5.3.2. Sauter Mean Diameter (SMD)

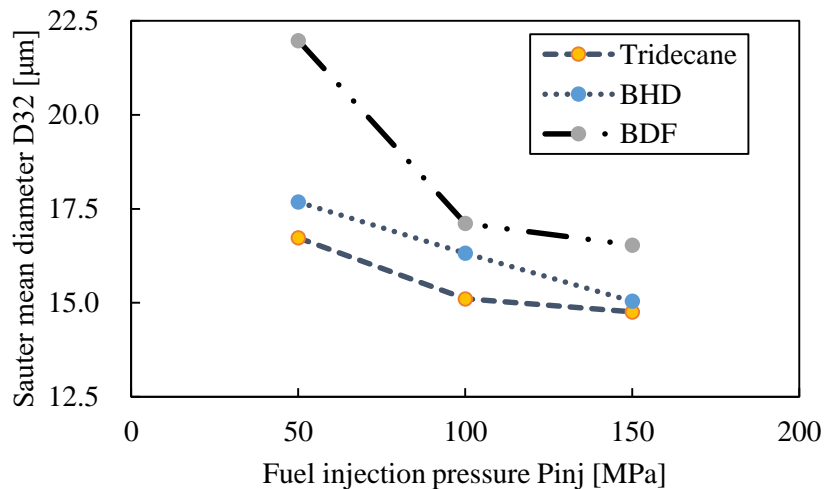


Figure 6.13. SMD with different injection pressure at non-evaporating condition ($P_{inj}=50, 100, 150$ MPa)

A comparison of SMD from Tridecane, BDF and BHD can be seen in Figure 6.13. Figure 6.11 represents that SMD from different injection pressures from various fuels. It can be seen that injection pressure increased, SMD from all fuel are decreased. At $P_{inj}=50$ MPa, SMD of BHD is smaller 19.53 % than BDF, but higher 5.4% than tridecane, whereas, SMD of BDF is

the largest than BHD and tridecane. The figure shows a trend of reduction in SMD for all fuels as the injection pressure increased. As injection pressure increased from 50 to 150 MPa, SMD of BHD, BDF, and tridecane are decreased from 14.91, 24.73, and 11.76 % respectively. Fuel viscosity and surface tension affected by mean droplet size as shown in Fig. 6 (a), with the effects being most significant at lower injection pressures [10].

6.6. Conclusions

The viscosity, density and surface tension have big influences in non-evaporating spray characteristics. High boiling point fuel has high in viscosity, density and surface tension. These fuel properties have negative affected in diesel engine. JME100 and BDF have high spray penetration tip than other fuels. Spray droplets are higher than other fuels. Higher spray droplet can make difficult momentum in the fuel to move. The atomization is difficult and unperfected combustion will appear. Therefore, it is important to mix with low boiling point fuel such as tridecane. The mixing fuel (JME25, JME50 and JME75) have improved the fuel properties compared to JME100. Therefore, the spray characteristics also improved and good atomization in the fuel will occurs.

6.7. References

- [1] Senda, J., Ikeda, M., Yamamoto, M., Kawaguchi, B and Fujimoto, H. 1999. Low Emission Diesel Combustion System by Use of Reformulated Fuel with Liquefied CO₂ and n-Tridecane, *SAE Paper* 1999-01-1136.
- [2] Senda, J., Higaki, T., Sagane, Y., Fujimoto, H., Takagi, Y., and Adachi, M. 2000. Modeling and Measurement on Evaporation Process of Multicomponent Fuel”, *SAE Paper* 2000-01-0280.
- [3] Kamimoto, T., Matsuoka, N., Sugiyama, H., and Aoyagi, H. 1972. Transactions of the Japan Society of Mechanical Engineers, 40, no.339, pp 3206-3215.
- [4] Sibers, L. D. 1985. Ignition delay characteristics of alternative diesel fuels: Implications on cetane number. *SAE Paper* 852102.
- [5] Adebayo, G. B., Ameen, O. M., and Abass, L.T. 2011. Physico-chemical properties of biodiesel produced from jatropha curcas oil and fossil diesel. *J. Microbiol. Biotech. Res*, 1 (1): 12-16.
- [6] Hashimoto, N., Nishida, H., and Ozawa, Y. 2014. Fundamental combustion characteristics of jatropha oil as alternative fuel for gas turbines. *Fuel*, 126, 194-201.

-
- [7] Mo J, Tang C, Li J, Guan L, Huang Z. 2016. Experimental investigation on the effect of n-butanol blending on spray characteristics of soybean biodiesel in common-rail fuel injection system. *Fuel*. 182. 391-401.
- [8] Senda J, Okui N, Suzuki T, Fujimoto H. 2014. Flame structure and combustion characteristics in diesel combustion fueled with bio-diesel. *SAE Technical Paper Series*. 2004-01-0084.
- [9] Wang D, Fan L.S. 2013. Particle characterization and behavior relevant to fluidized bed combustion and gasification system. *Fluidized Bed Technologies for near-zero emission combustion and gasification. Woodhead Publishing Limited, Number 52*. 42-73.
- [10] Heywood J.B. 1988. *Internal combustion engine fundamentals*. McGraw-Hill Series. ISBN 0-07-028637-X.
- [11] Suh H.K, Lee C.S. 2016. A review on atomization and exhaust emissions of a biodiesel-fueled compression ignition engine. *Renewable & Sustainable Energy Reviews*, 58, 1601-1620.
- [12] Lefebvre A.H. 1989. *Atomization and sprays*. New York: Taylor & Francis. ISBN 0-891116-603-3.
- [13] Koji Kitaguchi, Masashi Matsumoto, Tadayoshi Minami, Takao Kawabe, Tadanori Oshida, Shirotsuke Okada, Jiro Chida, . 2012. Prediction of Ultra High Pressure Injection and High Density Field Diesel Spray Characteristics by Experimental Formula and Numerical Calculation (2nd Report). *Atomization symposium*.
- [14] Miyata S, Kuwahara Y, Kobashi Y, Kuwahara K, Matsumura E, Senda J. 2015. Artificial control of diesel spray and flame feature by using dual-component fuel. *JSAE 20159115/ SAE 2015-01-1916*.
- [15] Gao Y, Deng J, Li C, Dang F, Liao Z, Wu Z, Li L. 2009. Experimental study of the spray characteristics of biodiesel based on inedible oil. *Biotechnology Advances*. 27, 616-624.
- [16] Yamaji T, Asaka K, Kobashi Y, Sato S, Suzuki Y. 2015. A comparative analysis of combustion process, performance and exhaust emissions in diesel engine fueled with blends of jatropha oil-diesel fuel and jatropha oil-kerosene. *JSAE 20159797/SAE 2015-32-0797*.
- [17] Bhikuning A, Matsumura E, Senda J. 2018. A review: non-evaporating spray characteristics of biodiesel jatropha and palm oil and its blends. *International Review of Mechanical Engineering*. Vol 12,4 ,364-370.
- [18] Dent, J. C. 1971. Basis for the comparison of various experimental methods for studying spray penetration. *SAE Paper 710571, SAE Trans.*, Volume 80.

Chapter 7. Evaporating Characteristics

7.1 Introduction

This chapter discusses the evaporating spray characteristics using the shadowgraph technique. The fuels tested are from jatropha methyl ester (JME25, JME50, and JME75), bio-hydro fined diesel oil (BHD) and biodiesel fuel (BDF).

7.2. Experimental Method

The evaporating characteristics include parameters such as spray-tip penetration, spray cone angle, and droplet size distribution. The design of visualize and fuel spray characteristics in of constant volume vessel is the same as non-evaporating spray which is shown in Figure 6.2. Furthermore, spray shadowgraph photography is used to take the evaporating spray is shown in Figure 6.3. Moreover,super high spatial resolution photography (SHSRP) for SMD calculating is the same as non-evaporating spray which is shown in Figure 6.4.

7.3. Experimental Conditions

Table 7.1. The experimental conditions in all Fuels

Test Fuel	JME25, JME50,JME75, JME100	BHD, BDF, n-tridecane (C ₁₃ H ₂₈)
Ambient Gas	N ₂	CO ₂
Ambient Temperature [K]	573	400,500,600
Ambient Pressure Pa[MPa]	1.50	1.42, 1.77, 2.13
Ambient Density ρ_a [kg/m ³]	18.75	
Injection Pressure P _{inj} [MPa]	100	
Injection Amount M _{inj} [mg]	5.7	
Nozzle Type	G3P (Single hole)	
Hole Diameter d _h [mm]	0.123	

7.4. Results and Discussion

7.4.1 Evaporating Spray from Jatropha Methyl Ester (JME) and its blends

7.4.1.2. Fuel Distillations and Spray Image

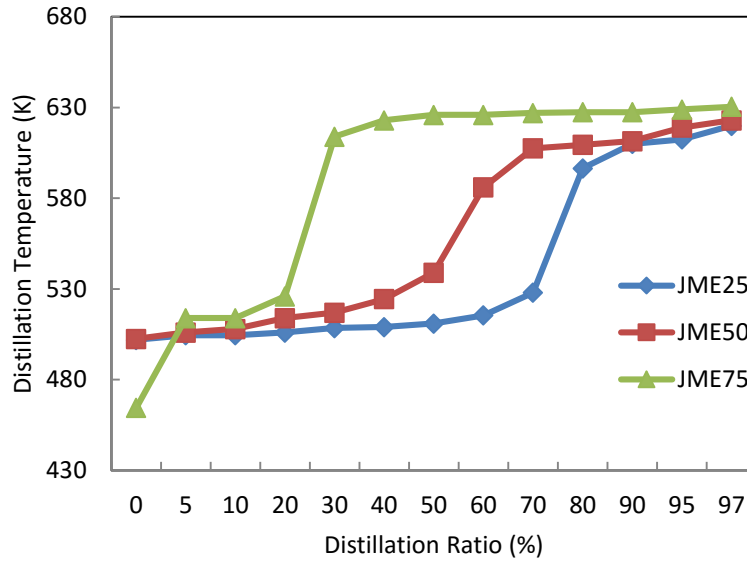


Figure 7.1. Distillation Curves for JME blends

The distillation curves of each fuel are shown in Figure 7.1. As mixing ratio of lower boiling point fuels increases, the distillation curve shifts to lower temperature side. In fact, the fuel vaporizability is improved by mixing higher volatility fuels.

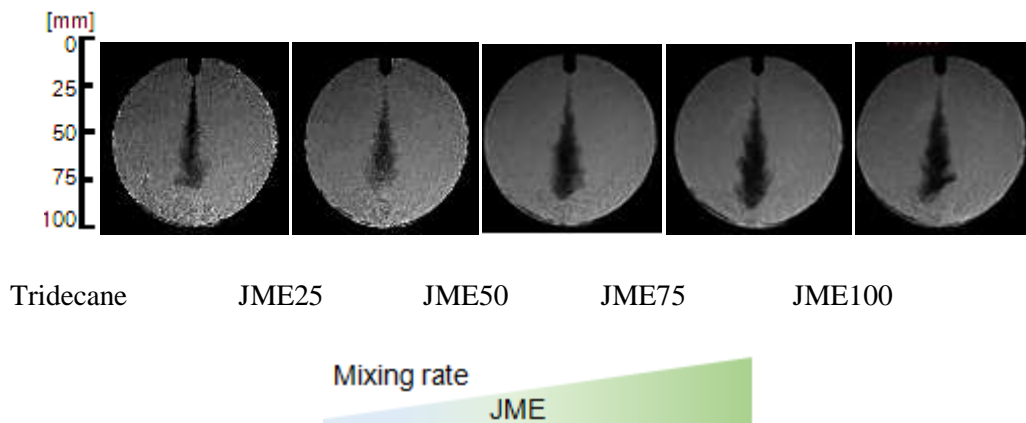


Figure 7.2. Spray Image for Evaporating of JME and its Blends ($t/t_{inj}=1.0$, $T_a=573$ K, $P_a=1.85$ MPa).

The figure 7.2 shows the spray image for each fuel taken by shadowgraph photography. As can be seen in the figure, the spray of JME 100 region spread extensively. As an increase in tridecane mixing ratio, the region seems to be diluted and the dispersion of spray increases. From the pictures describes that the vapors are diluted in the downstream region of the mixed spray. This happens because of mixing by low boiling point (tridecane), makes advanced in the atomization and the evaporation of the spray.

7.4.1.3. Spray Tip Penetration

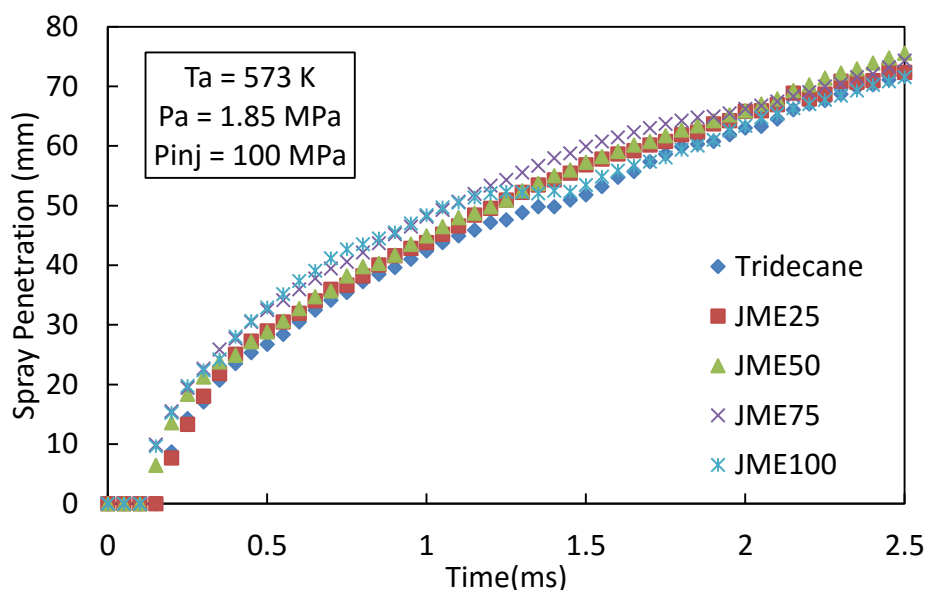


Figure 7.3. Spray Tip Penetration in Evaporating Condition for Various Fuels

Figure 7.3 shows the spray tip penetration in evaporating condition for jatropha methyl ester (JME) and its blends. As seen in Figure 7.1 that JME100 which is true biodiesel from jatropha has the highest spray tip penetrations. JME75 which is has 75% blending with jatropha (75%) and tridecane (25%) is pointed high after JME100. This happened because high boiling point in the fuel makes higher spray penetration. Heavier quality of JME100 disturbs the atomization and the evaporation of spray droplets. Spray droplets of JME100, which has higher density, maintain greater momentum to axial direction. Nevertheless, the mixed fuel sprays penetrate slower.

7.4.1.4. Spray Angle

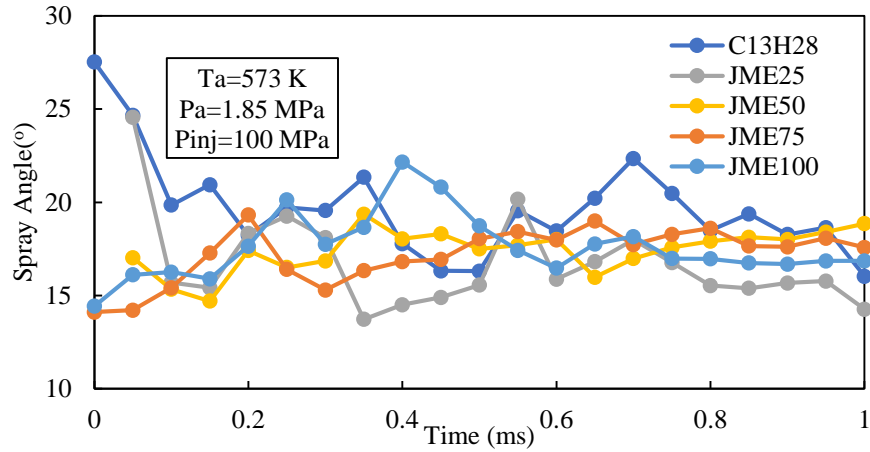


Figure 7.4. Spray Angle in Evaporating Condition for Various Fuels.

Figure 7.4 describes the spray angle of JME and its blends. As seen in Figure 7.3 that the results of spray angle are fluctuates. However, as seen in generally, fuel which higher mix with high boiling fuel has lower spray angle. This happened due to the viscosity in the fuels are improved affected the momentum in fuels to make easier to move. These results are the same as previous results by another researchers [1,2].

7.4.2. Evaporating Spray from Bio-Hydro Fined Diesel (BHD) and Biodiesel Fuel (BDF)

7.4.2.1. Fuel Distillation and Spray Image

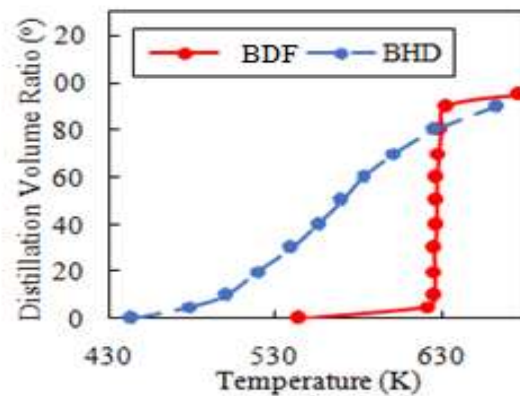


Figure 7.5. Fuel Distillation of BDF and BHD

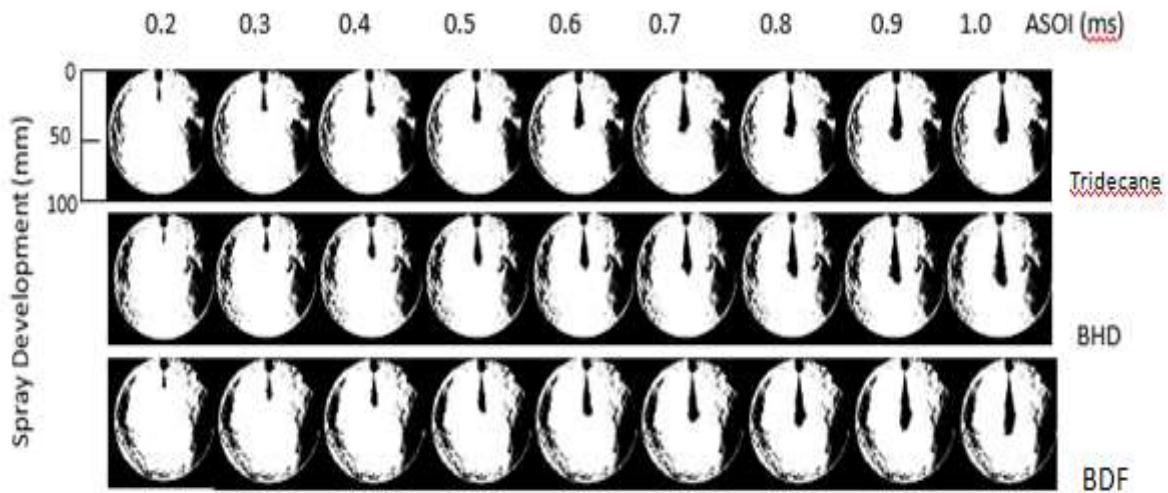


Figure 7.6. Spray Evolution Process at $T_a = 500$ K

Figure 7.5 describes the fuel distillation between BDF and BHD. BDF has a higher boiling point than BHD. It can be indicated that BHD has better spray atomization than BDF. Figure 7.6 shows the spray evolution process from several fuels at evaporating condition (500 K) in different time after the start of injection (ASOI) from 0.2 to 1.0 ms. From Figure 7.6 shows those spray characteristics are developed by the elapsed time. It can be seen that at the beginning of injection start, tip penetration of all fuels seems no differences. However, after time injection increased, BDF has larger tip penetration than BHD and $C_{13}H_{28}$. This tendency happened due to high viscosity and density in BDF can make larger in spray tip penetration and narrower spray angle as compared to BHD and $C_{13}H_{28}$ (tridecane).

7.4.2.2. Spray Characteristics

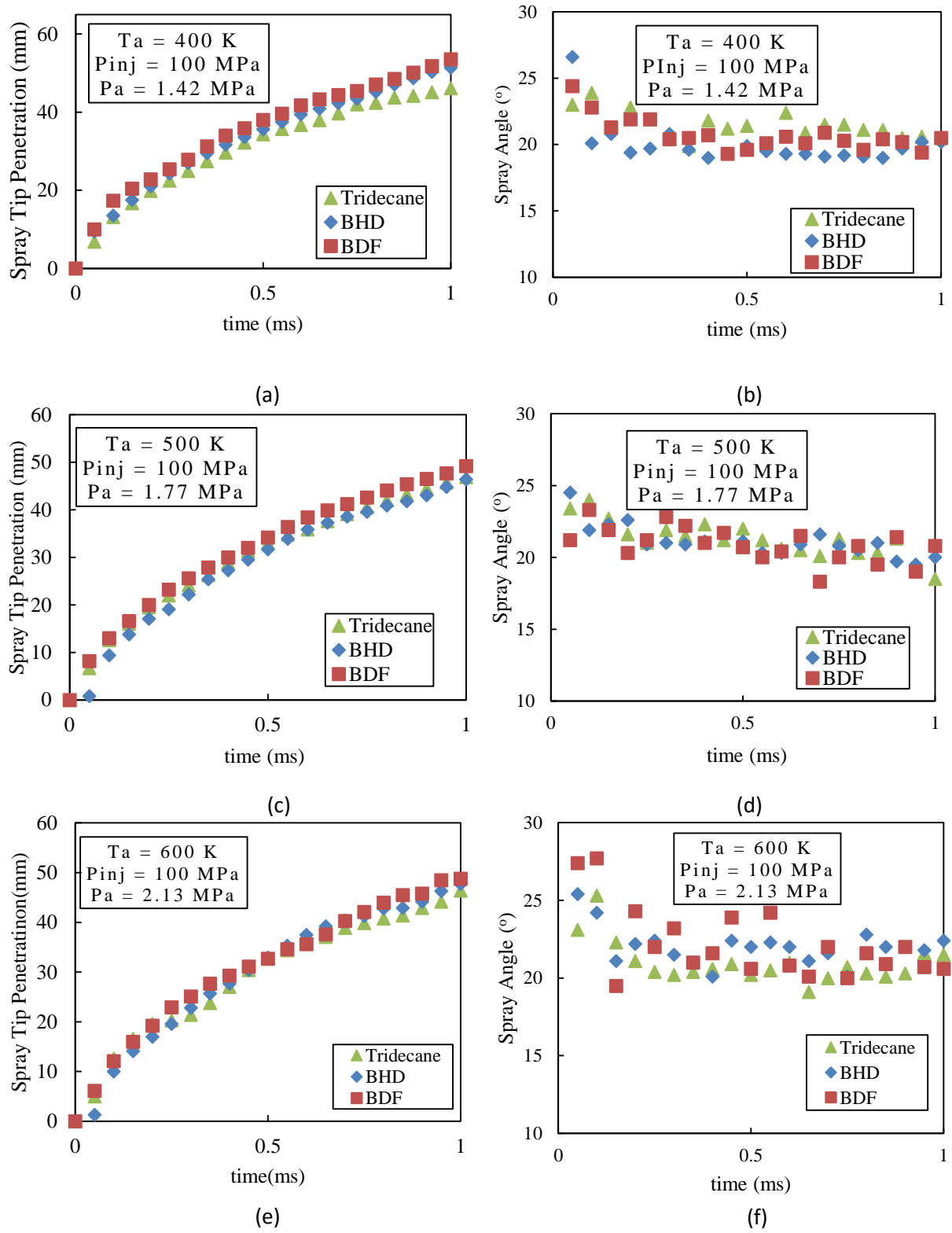


Figure 7.7 Spray Tip Penetration and Spray Angle in Evaporating Condition for Various Fuels

Figure 7.7 (a) – (f) show the spray tip penetration and spray angle in evaporating conditions for various fuels with temperature ambient of 400,500 and 600 K. Figure 7 (a), (c), and (e) show that BDF has higher spray tip penetration than BHD and tridecane. Figure 5 (b), (d), and (f) show the spray angle from various fuels in a different ambient temperature of 400, 500 and 600 K. Figure 5 (c) at ambient temperature 400 K, $t = 1.0$ ms, and $P_{inj} = 100$ MPa shows that spray tip penetration of BDF is higher 3.92 to 13.83% than BHD and C13. The higher spray tip penetration in evaporation condition in BDF occurs because of higher boiling point temperature and distillation of BDF compared to BHD and C13. As the temperature ambient increased (500 to 600 K), the spray tip penetration of BDF has nearly the same as BHD and BDF which is probably due to the same momentum appeared in both of sprays. Moreover, the evaporating conditions can also make narrower the spray angle in the fuel than of the non-evaporating conditions. The micro-explosion can be occurred and can improve spray penetration and deployment [3]. These results of the evaporating spray tip penetration and spray angle are similar with results by previous research [4,5].

7.4.2.3. Sauter Mean Diameter

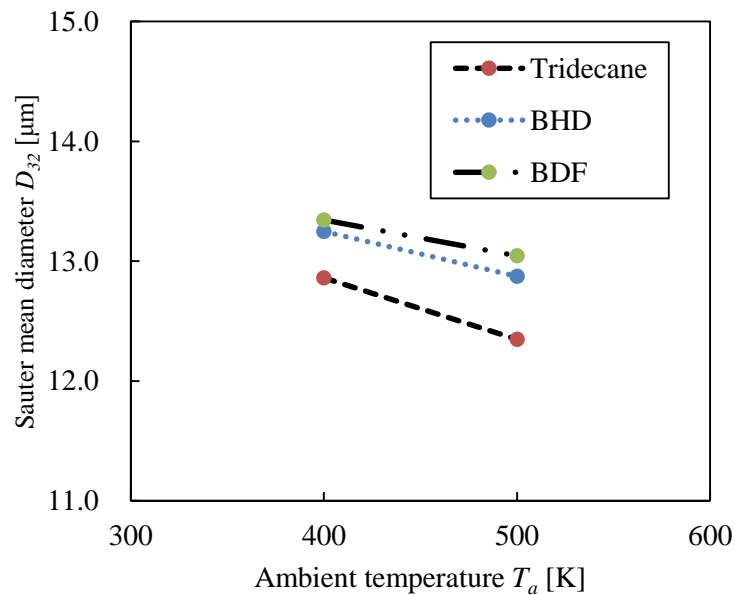


Figure 7.8. Sauter Mean Diameter from Various Fuels ($T_a = 400, 500$ K)

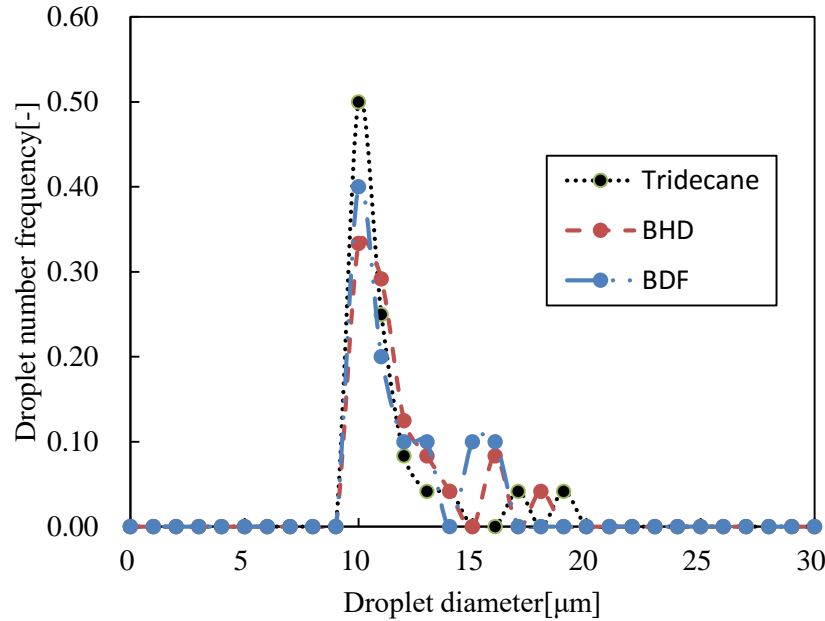


Figure 7.9. Droplet Number Frequency from Various Fuels ($T_a = 500$ K; $P_{inj} = 100$ MPa; $P_a = 1.77$ MPa)

Figure 7.8 describes SMD with different ambient temperatures at 400 and 500 K. From all tendencies, the increased ambient temperature from 400 to 500 K can affect a decreased of SMD from all fuels. From figure shows that SMD of BHD at ambient temperature 400 K to 500 K is reduced up to 2.81%. Also, from the figure is shown that BDF has the highest SMD than BHD and C13. This because of WCO has higher in boiling point and distillation as compared to tridecane and BHD.

Figure 7.9 shows droplet number frequency or SMD distributions from all fuels. It can be seen in that tridecane sprays has a higher number of frequency for small droplets and lower frequency of larger droplets than BHD and BDF. This occurred because tridecane has lower boiling point temperature and distillation than BHD and BDF. In this study, droplet number frequency of BDF is higher than BHD may be occur because the variations of the experimental. The research of SMD versus injection pressures also had similar results by a previous study [6,7].

7.5. Conclusion

The boiling point in fuel properties has a huge impact in the evaporating spray characteristic. The high boiling fuel has disadvantages such as the fuel is difficult to atomize due to high viscosity and density in the fuel. The mixing with low boiling point is one of the best solutions to improve the fuel properties in order to improve the atomization fuel in the engine.

In this study, high boiling fuel (jatropha methyl ester/JME) is mixed with low boiling point fuel (tridecane). As results show that the JME25, JME50 and JME75 have better spray characteristics than JME100. JME 100 has highest viscosity and density, therefore, it has difficulty in atomization because the momentum in the fuel is difficult to move. Higher injection pressures are also has impact in spray evaporating atomization in the fuel. High injection pressure makes good in atomization in the fuel. Moreover, in evaporating condition, the micro-explosion can be occurred and can improve spray penetration and deployment. Therefore, a good atomization in the fuel can be occurred in the engine.

7.6. References

- [1] Li T, Zhang X. Q, Wang B, Guo T, Shi Q, Zheng M. 2017. Characteristics of non-evaporating, evaporating and burning sprays of hydrous ethanol diesel emulsified fuels. *Fuel*. 191, 251- 265.
- [2] Nishida K, Gao J, Manabe T, Zhang Y. 2008. Spray and mixture properties of evaporating fuel spray injected by hole-type direct injection diesel injector. *International Journal of Engine Research*. 9, 347-360.
- [3] Ma Y, Huang S, Huang R, Zhang Y, Xu S. 2016. Spray and evaporation characteristics of n-pentanol-diesel blends in a constant volume chamber. *Energy Conversion and Management*. 130, 240-251.
- [4] Miyata S, Kuwahara Y, Kobashi Y, Kuwahara K, Matsumura E, and Senda J. 2015. Artificial control of diesel spray and flame feature by usimh dual-component fuel. JSAE 20159115/ SAE 2015-01-1916.

[5] Nishida K, Gao J, Manabe T, and Zhang Y. 2008. Spray and mixture properties of evaporating fuel spray injected by hole-type direct injection diesel injector. *International Journal of Engine Research*. 9, 347-360.

[6] Gong Y, You L, and Liang X. 1992. An Investigation on Droplet Size Distribution and Evaporation of Diesel Fuel Sprays at High Injection Pressure by Using Laser Diagnostic Technique. *SAE Technical Paper* 920090.

[7] Li T, Nishida K, Hiroyasu H. 2011. Droplet size distribution and evaporation characteristics of fuel spray by swirl type atomizer. *Fuel*. 90, pp 2367-2376.

Chapter 8. Laser Induced Scattering

8.1. Introduction

In this chapter, laser induced scattering from biodiesel fuels and its blends will be discussed. The fuels tested are from jatropha methyl ester (JME25, JME50, and JME75), bio-hydro fined diesel oil (BHD) and waste cooking oil (BDF).

Laser induced scattering was used to image the liquid phase portion of non-evaporating spray. The liquid length spray is very important to understand because it defined the behavior of the spray in the combustion chamber. The defined of liquid lengths have been proposed from many researchers. The Figure 8.1 shows the definition of liquid length [1].

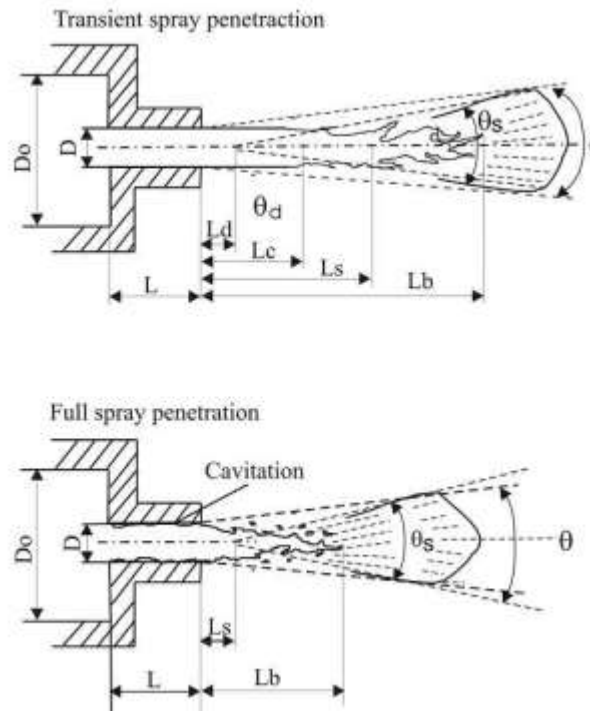


Figure 8.1. The structure of complete and incomplete spray [1]

Hiroyasu & Arai proposed liquid length equation based on the experimental results in complete sprays as follow.

$$L_b = 7d \left(1 + 0,4 \frac{R}{D} \right) \left(\frac{\rho_g}{\rho_l U_o^2} \right)^{0,05} \left(\frac{L}{D} \right)^{0,13} \left(\frac{\rho_l}{\rho_g} \right)^{0,5} \quad (1)$$

In 1983, Bracco[2] also proposed the liquid length equation as follow:

$$L_b = 7,15 \left(\frac{\rho_l}{\rho_g} \right)^{0,5} \quad (2)$$

According from the research in the liquid length, an increase the ratio or percentage in density makes a decreases in a liquid length because the increase of the interaction between spray and the environment [3-5]. Moreover, the relationship between length and nozzle diameter. When the control of volume pressure is high, it also can influence the decrease of liquid length penetration [6,7].

The analysis of the liquid length penetration is useful to determine the geometric design of combustion chambers for high speed regime diesel engines with direct injection. For example, in low speed regime and light load the hydrocarbon emissions will be reduced if the contact of the spray (liquid length) with the combustion chambers wall is avoided. For high speed regimes and heavy loads, the reduction of fumes can be achieved by contact between the spray and the chamber wall. Because of these, the necessity to measure the liquid penetration in diesel engines of direct injection emerges, motivating the use of measure techniques even more complex and sophisticated [8].

8.2. Experimental Method

Figure 8.2 shows a schematic diagram of the optical system for sheet scattered photography. The sheet scattered light was photographed at 20000fps with a high-speed video camera by making the second harmonic emitted from the YAG laser (Lee Laser: LDP 100 MQG), wavelength λ : 532 nm) as a light source. Laser light was changed to light sheet by cylindrical lens (Seika Corporation: BZ-60) and irradiate to spray cross section, then the light through another single-convex lens ($f=1,200$ mm) to focus on high speed video camera (Vision Research Inc.: Phantom v2011). The ambient temperature was room temperature, and injection pressures were changed to 50, 100, and 150 Mpa respectively.

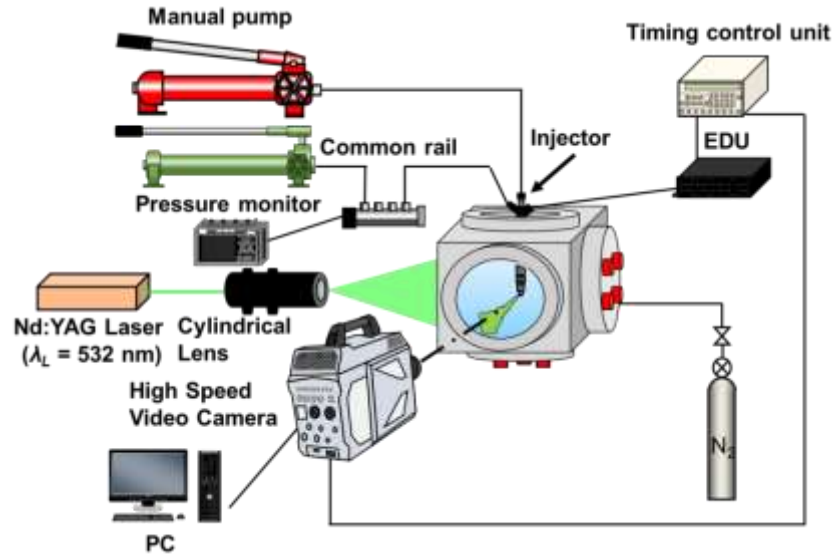


Figure 8.2. Schematic Diagram of Sheet Scattered Photography.

8.3. Experimental Condition

Table 8.1 shows the experimental conditions for LIS. The discussions were divided into two experiments by different injection pressure, there are: first experiment, fuels tested are JME25, JME50 and JME75 in non-evaporating conditions and injection pressure is 100 MPa. Second experiment are BHD, BDF and $C_{13}H_{28}$ with injection pressures are 50, 100, and 150 MPa.

Table 8.1. Experimental Conditions of Laser Induced Scattering (LIS)

		Test 1	Test 2
Test Fuel		JME25, JME50, JME75	BHD, BDF, n-tridecane ($C_{13}H_{28}$)
Ambient gas		N_2	
Ambient temperature	T_a [K]	Room temperature	
Ambient density	ρ_a [kg/m ³]	18.75	
Injection pressure	P_{inj} [MPa]	100	50, 100, 150
Injection quality	Q_{inj} [mg]	5.7	
Nozzle type		G3P (Single hole)	
Hole diameter	d_h [mm]	0.123	

8.4. Result and Discussion

8.4.1. Jatropha Methyl Ester (JME) and its Blends

The photograph of laser sheet scattering can be seen in Figure 8.3. It can be seen in the Figure 8.3 that the spray of JME75 was spread intensively. The spray distance of JME75 is higher than JME25 and JMR50. As the mixing ratio of n-tridecane increases, the region seems to be diluted and the dispersion of spray increases. From the pictures, it can be understandable that the vapors are diluted in the downstream region of the mixed spray. This happens due to mix with low boiling point (tridecane), thus can make advanced in the atomization and the evaporation of the spray.

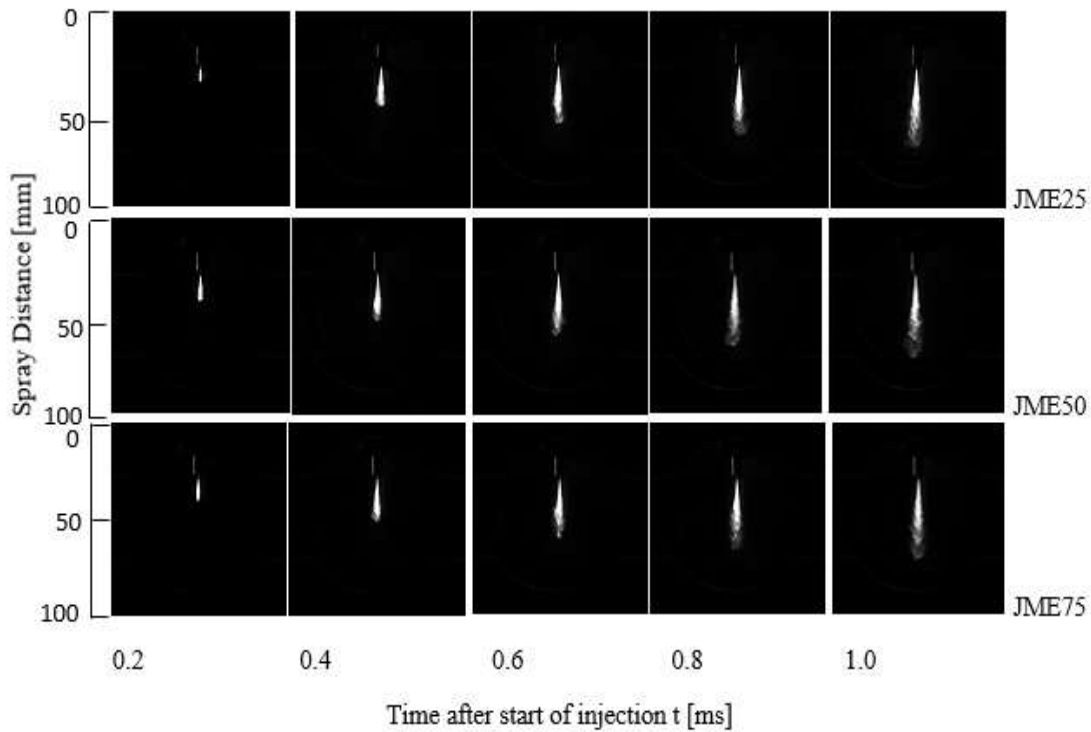


Figure 8.3. Sheet Scattered Photography Images at Different Time ($P_{inj}=100$ MPa)

8.4.1.1. Spray Characteristics

In this study, the spray characteristics are liquid length and spray angle. In this study, the liquid lengths of JME are in the constant of injection pressure. To determine the observations of fuels are from the fuel properties. Liquid phase region is defined as the area of 3% or less of the maximum intensity in each image [9]. Figure 8.4 shows the liquid length penetration from JME25, JME50 and JME75. As can be seen on Figure 8.4, JME75 has higher liquid phase length than JME25 and JME50. This happened that mixing ratio of lower boiling point fuels increases, liquid phase length decreases because early evaporation is promoted in case of the fuel spray.

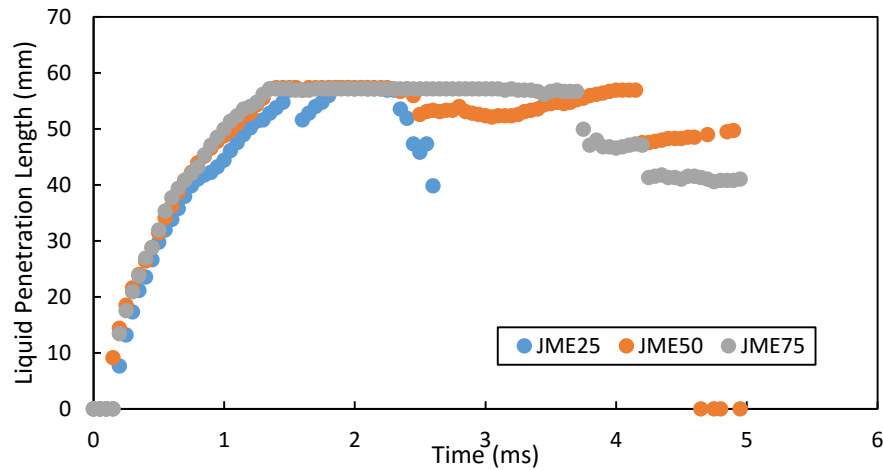
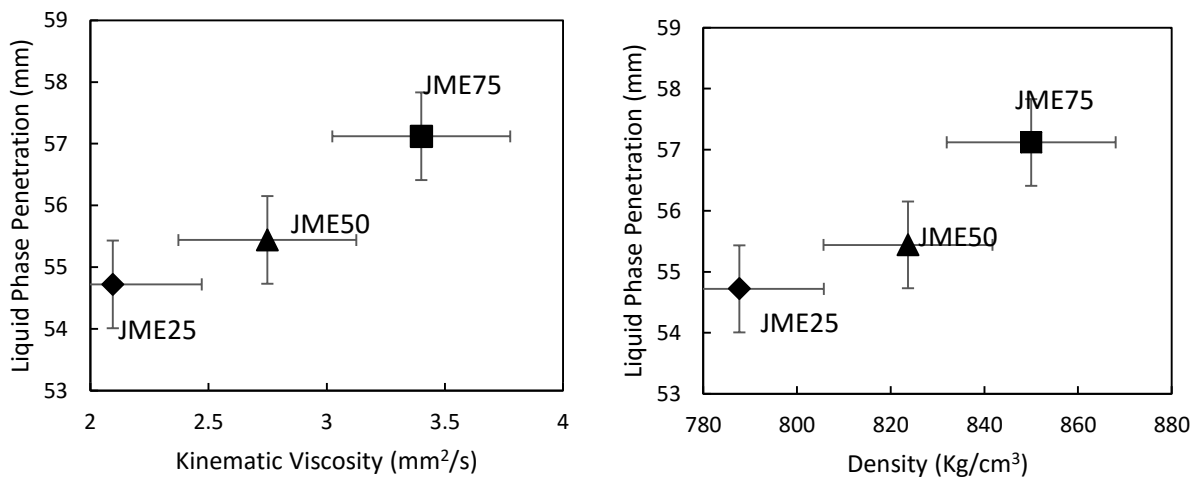


Figure 8.4. Liquid Penetration Length in Various Fuels



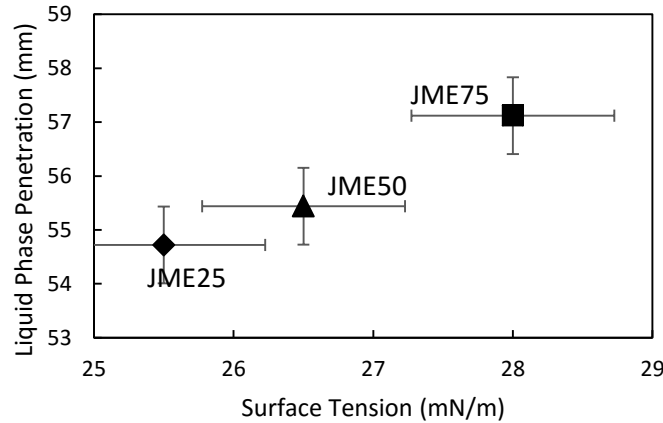


Figure 8.5. Effect of Physical characteristics in Fuel on Liquid Phase Penetration

The effect of physical characteristics with liquid length can be seen in Figure 8.5. The data points plotted in Figure 8.5 represent the median quasi-steady state liquid lengths data. As can be seen in Figure 8.5 that the liquid length of JME75 is higher than JME25 and JME50. Figure 8.5 shows the relationship between liquid length and viscosity. The viscosity effects in the liquid length, higher viscosity in the fuel makes liquid phase penetration increases. The effect of low volatility makes lower in liquid penetration length. Moreover, density and surface tension can also effect in the liquid phase length. Higher density and surface tension makes higher in liquid phase penetration. This also shows a good agreement with previous research by Arai et al. 1984 and Siebers. 1998.

8.4.1.2 Spray Angle (JME25, JME50, and JME75)

In this study, calculating the spray angle in liquid phase is the same as spray penetration length in chapter 6 and 7. Figure 8.6 shows the analyzing of spray angle in liquid phase penetration.

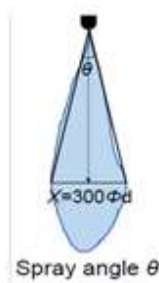


Figure 8.6. Definition of Spray Angle.

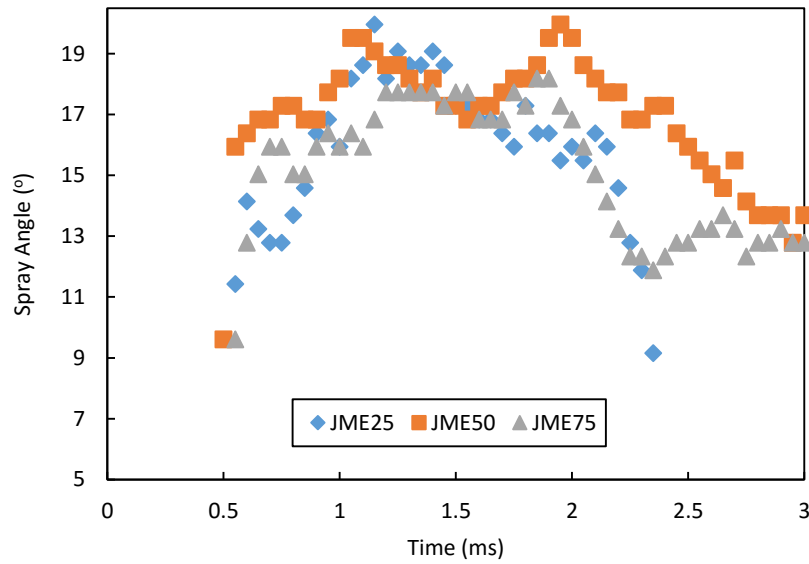


Figure 8.7. Spray Angle in Liquid Phase for Various Fuels

Spray angles in JME25, JME50, and JME75 are shown in Figure 8.7. From Figure shows that spray angles have irregular graphic. Nevertheless, the spray angle in the Figure can conclude that spray angle JME25 has higher than JME50 and JME75. The large value of spray angle happened due to the cavitation effect in the nozzle since the needle lift was small during that time [10]. Moreover, another possibility that at the beginning of injection, fuel droplets were injected into the quiescent air, which pushed the air in front of the nozzle hole. Therefore, the fuel spray was retarded and pushed in the radial direction [11].

8.4.2. Bio-Hydro Fined Diesel Oil (BHD), Biodiesel Fuel (BDF), Tridecane ($C_{13}H_{28}$)

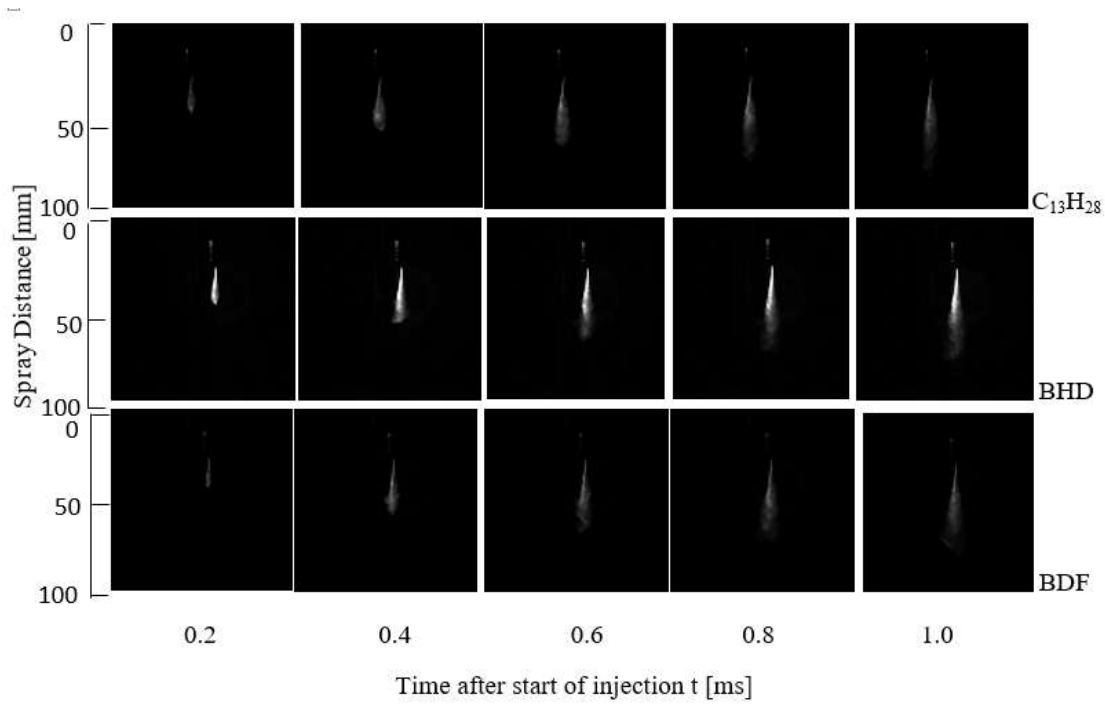


Figure 8.8. Sheet Scattered Photography Images at Different Time ($P_{inj}=100$ MPa)

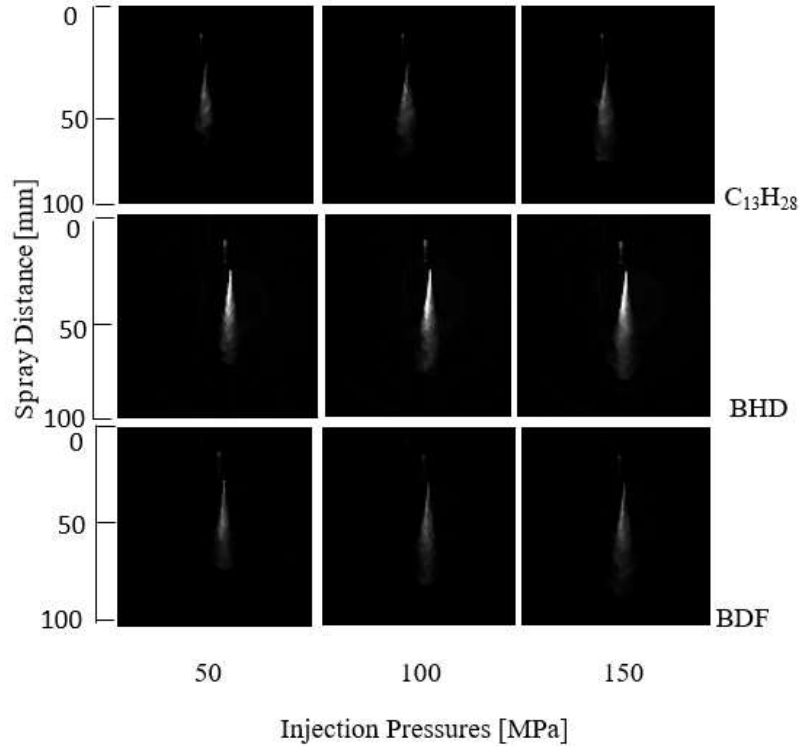


Figure 8.9. Sheet Scattered Photography Images at $t=100$ ms

Figure 8.8 shows the spray development for liquid spray in injection pressure of 100 MPa with different times. As can be seen that sprays are dispersed by following time from nozzle tip. Figure 8.9 shows the sheet scattered photography at $t=100$ ms with different injection pressures. As can be seen that higher injection pressures makes higher in spray development. This happened because of as the injection pressure increased, the spray liquid length can be reacted to reach steady region earlier.

8.4.2.1 Spray Characteristics

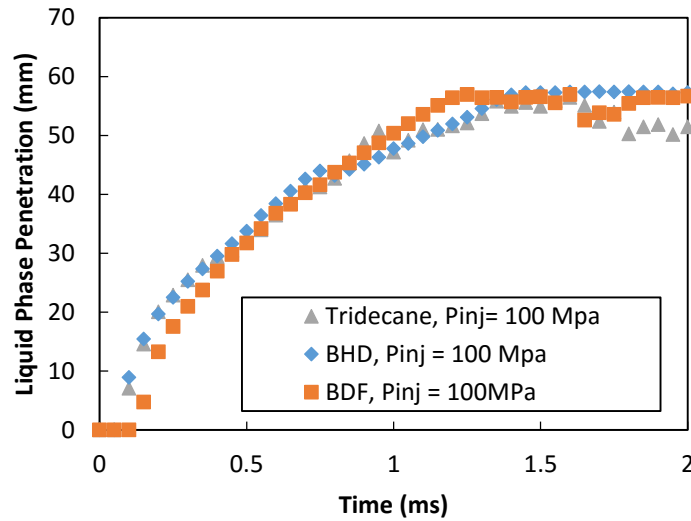


Figure 8.10. Liquid Phase Penetration from Various Fuel at 100 MPa

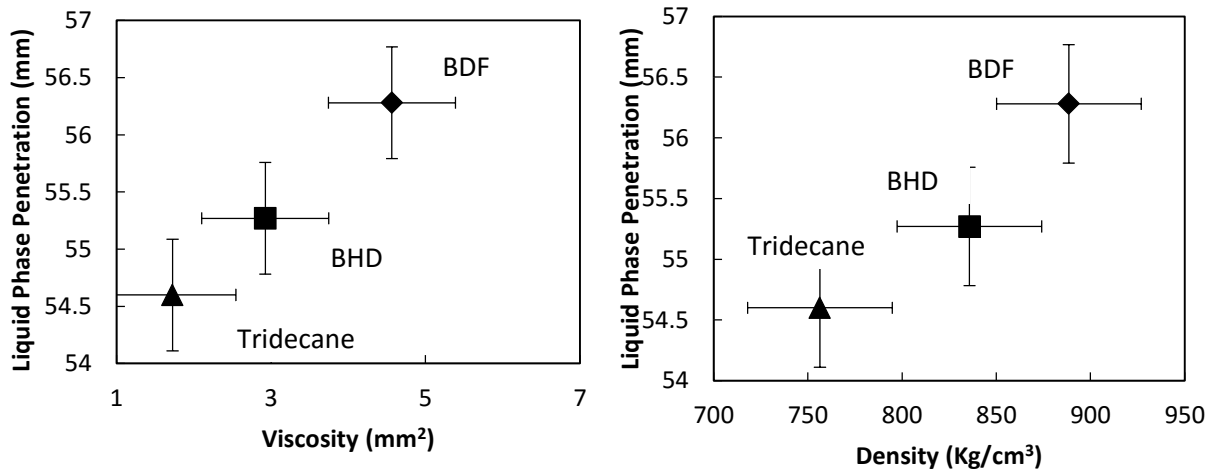


Figure 8.11. Effect of Physical characteristics in Fuel on Liquid Phase Penetration in Various Fuels

Figure 8.10 shows the spray development in liquid phase at injection pressure 100 MPa. As can be seen in Figure that tridecane as high volatility has low liquid length as compared to BHD and BDF. BDF as low volatility has higher in liquid length. The liquid length for these are can be written as tridecane<BHD<BDF. The liquid lengths also effected by fuel properties as viscosity and density. The data points in Figure 8.11 are indicated the average of quasi-steady state liquid lengths data. Figure 8.11 shows the effect of physical characteristics on liquid phase penetration. As can be seen in figure that BDF which is high viscosity and density effect for high liquid lengths. BHD has better in viscosity and density than BDF is pointed in the middle between BDF and tridecane. This can be concluded that low density and viscosity in the fuel makes low in liquid length.

8.4.2.2. Spray Angle (Tridecane, BHD, and BDF)

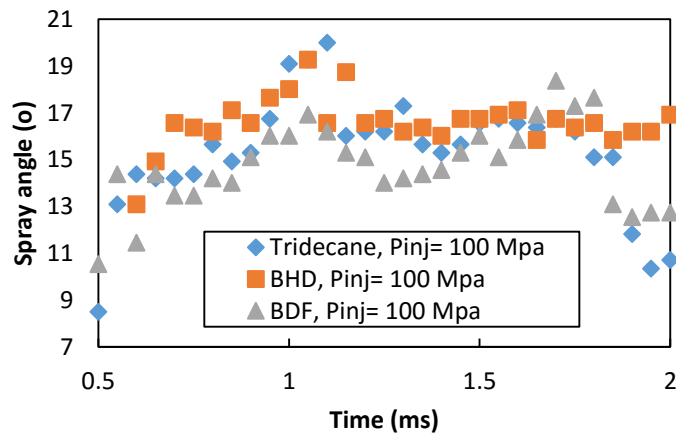


Figure 8.12. Spray Angle in Liquid Phase for Various Fuels

Figure 8.12 shows the spray angle in liquid phase for various fuels. As can be shown that the angles are in irregular positions by times. However, the as can be seen at time =1.1 ms, the spray angle of tridecane is higher than BHD and BDF. Also, Figure 8.13 can be shown as a whole that BDF has the smallest spray angle than other fuels and tridecane has the largest value from among the fuels. This reason might be the same as Figure 8.7 that the large value of spray angle happened due to the cavitation effect in the nozzle since the needle lift was small during that time [10].

8.4.2.3. The Effect of Liquid Length with Different Injection Pressures

In this study, the effect of liquid length with different injection pressures is shown in Figure 8.14. BHD was chosen for the analysis due to a second generation oil that have some benefits such as higher efficiency and reduced the emissions as compared to BDF and JME.

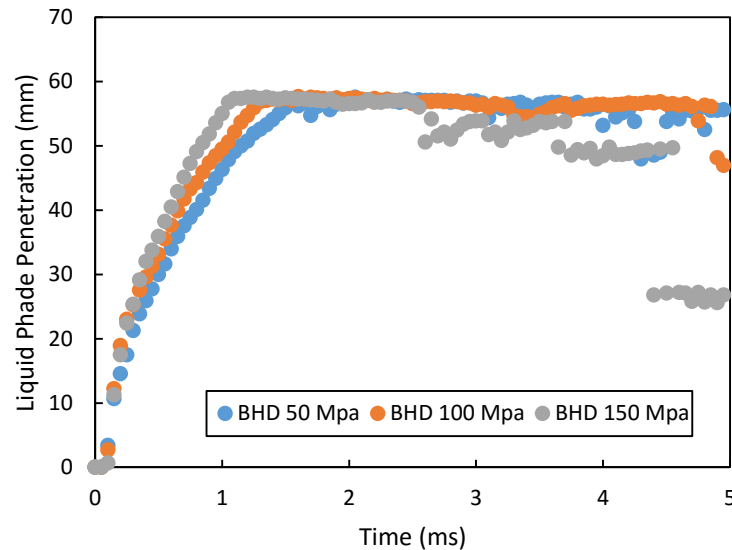


Figure 8.13. Liquid Phase Penetration of BHD in Different Injection Pressures.

As can be shown in Figure 8.13 that higher injection pressures make higher in liquid phase penetration. The liquid length of fuels is almost depends on the injection pressures. BHD with injection pressure of 150 MPa has higher liquid phase than 50 and 100 MPa. Since in the non-evaporating spray stated that higher injection pressures can make improve the evaporation in diesel engine. However, higher injection pressures in liquid phase can effect higher in the liquid phase. However, the longer liquid length affects liquid impingement in diesel engine and also increase the emissions (unburned carbon) due to incomplete combustion occurred. Therefore, this statement shows that the liquid lengths is not much affected by injection pressures. This results have the same agreement from previous research from Johnson et al. 2012.

8.5. Conclusion

In this study, the liquid lengths penetration from JME and its blends, tridecane, BHD, and BDF are discussed. The liquid lengths are influence by the fuel properties. In this study, the experimental condition was in the room temperature which the boiling points of fuels cannot be determined as influences by liquid lengths. As can be seen from the analyzing of liquid phase penetration that liquid length are effected to densities, viscosities and surface tensions in fuels. Higher viscosity, density, and surcafe tension can be effected to produce a higher in liquid length. Moreover, high volatility fuels effect lower in the liquid lengths. This because of an increase in the interaction between spray and the environment. Nevertheless, Injection pressures in liquid lengths haveno effect in diesel engine and it has a good agreement with another research in the past.

8.6. References

- [1] Hiroyasu, H., and Arai, M. 1990. Structures of Fuel Sprays in Diesel Engines. *SAE Technical Paper*, 900475.
- [2] Bracco, F. V. 1983. Structure of High Speed Full Cone Sprays. Recent Advances in Gas Dynamics, Plenum Publishing Corporation, N.Y.
- [3] Arai, M., Tabata, M., Shimizu, M. and Hiroyasu, H. 1984. Disintegrating Process and Spray Characterization of Fuel Jet Injected by a Diesel Nozzle. *SAETechnical Paper*, 840275
- [4] Siebers, D. L. 1998. Liquid-Phase Fuel Penetration in Diesel Sprays. *SAE Technical Paper*, 980809.
- [5] Naber, J. D. andSiebers, D. L. 1996. Effects of Gas Density and Vaporization on Penetration and Dispersion of Diesel Sprays. *SAE Technical Paper* 960034.
- [6] Ha, J., Sato, G. T., Tanabe, H., Fujimoto, H. andKuniyosh,i H. 1983. Investigation on the Initial Part and the Spray Formation Delay of Diesel Spray. *SAE Technical Paper*, 830451.
- [7] Xu, M. and Hiroyasu, H. 1990. Development of a New Optical Technique for Measuring Diesel Spray Penetration. *SAE Technical Paper*, 902077.
- [8] Simon, M. M., Fausto, A.S.C., Vicente, R. B., and Jose, M.R. 2010. *Fuel Injection. Liquid sprays characteristics in diesel engines*. Sciyo Publisher.
- [9]Jiro, S; Tomoki, I; Teruaki, H; Sho, S; Yoshimitsu, W; and Hajime, F. 2007. Spray and combustion characteristics of reformulated biodiesel with mixing of lower boiling point fuel. *SAETechnical Paper*, 2007-01-0621.

[10] Gavaises, M. and Andriotis, A., 2006. Cavitation Inside Multi-hole Injectors for Large Diesel Engines and Its Effect on the Near-nozzle Spray Structure. SAE Technical Paper 2006-01-1114.

[11] Taşkıran, O. O and Metin E. 2011. Experimental study on diesel spray characteristics and autoignition process. *Journal of Combustion* vol. 2011, Article ID 528126, 20 pages.

Chapter 9. Combustion, Emissions and Heat Balance Analysis

9.1. Introduction

Analyzing the combustion and emissions in diesel engines are important to understand. The results will show the differences between the combustion characteristics by using different fuels. The fuels are bio-hydro fined diesel oil (BHD), Biodiesel fuel (BDF) and diesel oil (JIS). Moreover, knowing the results from the emissions are also crucial to comprehend.

BDF is the first generation oil, made from waste cooking oil and produced by using transesterification process which is need a catalyst (KOH or NaOH) to make a biodiesel. Biodiesel from the first generation oil has several disadvantages such as high viscosity and density that can cause operational trouble in diesel engines due to some deposits in the engines. BHD is the second generation oil, made from waste cooking oil and produced by using hydro finning process without esterification. The advantages of BHD oil is that the fuel properties are nearly the same as diesel oil. Therefore, to understand the combustion, emissions and heat balance by using BHD, BDF, and JIS are important to analyze. In this chapter, the combustion, emissions and heat balance in diesel engine will be discussed and analyzed.

9.2. Materials and Method

9.2.1. Materials

The fuel tested are biodiesel fuel (BDF), bio hydro-fined diesel (BHD) and diesel fuel (JIS). BDF and BHD are collected from Revo International- Japan. BDF is biodiesel from waste cooking oil. The fuel properties can be seen in Figure 9.1.

From Table 9.1 shows that the BHD has good caloric value because near to diesel oil JIS No.2. Moreover, second generation oil (BHD) has fuel properties that nearly similar the same as light oil JIS No.2 (JIS). Nevertheless, biodiesel fuel (BDF) has higher in density and viscosity as compared with JIS and BHD, but LHV's value is lower than BHD and JIS. The oxygen contents in BDF is higher (pointed 10.9%) than JIS and BHD. The higher oxygen content in BDF could improve the combustion process and the oxidation potential could decrease. It can be seen also that BHD has oxygen content of 0.4%. Oxidation stability is one of the problems in technical issues because it can affect the quality of the fuel. In biodiesel, the fatty acid chains of Polyunsaturated can affect the oxidation stability in the fuel [1].

Table 9.1. Fuel properties from various fuels.

Properties	Unit	Light Oil JIS No.2	BHD	BDF
Density (15°C)	g/cm ³	0.8352	0.8358	0.885
Viscosity (40°)	mm ² /s	2.7	2.925	4.565
Oxygen Content	%	0	0.4	10.9
Carbon Content	%	86.5	85.89	77.2
Hydrogen Content	%	13.5	12.8	11.9
LHV	MJ/kg	42.88	42	37

9.2.2. Experimental Method

Table 9.2. Engine specifications

Type	Supercharged Direct-Injection Single Cylinder 4 Stroke
Bore [mm]	85 x 96.9
Displacement [cm ³]	550
Compression ratio	16.3
Combustion chamber shape	Re-entrant
Fuel Injection system	Common rail
Number of holes	7
Nozzle diameter [mm]	0.125
Injection angle [deg.]	156
EGR system	Low-pressure loop EGR

In this study, the engine specifications shows in Table 9.2. a single-cylinder direct injection diesel engine with a low pressure EGR system (bore x stroke: ϕ 85 x 96.9 mm, exhaust 550 cc air volume and compression ratio 16.3) was used. Table 2 shows the specifications of the diesel engine, and Figure 1 shows the schematic diagram of experiment. During the experiment the temperature of the cooling water is set to 80 ± 5 ° C, and the air temperature enters to 40 ° C. Also, S / C (Super Chargers), SCV (Swirl Control Valve) rotating is independent of the engine. Low pressure Recirculation Gas EGR (Recirculation System) with Control Valve and DPF (Diesel Particulate Filter) were also used. Gas analyzer is horiba MEXA-1500D and AVL smoke meter is used to determine the filter smoke number (FSN according to ISO 10054) and the soot content in exhaust diesel engine.

Table 9.3. Experimental conditions.

Test fuel	Light Oil JIS#2, BHD, BDF	
Engine Speed [rpm]	2000 rpm	
Pilot injection timing [deg.BTDC]	18.0	
Main injection timing [deg.BTDC]	2.0	
Rail pressure [MPa]	160	
Boost pressure [kPa]	130	
EGR ratio [%]	0 ; 10 ; 20	
Swirl ratio [-]	2.05	
Load	Low load	Partial load
Main injection quantity (mg/str.)	8.4	27.4
Pilot injection quantity (mg/str.)	2.0	2.0
Total injection quantity (mg/str.)	10.4	29.4

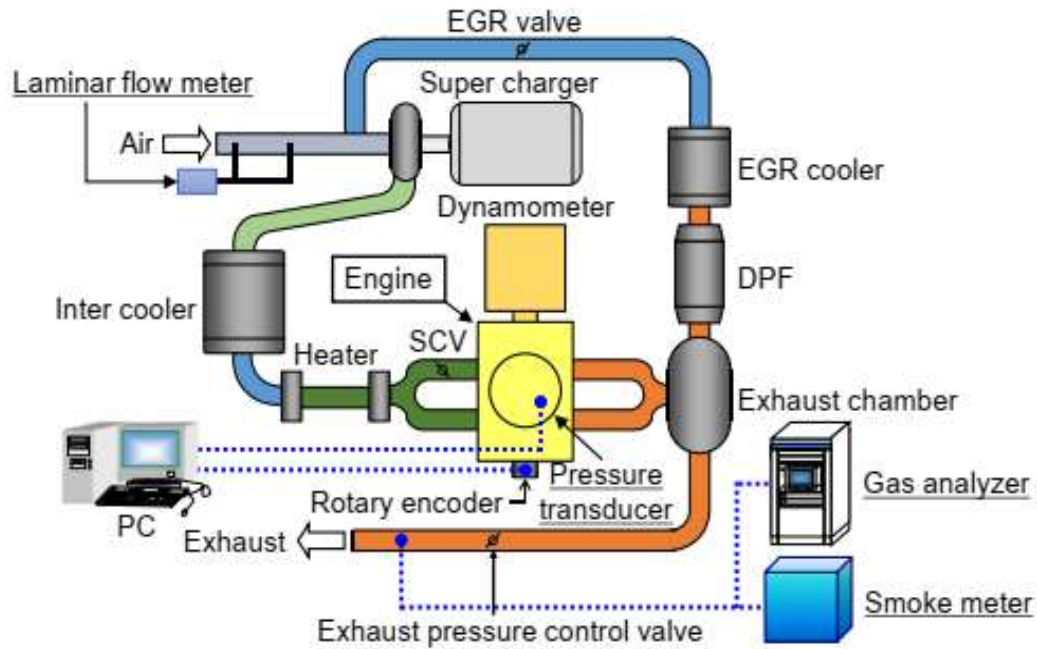


Figure 9.1. Schematic diagram of experiment

In engine test, the fuel consumption is measured as a flow rate mass flow per unit time \dot{m}_f . The parameter is brake specific fuel consumption (BSFC). It measures the efficiency in the engine is using the specific fuel to produce work.

$$\text{BSFC} = \frac{\dot{m}_f}{W_b} \quad (1)$$

Where W_b is brake engine power. \dot{m}_f is the fuel mass flow rate. The specific fuel consumption has units. The ratio of work produced per cycle to the amount of fuel energy supplied per cycle that can be released in the combustion process is commonly used for this purpose [4].

The measure of fuel efficiency is given by,

$$\eta_f = \frac{1}{\text{SFC} Q_{HV}} \quad (2)$$

The fuel energy supplied to the engine per cycle is not fully released as thermal energy in the combustion process because the actual combustion process is incomplete [4].

While torque is a valuable measure of a particular engine's ability to do work, it depends on the engine size. A more useful relative engine performance measure is obtained by dividing the work per cycle by the cylinder volume displaced per cycle [4]. The parameter so obtained has units of force per unit area and is called the mean effective pressure (mep), the equation is shown below.

$$\text{Mep} = \frac{P n_R}{V_d \cdot R} \quad (3)$$

Where n_R is the number of crank revolutions for each power stroke per cylinder. For design calculations, the engine displacement required to provide a given torque or power, at a specified speed, can be estimated by assuming appropriate values for bmep for that particular application.

9.3. Experimental Results

9.3.1. Engine Performances

9.3.1.1. Brake Specific Fuel Consumption (BSFC)

BSFC in variation of loads (low and partial) and EGR (zero, 10, and 20%) is presented in Figure 9.2. From figure shows that BHD and JIS at low and partial loads have lower BSFC than DF. However, BDF has the highest BSFC as compared to JIS and BHD. It is believed that higher BSFC is due to high density, viscosity and also lower calorific value. Adding EGR 20% at low load in BHD, it can increase BSFC up to 2.58% compared to JIS. Moreover, at low load and EGR 20%, BSFC at JIS is 2.93% lower than JIS with EGR 10%. This can conclude that at low load, using EGR 20% can be effective in reducing BSFC. Similar trends of decreasing in BSFC with EGR are also reported by Hawi et al. [2]. They studied that the decrease of BSFC with EGR at low load is due to an increase in intake charge temperature that would affect to increase the combustion rate, causing a decrease in BSFC.

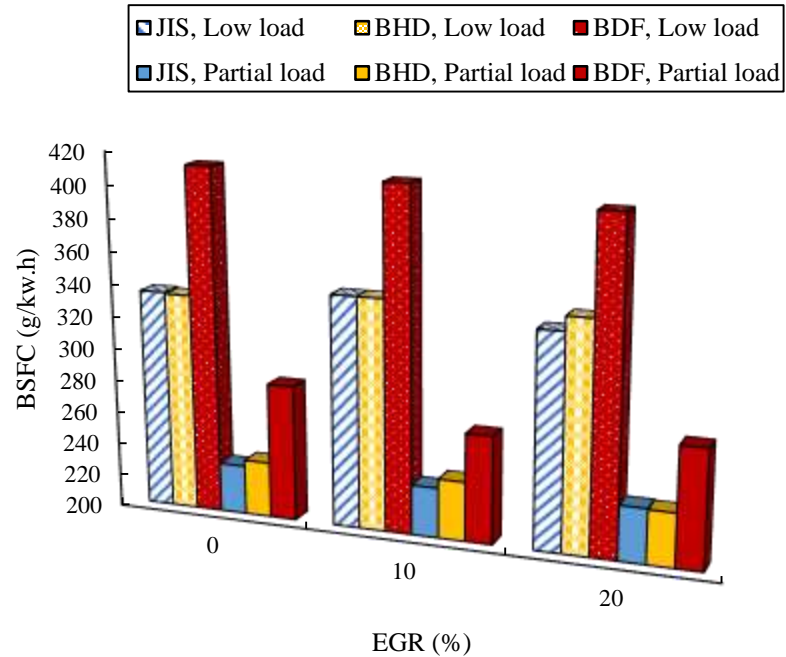


Figure 9.2. Brake specific fuel consumption from various fuels

In partial load and zero EGR conditions, BHD has 1.64% higher than JIS, but lower 17.5% than BDF. At EGR 10%, BHD has 2.39% higher than JIS and 11.16% lower than BDF. Moreover, at EGR 20%, BSFC of BHD is lower 2.28% than JIS and 14.6% lower than BDF.

9.3.1.2. Thermal Efficiency

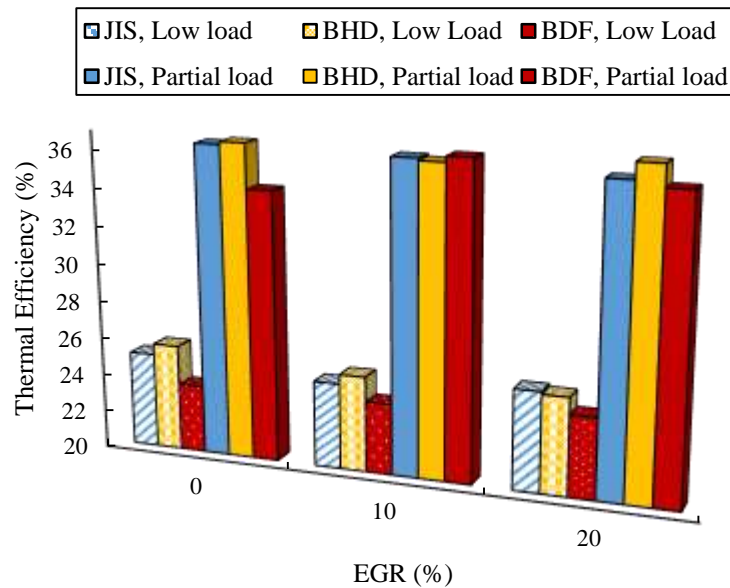


Figure 9.3. Thermal efficiency from various fuels

Thermal efficiency of JIS, BHD and BDF are shown in Figure 9.3. The results show that at low load and partial load with zero EGR, BHD has the highest thermal efficiency compared to JIS and BDF. At low load and zero EGR, thermal efficiency of BHD is increased up to 2.28% - 8.1% than JIS and BDF. The increasing of thermal efficiency due to BHD has oxygen content of 0.4%. The oxygen content in BHD can cause complete combustion that can extend premixed in combustion phase [3]. Moreover, at low load, using EGR 10% can also raise the thermal efficiency of BHD up to 2.08% than JIS and 5.19% than BDF. However, at EGR 20%, thermal efficiency of BHD is slightly reduced to 0.54% than JIS.

At partial load and zero EGR, thermal efficiency of BHD is increased to 0.41% than JIS and raised up to 6.35% compared to BDF. However, the using of EGR in partial load can make lower in thermal efficiency. From Figure 4 it shows that there were tendencies that thermal efficiency of JIS and BDF decreased with added EGR 20%. This happened because of the recirculation of too much exhaust gases and much of air for combustion can cause leading to decrease in thermal efficiency [2].

9.3.1.3. Brake Mean Effective Pressure

Brake mean effective pressures of (BMEP) of JIS, BHD and BDF are shown in Figure 9.4. The results show that from all tendencies, JIS has higher in BMEP compared to BHD and BDF. At low load and zero EGR, BMEP of BHD is higher 2.46% than JIS and 11.86% higher than BDF. Higher BMEP in BHD can cause by having low viscosity in BHD as compare to BDF. Therefore, good spray atomization in the oil and fully mixed air fuel mixture can be achieved. However, BDF has lower BMEP compared to BHD. This is because of BDF has higher in viscosity that would have difficult in atomize.

By changing load from low to partial, BMEP have tendencies to increase. At low load and zero EGR, BMEP in BHD can raised up to 68.24% compare to partial load and zero EGR. This happened because by adding partial load into the engine, therefore, the value of torque is increased and it can make the BMEP changed by loads. At partial load and zero EGR, BMEP of BHD is increased 3.1% than JIS and also higher 10.65% than BDF. At partial load, adding EGR up to 20%, all oils have tendencies to decrease the value of BMEP. This can be concluded that the use of EGR 20% can make BMEP decrease in the diesel engine.

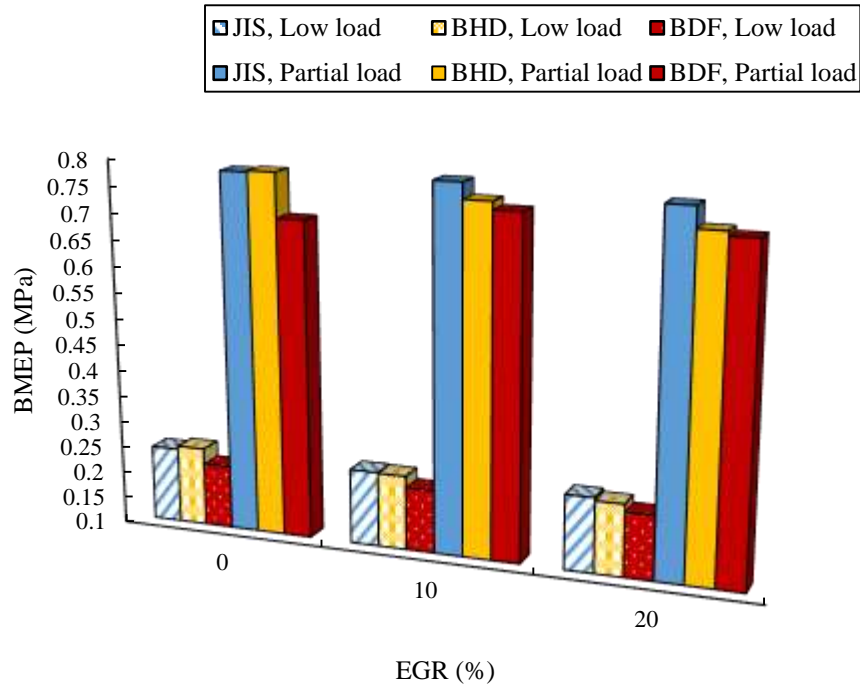


Figure 9.4. Brake mean effective pressures

9.3.2. Emissions Characteristics

9.3.2.1. Carbon monoxide (CO)

Carbon monoxide (CO) emissions from internal combustion engines are controlled by primarily the fuel/air equivalence ratio [4]. CO formation is one of the principal reaction steps in the hydrocarbon combustion mechanism, which can be summarized as [5],



Where R is the hydrocarbon radical. The principal CO oxidation reaction in hydrocarbon-air flame is



CO emissions from JIS, BHD and BDF can be seen in Figure 9.5. In general, at low load, CO emissions have not changes dramatically. At low load and EGR zero, 10, and 20%, CO emission in BHD is the lowest than JIS and BDF. Nevertheless, BDF has the highest CO emissions than JIS and BHD. At low load and zero EGR, CO emissions in BHD is lower 33.12 - 52.45% than JIS and BDF. Moreover, at

EGR 10% CO emissions in BHD was down to 9.54% than EGR zero and at EGR 20% increased to 9.97% than EGR 10%. The increase of CO emission at EGR 20% can reduce oxygen in the combustion chamber and can influence the reaction rates of mixture between air and fuel and affect lower temperature [8]. CO emissions results are came from incomplete combustion and also depend on air fuel ratio [6].

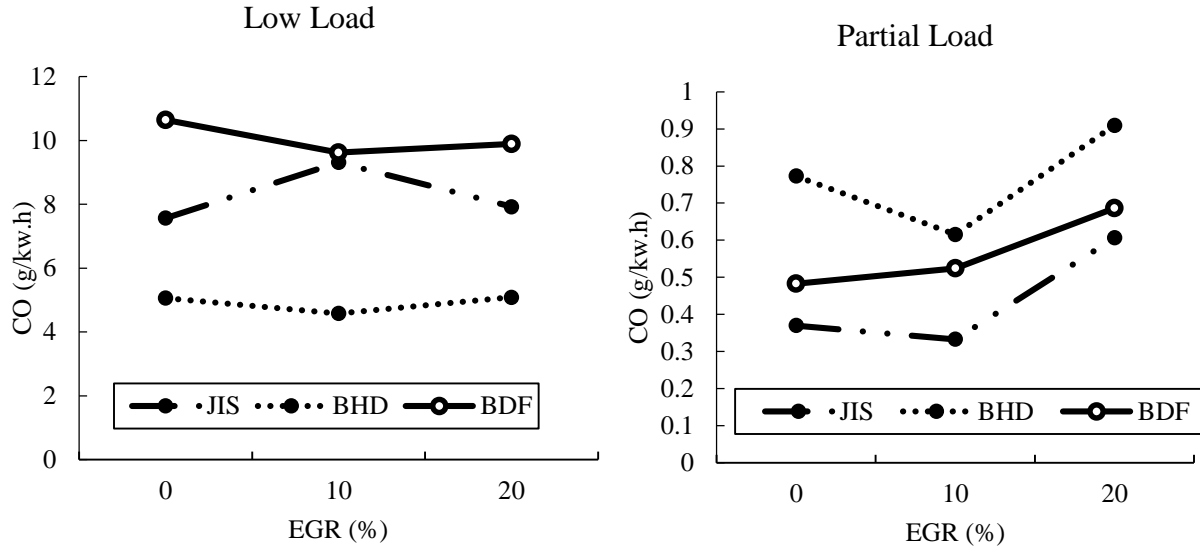


Figure 9.5. CO Emissions in low and partial loads

At partial load, EGR zero, 10, and 20%, CO emissions in JIS, BHD and BDF were increased by adding EGR 20%. In addition, at partial load, CO emissions of BHD are the highest from JIS and BDF. At EGR zero, CO emissions of BHD increased up to 52.19% than JIS. And at EGR 20%, CO emissions of BHD were raised up to 33.37% than JIS. This is because BHD has small content of oxygen (0.4%) that results in lower local oxygen concentration and that could raise the CO emissions [7].

9.3.2.2. Nitrogen oxides (NOx)

NOx emissions from JIS, BHD, and BDF are shown in Figure 6. As can be seen in Figure 9.6, at low and partial load, using EGR can effective to reduce NOx emissions in JIS, BHD and BDF. By adding the lower oxygen exhaust gas into the intake, diesel engine with EGR system can make lower combustion temperature because of the spatial broadening of the flame due to the reduction in the oxygen molar fraction and then reduce NOx emissions [8]. For BHD in low load, using EGR 10 and 20% can reduce NOx emissions ranged from 27.90 to 56.77%. Moreover, using EGR 10 and 20% in BHD at partial load can decrease NOx emissions ranged from 46.78% to 83.07%. For JIS in low load, using EGR 10 and 20% can decrease the NOx emissions from 33.84 to 56.66%. Other than that, using EGR 10 and 20% for JIS at

partial load can reduce the NO_x emissions from 40.29 to 81.92%. For BDF in low load, using EGR 10 and 20% can reduce NO_x emissions from 24.89 to 60.30%. Furthermore, at partial load, adding EGR 10 and 20% can cause the NO_x emissions reduced from 45.34 to 85.43%.

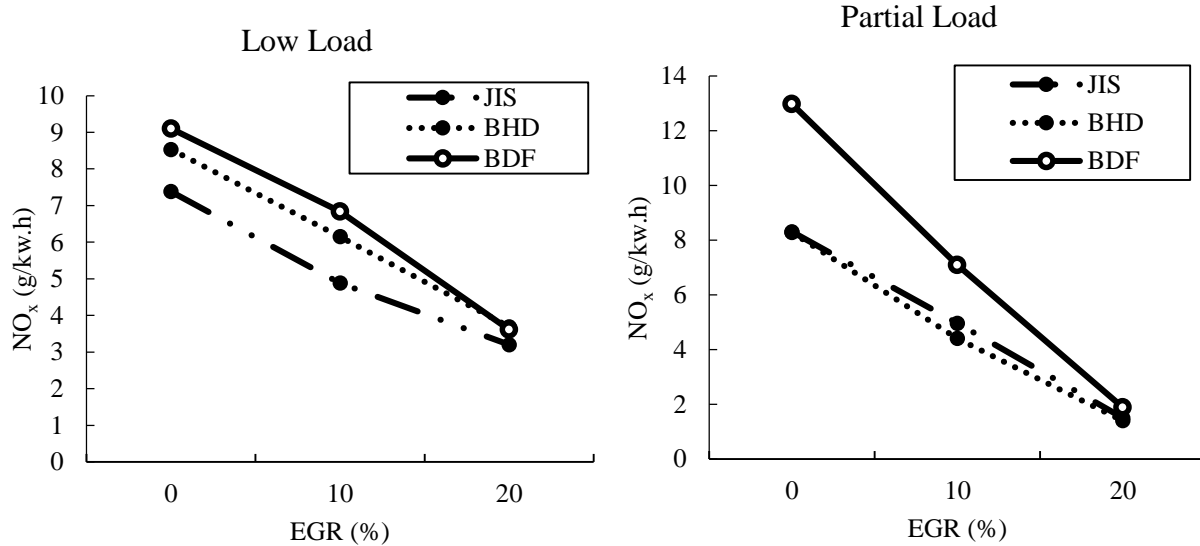


Figure 9.6. NO_x Emissions in low and partial loads

9.3.2.3. Hydro Carbon Emissions (THC)

Hydrocarbon emissions (THC) of JIS, BHD and BDF are shown in Figure 9.7. From all tendencies show that at partial load, adding EGR 10, and 020% can effect THC emissions decreased. At low load, by adding EGR 10 and 20% in BHD can increase THC emissions from 1.74 to 1.91%. Higher in THC emissions is explained because of the higher fuel amount injected to fulfill demands from unburned fuel in higher amount [9]. The increase of EGR rate can reduce oxygen in the combustion chamber. Therefore, incomplete combustion will occur and resulting in higher CO and THC emissions. Nevertheless, in partial load, added EGR 10 and 20% in BHD can reduce the THC emissions ranged from 9.36 to 13.38%.

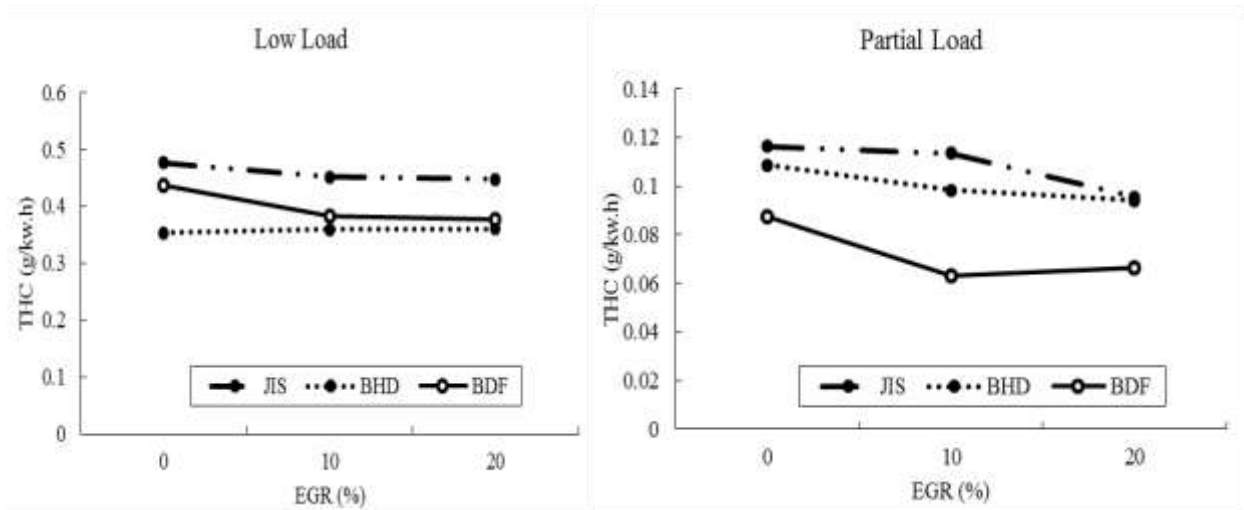


Figure 9.7. THC emissions in low and partial load.

9.3.2.4. Smoke

Smoke emissions from JIS, BHD and BDF are can be seen in Figure 9.8. It can be seen from Figure 9.8, at low load and zero, 10, and 20% of EGR show that smoke of BHD was higher than JIS and BDF. At partial load, from all tendencies show that adding EGR 10 and 20% can make smoke emissions increased for all fuels tested. As can be seen that at partial load, EGR 10 and 20%, smoke emissions raised to 29.83-71.07% for BHD comparing to EGR zero. There are possibilities that smoke emissions in fuels were high, the insufficient pressure and temperature can cause incomplete combustion and increase smoke emissions in the engine. However, the increased of CO emissions can affect high in smoke emissions. As compared to BDF, the smoke emissions were reduced at low and high load. The reduced of emissions in BDF due to high oxygen content in the oil. Therefore, when the engine was running, it would make easier to be burn at higher temperature.

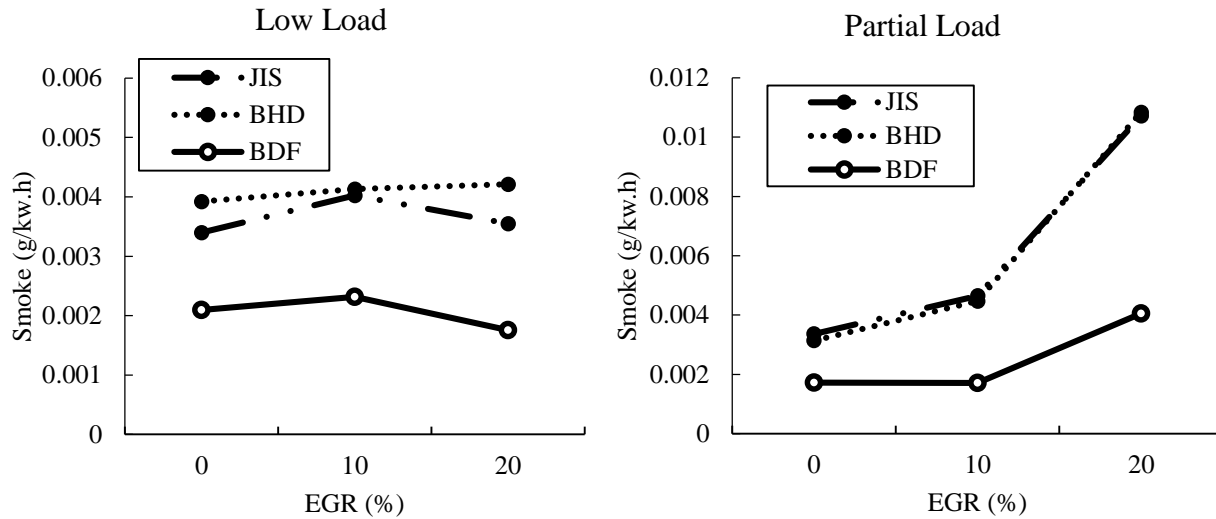


Figure 9.8. Smoke emissions in low and partial loads

9.3.3. Engine Combustion Analysis

9.3.3.1. Peak Cylinder Pressures and Heat Release

The cylinder pressure and heat release rate with crank angle (CA) for JIS, BDH and BDF at different loads (low; partial) and EGR rate (zero; 10, and 20%) are given in Figure 9.9 and 9.10.

In Figure 9.9 and 9.10, the cylinder pressure at low and partial load with EGR zero, 10, and 20% are shown. At low and partial load, the increase of EGR rate makes lower in peak cylinder pressure. In addition, at low load peak pressure of BDF is higher than JIS and BHD and at partial load peak pressure of BDF was nearly the same as JIS, this occurred because BDF has high oxygen content leading to increase of rate combustion, peak temperature and pressure [10]. At low load and zero EGR, it recorded that peak cylinder pressure of JIS was 7.00 MPa (10.5 °CA), BHD was 6.94 MPa (11°CA), and BDF was 7.10 (11 °CA). By adding EGR 10 and 20% at low load, it shows that peak cylinder of JIS decreased in the ranged from 0.10 to 1.3% in comparison with EGR zero. Moreover, by adding EGR 10 and 20% at low load, it decreased peak cylinder pressure of BHD from 6.86 MPa (11°CA) to 6.79 Mpa (11°CA) and also reduced peak cylinder of BDF from 7.04 MPa (11°CA) to 6.98 MPa (11°CA). At partial load and zero EGR, it shows that peak cylinder pressure at 15 °CA of JIS was 8.13 MPa, BHD was 8.02 MPa and BDF was 8.12 MPa. Adding EGR 10 and 20% at partial load can decrease peak cylinder pressure at 15 °CA of JIS from 8.013 to 7.60 MPa, BHD from 7.79 to 7.46 MPa, and BDF from 7.96 to 7.61 MPa. The use of EGR may increase the intake charge specific heat capacity and availability to reduce O₂ that has negative effect to combustion because it can reduce values of peak cylinder [11]. Furthermore, the

separation between O₂ and H₂O can reduce the temperature in the flame because of the process of endothermic; this can cause to reduce NO_x formation [11]. Moreover, reduction in the temperature in the combustion can also cause the peak heat release rate is decreased by using the EGR.

Figure 9.10 shows the heat release rate for low and partial load for various fuels. Adding EGR rate can cause the longer ignition delay of the fuels. As can be seen in Figure 9.10 at low load and EGR zero, the peak heat release of BHD is slightly higher than JIS and BHD. The shorter ignition delay of BDF is due to higher in viscosity. Moreover, slower ignition delay occurred because much fuel accumulated in the combustion chamber at the time of premixed burning phase [12]. At low load, using EGR 10 and 20% can cause reduction of heat release of BHD from 3.85 to 9.11% in comparing to EGR zero. At partial load, adding EGR 10 and 20 % can decrease heat release from 5.52 to 10.16 % compared to EGR zero. This happened due to the oxygen content in the fuel can improve the combustion process to burn fuel completely [12]. However, at partial load with EGR and without EGR, it is found that JIS, BHD and BDF show comparable heat release rate. This occurred because the increased fuel injection pressure at partial load can improve fuel atomization and partially offset from the negative influence from high viscosity in biodiesel [13].

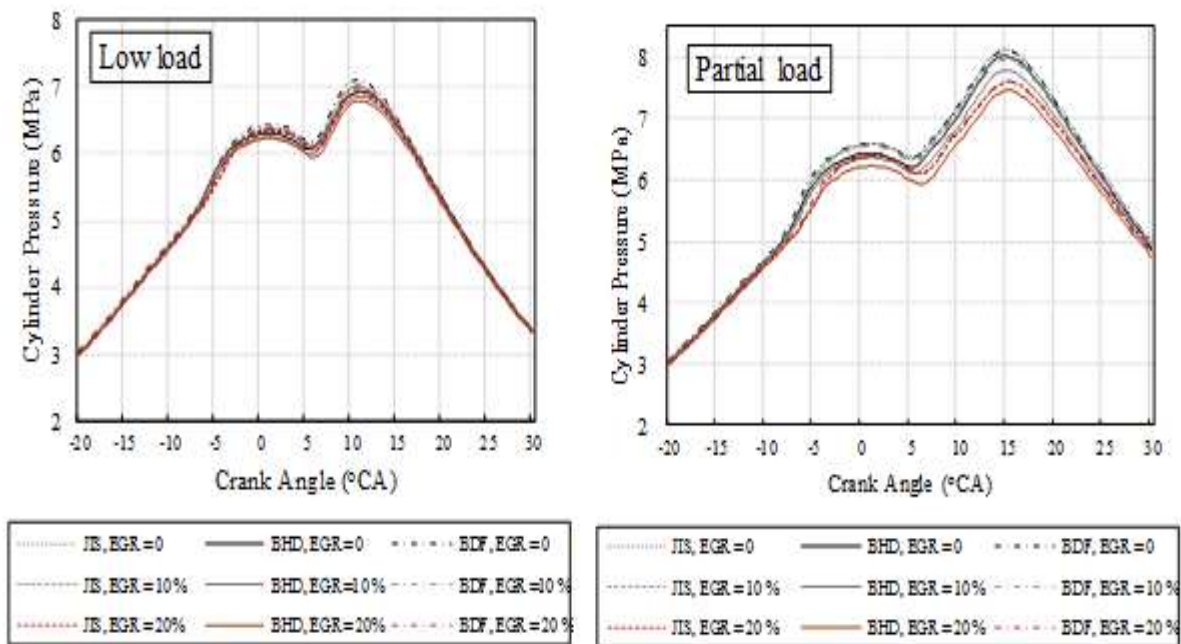


Figure 9.9. Cylinder pressure at low and partial with EGR 0, 10%, 20%

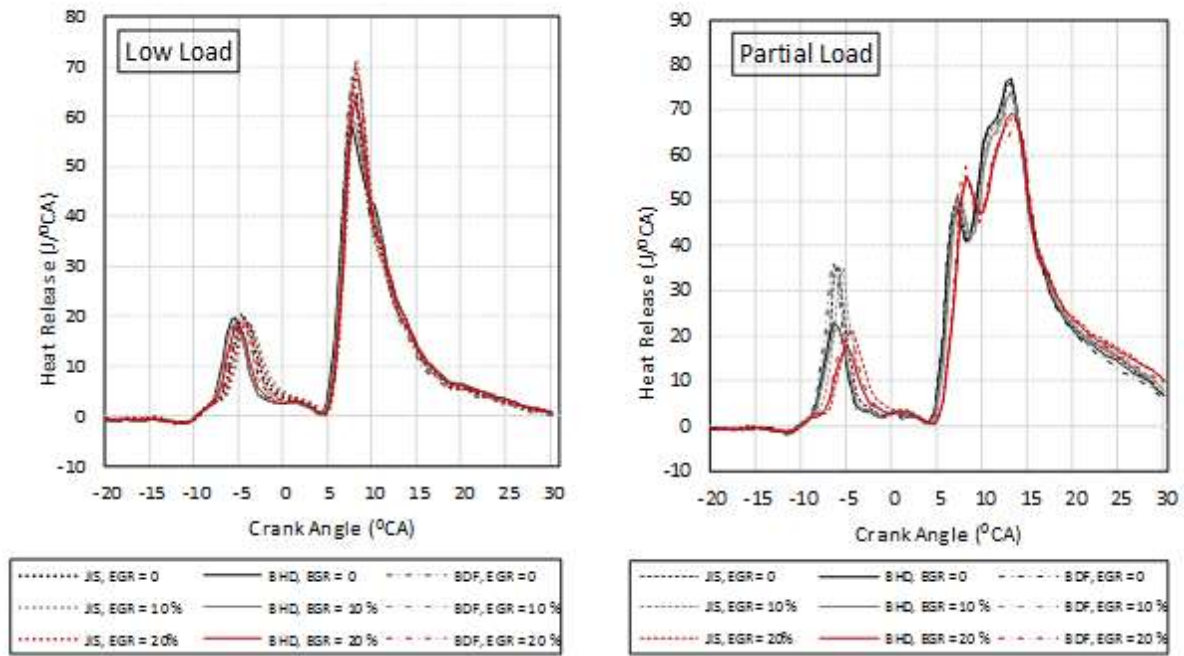
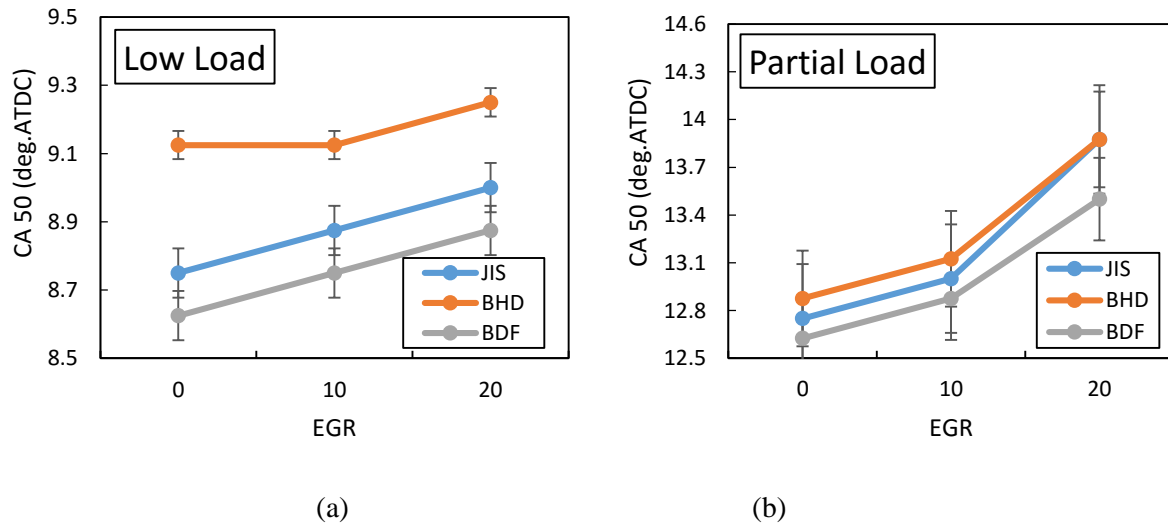


Figure 9.10. Heat release at low and partial load with EGR 0, 10%, 20%.

9.3.4. Correlation between Combustion Phasing and EGR Rate



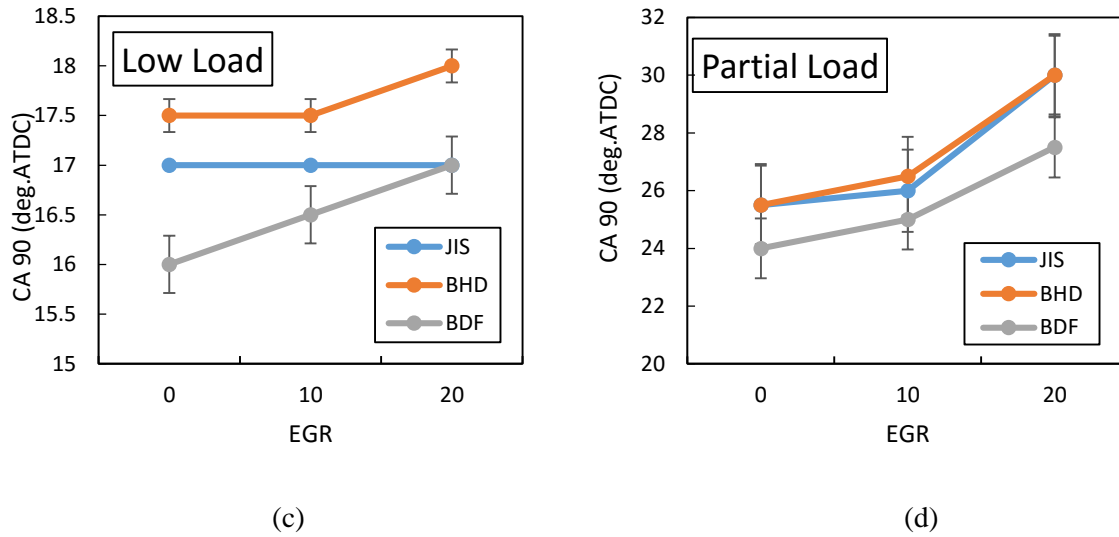
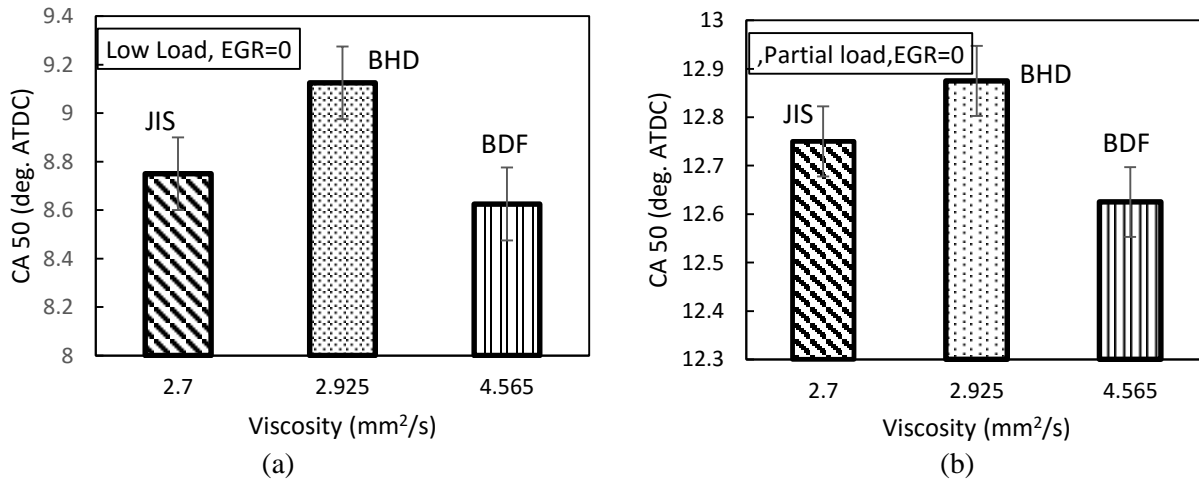


Figure 9.11. Combustion phasing CA50 and CA90 versus EGR rate

Figure 9.11 (a) - (d) show the combustion phasing of CA 50 and 90 to EGR rates. CA50 is defined as crank angle position where 50% of heat is released. CA 90% is defined as crank angle position where 90% of heat is released. At low load, less fuel was burned. Therefore, the combustion temperature was lower as compared with partial load. When the EGR rate increases, the combustion temperature in the cylinder decreases as does the oxygen concentration. Therefore, the ignition delay time increases and the mixture starts to burn unstable and eventually fails to ignite. The ignition of the air / fuel mixture is very depends on the temperature intake air and the boost pressure. Moreover, the increase of EGR makes combustion retarded for all fuels and reduces the reaction rate that can lead longer combustion rate even more retarded CA50 and CA90 [14].

9.3.5. Correlation between Combustion Phasing and Fuel Properties



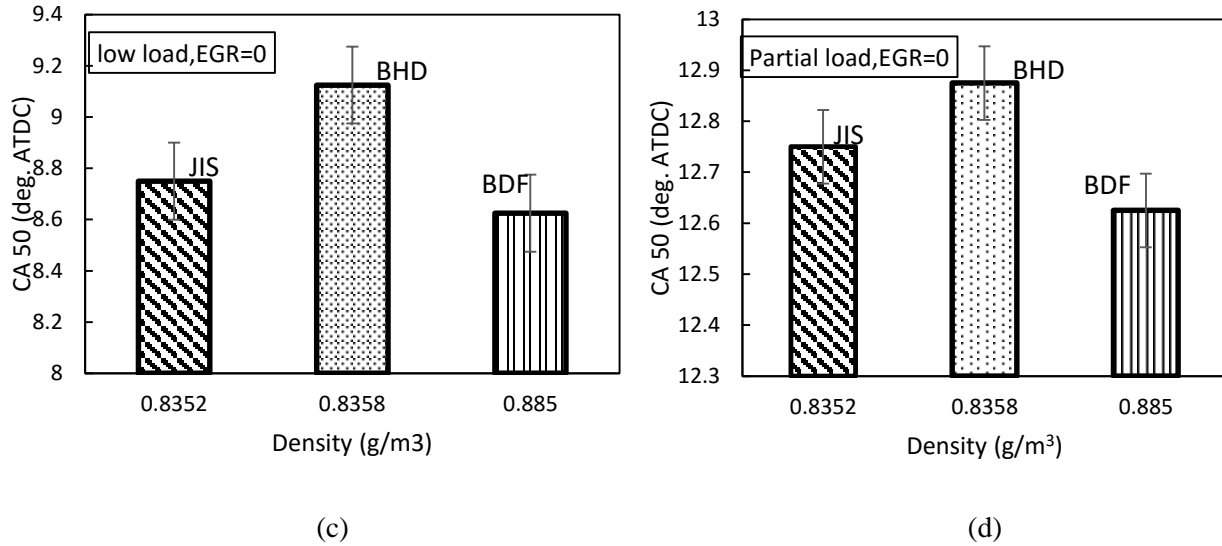


Figure 9.12. Correlation between CA50 with viscosity and density

Figure 9.12 (a)-(d) describe the correlation between CA50 with viscosity and density. As seen in the figure that the highest viscosity and density are lower in the position of CA50. This can be assumed that BDF has higher in density and viscosity makes early ignition delay and early start of combustion duration than JIS and BHD.

9.3.6. Correlation between Combustion Passing and Combustion Duration

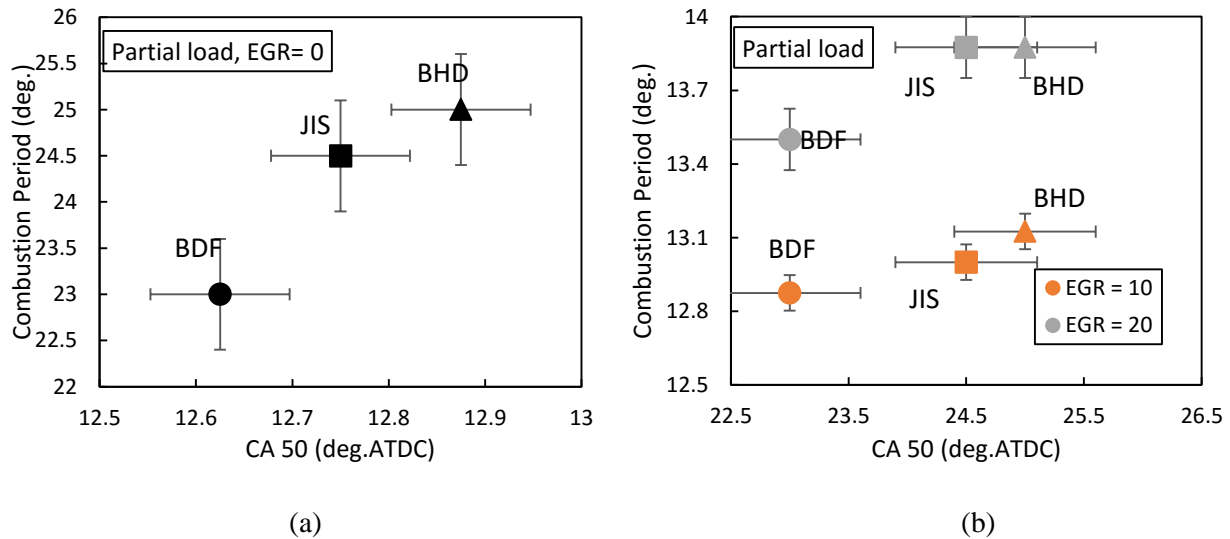


Figure 9.13. Correlation between CA50 with combustion period

Figure 9.13 (a) and (b) show the correlation between combustion period and CA50. The combustion period of BDF is shorter than BHD and JIS resulted the observed faster diffusion burn rate of biodiesel. As can be seen that at partial load without EGR, poorer mixture and smaller premixed fraction due to poorer volatility of BDF also caused longer combustion duration than that of JIS and BHD. Moreover, by increasing the EGR rates the ignition delay becomes longer due to the increased fraction of inert gas and the reduction of in-cylinder temperature [15]. It is also observed that the gap between BDF and JIS, BHD are becoming smaller as EGR increases. Combustion duration becomes longer and shorter when EGR increases. The exhaust gas in cylinder reduces the heat release rate which prolongs the combustion duration. Moreover, longer ignition delay leads to longer time for mixing and better mixture, which provides a rapid combustion [15].

9.3.5. Heat Balance Analysis

Since heat loss cannot be obtained from experiments, in this study, heat loss was calculated with reference to Tsurushima et al. [16]. Here the exhaust loss is calculated from the difference in enthalpy between intake and exhaust, and the constant volume specific heat of each chemical type is the value in the JANAF table [17] was used.

Heat Balance:

$$Q_{fuel} = G_{fuel} \cdot LHV \quad (6)$$

$$W_e = 2 \cdot 2\pi \cdot T \quad (7)$$

$$W_i = \oint p \cdot dV \quad (8)$$

$$Q_{unb} = G_e \cdot LHV_e \quad (9)$$

$$Q_{mec} = W_i - W_e \quad (10)$$

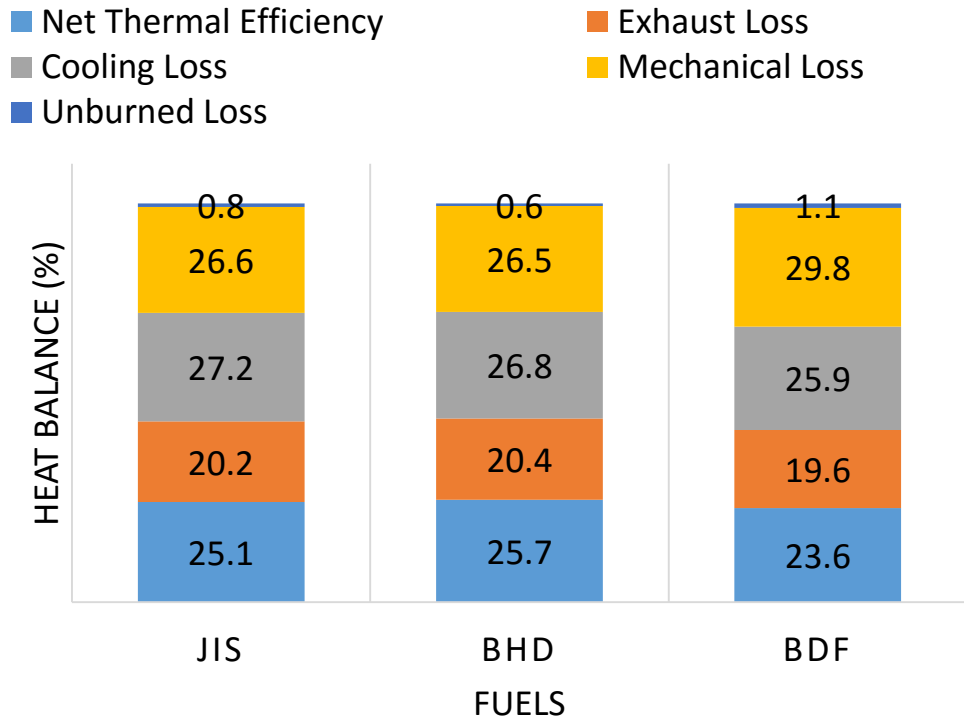
$$Q_{exh} = U_{ex} - U_{in} \quad (11)$$

$$Q_{cool} = Q_{fuel} - W_t - Q_{exh} - Q_{unb} \quad (12)$$

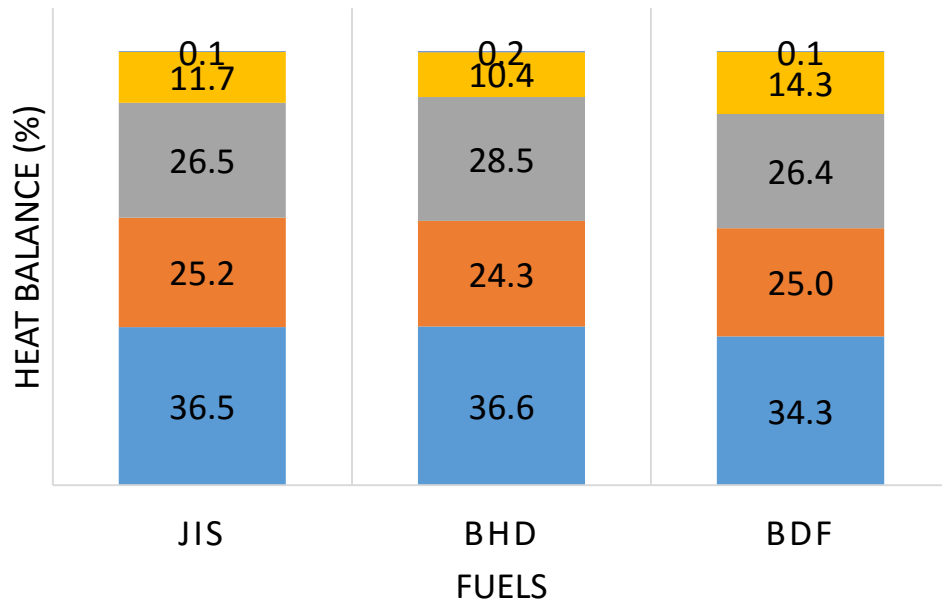
Q_{fuel}	: Input energy [J/cycle]
G_{fuel}	: Fuel consumption[g/cycle]
LHV	: Lower heating value [J/g]
W_e	: Net work [J/cycle]
T	: Torque [N · m]
W_i	: Illustrated work [J/cycle]
p	: In Cylinder Pressure [Pa]
V	: Engine Volume [m ³]
Q_{unb}	: Unburned loss [J/cycle]
G_e	: Mass of unburned components [g/cycle]
LHV_e	: Low caloric value for unburned components [J/g]
Q_{mec}	: Mechanical loss [J/cycle]
Q_{exh}	: Exhaust loss [J/cycle]
U_{ex}	: Exhaust enthalpy [J/cycle]
U_{in}	: Inhalation enthalpy [J/cycle]
Q_{cool}	: Cooling loss [J/cycle]

Figure 9.14 shows the heat balance without EGR in low and partial load. As can be seen in figure that the main heat loss for fuels at low load without using EGR are coming from mechanical loss, exhaust loss, and cooling loss. By increased the load at partial load, the mechanical loss are decreased, thus makes thermal efficiency in the engine is higher.

In Figure 9.15 shows the heat balance with EGR 10 and 20 in partial load. The EGR rate is calculated from the CO₂ concentration in the intake and exhaust. As can be shown in figure, the thermal efficiency is higher than without using EGR. This happened may be re-burning of hydrocarbons that enter the combustion chamber with the re-circulated exhaust gas. At part loads, exhaust gas has less CO₂ and fairly high amount of O₂. Also, partly-cooled EGR acts like a pre-heater of the intake mixture. When this exhaust gas is re-circulated in the cylinder, the unburned HC in exhaust gas burns because of sufficient O₂ available in combustion chamber and reasonably high intake temperatures [18].

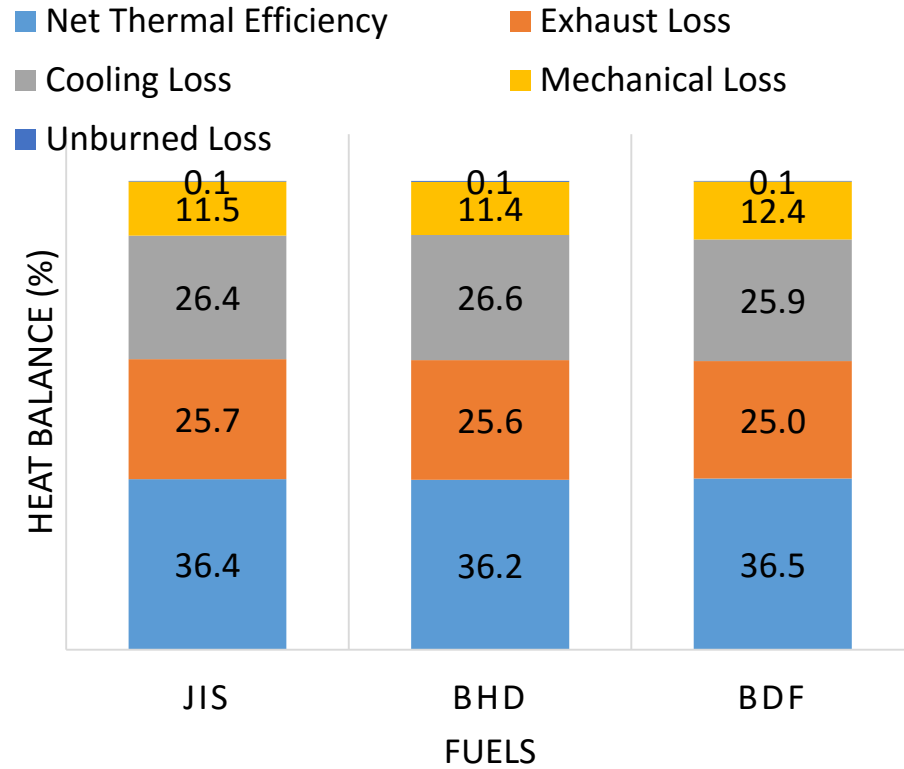


EGR=0, LOW LOAD

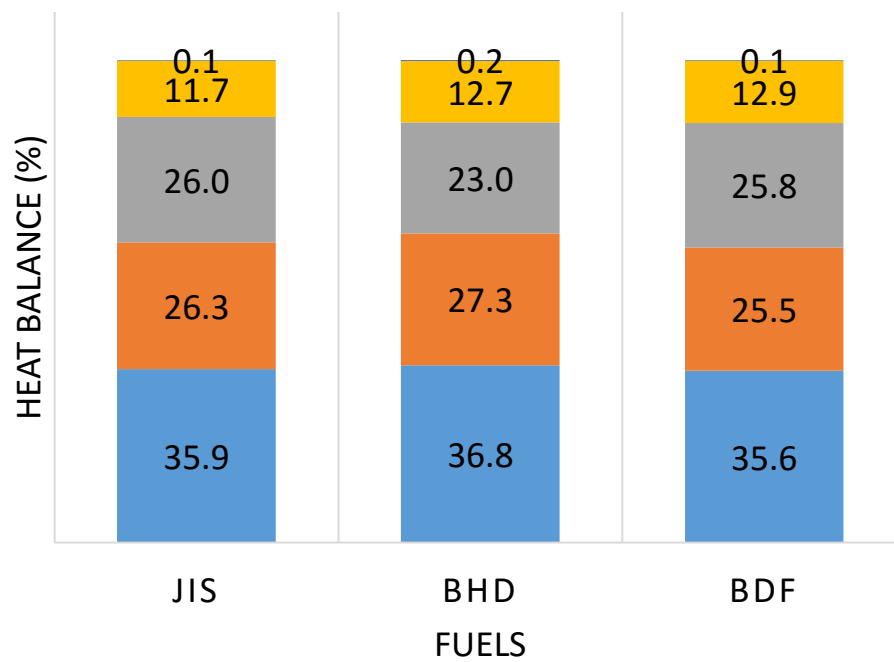


EGR = 0, PARTIAL LOAD

Figure 9.14. Heat Balance without EGR at low and partial load



EGR = 10, PARTIAL LOAD



EGR = 20, PARTIAL LOAD

Figure 9.15. Heat Balance with EGR 10 and 20 at Partial Load

9.4. Experimental Results in Different Injection Pressure

9.4.1 Experimental Condition

Table 9.4. Experimental Conditions in different injection pressures

Test Fuel	Light Oil JIS # 2 and BHD		
Engine speed (rpm)	2000		
Pilot injection timing (deg. BTDC)	18		
Main injection timing (deg. BTDC)	2		
Boost pressure (kPa)	130		
EGR ratio (%)	0		
Rail Pressure (MPa)	100	125	150
Main injection quantity (mg/str)	25	27.3	26.5
Pilot injection quantity (mg/str)	2	2	2
Total injection quantity (mg/str)	27	29.3	28.5

In this study, different injection pressures have been examined. Table 9.4 is the experimental conditions for different injection pressures ($P_{inj} = 100, 125$ and 150 MPa).

9.4.2 Results and Discussions

9.4.2.1 Combustion Characteristics

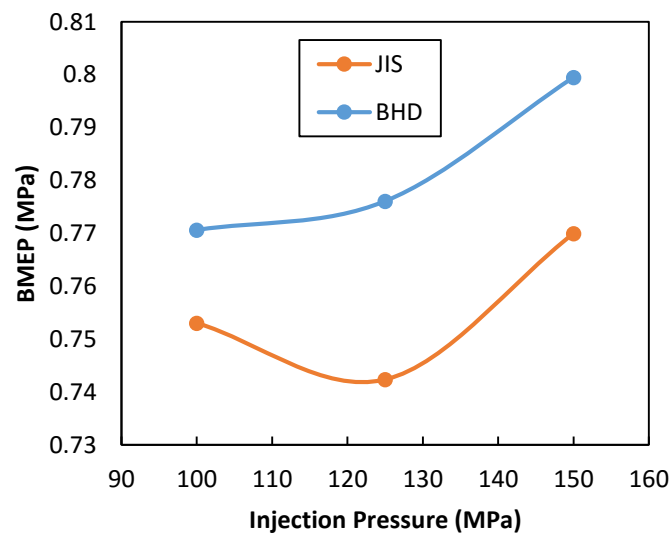


Figure 9.16. Brake mean effective pressures in different injection pressures

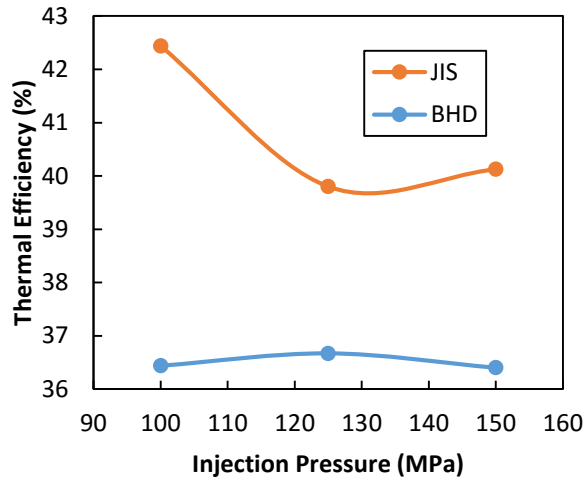


Figure 9.17. η_{th} in different injection pressures

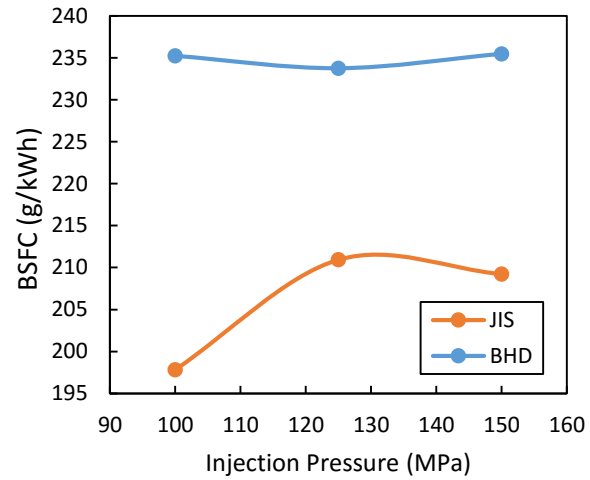


Figure 9.18. BSFC in different injection pressures

Figure 9.16 shows the BMEP from all fuels. As can be seen in Figure 9.16 that BMEP increases with the increases in injection pressures. Moreover, in Figure 9.17 and 9.18 that as the fuel injection pressure increases, the brake specific thermal efficiency (BSFC) increases and the fuel consumption decreases. This can be concluded that as the injection pressure increases, the atomization in the injected fuels are improved.

The increase of injection pressures in BHD can increase the thermal efficiency up to 0.62% in 125 MPa. However, by increasing the injection pressure in JIS the thermal efficiency can be decreased up to 5.4% than in $P_{inj}=100$ MPa. This can be concluded that for BHD is efficient in using high injection pressures (125 MPa) because the fuel can be atomized and the combustion can be improved.

9.4.2.2. Heat Release Rate and Cylinder Pressures

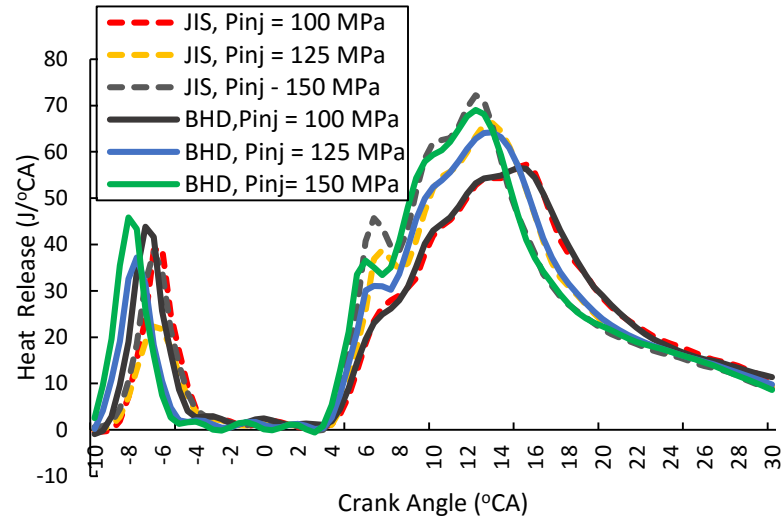


Figure 9.19. Heat release rate at Pinj = 100, 125 and 150 MPa

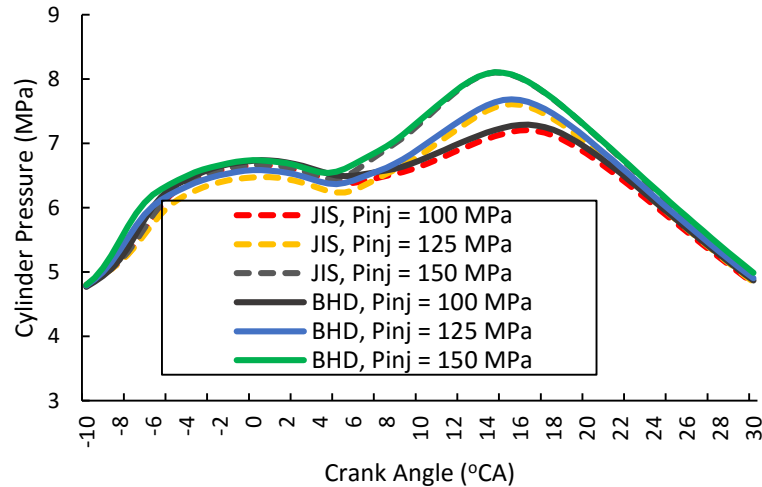


Figure 9.20. Cylinder pressure in different injection pressures

Figure 9.19 shows heat release rate of various fuels in different injection pressures. The increase of injection pressures resulted the shorter ignition delay. As can be seen that heat release rates throughout the combustion process are increased by increased fuel injection rates (achieved by increasing the fuel injection pressures). As can be shown that combustion of BHD is improved by increasing of injection pressures. The fuel atomized into fine droplets, undergoes evaporation by receiving the heat by diffusion

from the cylinder and the point at which combustion is initiated, the cumulative heat release increased rapidly with crank angle [19]. Figure 9.20 shows the cylinder pressure from various fuels in different injection pressure. As the fuel injection pressure increases, the peak cylinder gas pressure for the biodiesel is also increased because when the fuel injection pressure is increased, the amount of fuel taking part in the combustion process is also raised resulting higher peak in-cylinder gas temperature [20].

9.4.2.3. Emissions

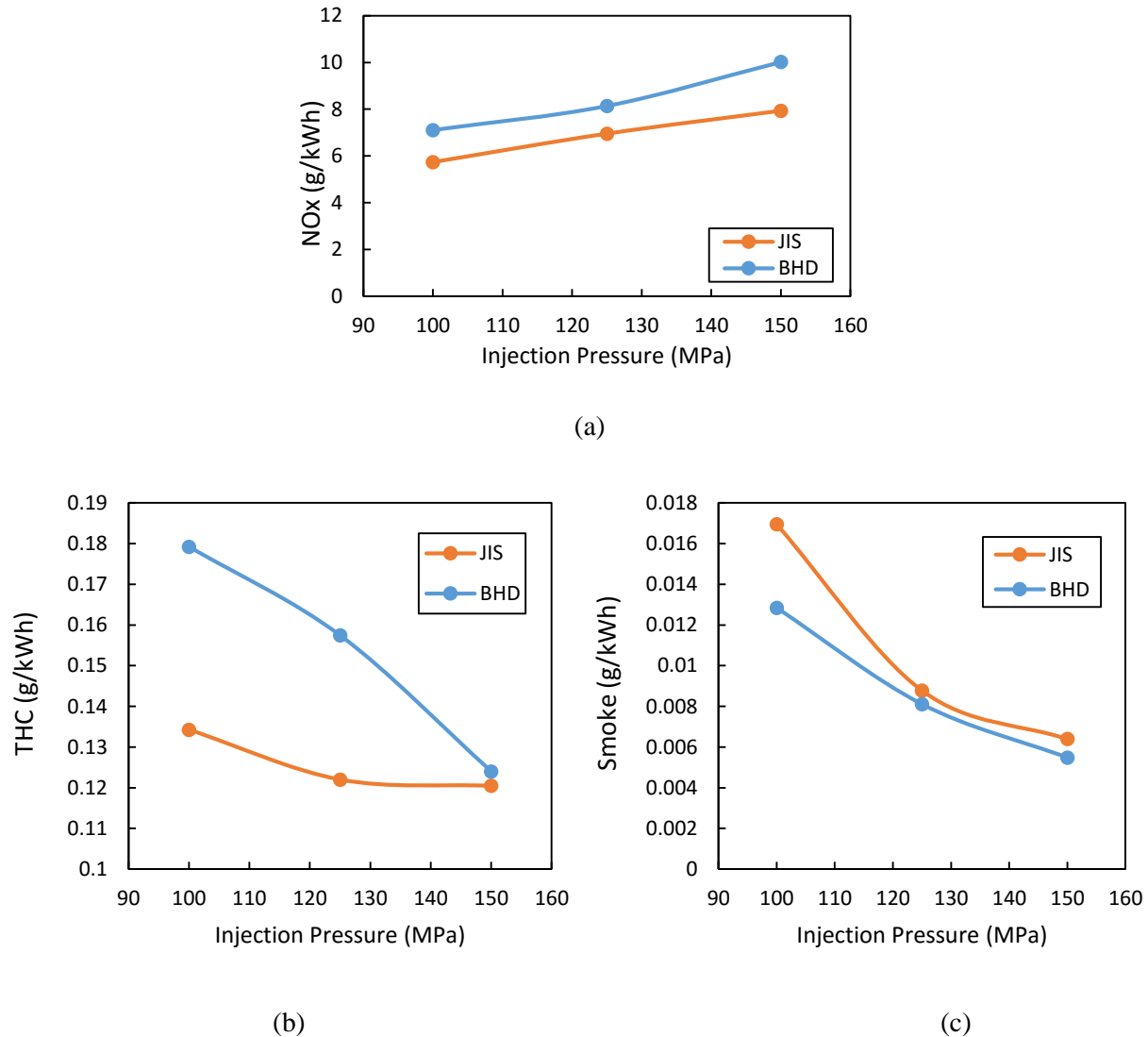


Figure 9.21. Emissions from various fuels in different injection pressures

Figure 9.21 shows the emissions from various fuels in different injection pressures. As can be seen that NOx emissions is higher by increasing of injection pressures. This happened because at higher injection pressure, the fuel droplet diameter decreased, and it vaporized more quickly, resulting in rapid

combustion during the premixed period. Thus the emissions of NO_x of increases with fuel injection pressure due to its higher gas temperature [21]. Moreover, THC and smoke emissions are decreased by increasing the injection pressure. The unburnt hydrocarbon emissions of biodiesel (BHD) are comparatively less as compared to the emissions from the diesel fuel. The suitable oxygen content in the fuel helps the fuel particles to get oxidized properly with the air resulting in lower HC emissions [21]. The smoke emissions is decreasing by higher injection pressure because in injection pressure, the fuels are having good atomization, so the efficiency of the fuel can be raised also can affect the decreasing in smoke emission.

9.4.2.4. Correlation between Combustion Phasing

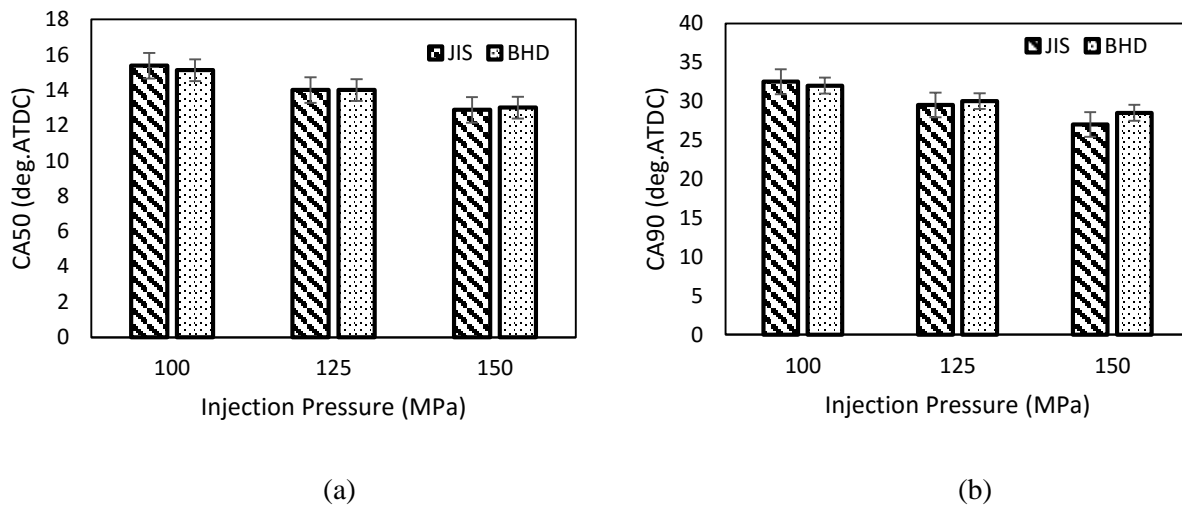


Figure 9.22. Correlation between CA50 and CA90 in different injection pressures

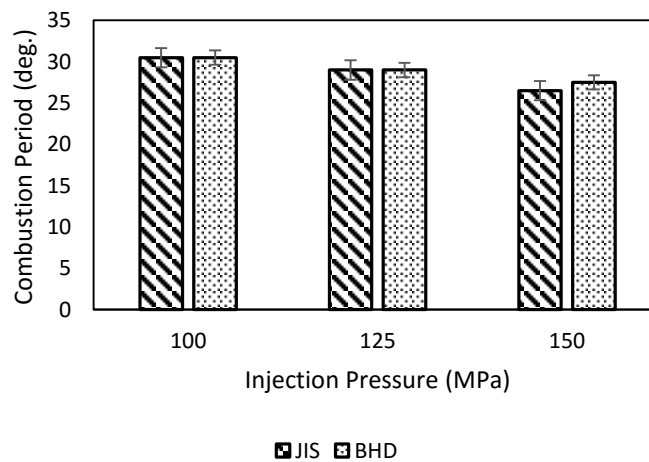


Figure 9.23. Correlation between combustion period and injection pressures

Figure 9.22 shows the correlation between combustion phasing of CA50 and CA90 in different injection pressures. It can be seen that CA50 and CA90 between all fuels (JIS and BHD) are not many differences. The increases of injection pressure, the combustion phasing CA50 and CA90 are decreased. This happened because the fuels are atomized resulted to improve the atomization. Figure 9.23 shows the combustion period in different injection pressures. The combustion period is becoming shorter in higher injection pressures. This is the correlation between ignition delays in the combustion. The ignition delays in higher injection pressures are decreased makes the combustion duration is shorter.

9.5. Conclusions

BHD has the highest thermal efficiency compared to JIS and BDF in low load with EGR zero and 10%. The thermal efficiency can reached to 2.28 to 8.1% as compared to JIS and BDF. Therefore, BHD can be an alternative fuel for the future.

BHD also can reduce the emissions such as NO_x and THC. Nevertheless, CO and smoke emissions have little higher than JIS and BDF. The using of EGR is effective in low load due to in partial load the emissions of CO, THC and smoke are increased.

BDF has a shorter ignition delay than JIS and BHD due to the compressibility is low, the viscosity is high and cetane number is high. A shorter ignition delay in biodiesel creates a relatively lower premixed burn fraction. In EGR =0, the peak cylinder pressure and heat release rate of biodiesel is lower than diesel oil because low caloric value in biodiesel.

As the fuel injection pressure increases, the brake thermal efficiency increases and the fuel consumption decreases. In higher injection pressure can improved the atomization in the fuel. Therefore, the emissions can also be decreased such as smoke and THC. However, NO_x is the biggest problems because it can be increased by the increase of injection pressure. Therefore, the combination between EGR rates is suitable in controlling the NO_x and higher injection pressure.

9.6. References

- [1] Pullen, J., Saeed, K. 2012. An overview of Biodiesel Oxidation Stability. *Renew SustEnerg Rev.* 16(8):5924-50.
- [2]Hawi, M., Kiplimo, R., and Ndiritu, H. 2015. Effect of Exhaust Gas Recirculation on performance and Emission Characteristics of a Diesel-Oiloted Biogas Engine. *Smart Grid and Renewable Energy*, 6, 49-58.

- [3] Muralidharan, K., Vasudevan, D., Sheeba, K.N. 2011. Performance, emission and combustion characteristics of biodiesel fuelled variable compression ratio engine. *Energ.* 36(8):5385-93.
- [4] Heywood, J. B. 1988. *Internal Combustion Engine Fundamentals*. McGraw Hill.
- [5] Bowman, C. T. 1975. Kinetics of pollutant formation and destruction in combustion. *Prog. Energy Combust. Sci.*, volume 1, pp. 33-45.
- [6] Park, S.H., Youn, I.M., and Lee, C.S. 2010. Influence of Two Stage Injection and Exhaust Gas Circulation on The Emissions Reduction in an Ethanol-Blended Diesel-Fueled Four-Cylinder Diesel Engine. *Fuel Processing Technology*, 91:1753-1760.
- [7] Zhong, W., Xuan T., He, Z., Wang, Q., Li, D., Zhang X., and Yin, HY. 2016. Experimental Study of Combustion and Emissions Characteristics of Diesel Engine /Second-Generation Biodiesel Blending Fuels. *Energy Conversion and management*, 121, 241-250.
- [8] SCR or EGR- Fleet Owner Magazine.
- [9] Serio, D.D., Oliveira, A.D., and Ricardo. 2017. Effects of EGR Rate on Performance and Emissions of a Diesel Power Generator Fueled by B7. *J. Braz.Soc.Mech.Sci.Eng.* 39:1919-1927.
- [10] Shehata, M. S. 2013. Emissions, performance and cylinder pressure of diesel engine fuelled by biodiesel fuel. *Fuel*, 112, 513 -522.
- [11] Pullen, J., Saeed, K. 2012. An overview of Biodiesel Oxidation Stability. *RenewSustEnerg Rev.* 16(8):5924-50.
- [12] Silitonga, A.S., Masjuki, H.H., Ong, H.C., and How, H.G. 2015. Engine performance, emission and combustion in common rail turbocharged diesel engine from jatropha curcas using artificial neural network. *JSAE 20159710/ SAE 2015-32-0710*.
- [13] Fahd, M. E. A., Wenming, Y., Lee, P. S., Chou, S. K., and Yap, C. R. 2013. Experimental investigation of the performance and emission characteristics of direct injection diesel engine by water emulsion diesel under varying engine load condition. *Applied Energy*, 102, 1042-1049.
- [14] Wang, S., Zhu, X., Somers, L. M. T., and Goey, L. P. H. D. 2017. Effects of exhaust gas recirculation at various loads on diesel engine performance and exhaust particle size distribution using four blends with a research octane number of 70 and diesel. *Energy Conversion and Management*, 149, 918-927.

- [15] Li, B., LI, Y., Liu, H., Liu, F., Wang, Z., and Wang, J. 2017. Combustion and emission characteristics of diesel engine fueled with biodiesel/PODE blends. *Applied Energy*, 206, 425-431.
- [16]Tsurushima, S., Miyamoto, T., Enomoto, Y., Asami, T., and Aoyagi Y. 2002. Evaluation of wall heat loss estimation method by heat balance and estimation accuracy Valence .*Transactions of the Japan Society of Mechanical Engineers (Part B)*, Volume 68, No. 674, pp. 2935-2942.
- [17] Takehiro Ito, “Industrial Thermodynamics (2)”, Corona (1994), p. 274.
- [18] Agarwal, D., Singh, S.K., and Agarwal, A. K. 2011. Effect of exhaust gas recirculation (EGR) on performance, emissions, deposits and durability of a constant speed compression ignition engine. Volume 88 (8), 2900-2907.
- [19]Ashok, B., K. Nanthagopal, B. Saravanan, K. Azad, B. S. Deepam Patel, and R. A. Ramasamy. 2019a. Study on isobutanol and calophylluminophyllum biodiesel as a partial replacement in CI engine applications. *Fuel* 235:984–94.
- [20]Nanthagopal, K., B. Ashok, B. Saravanan, S. M. Korah, and S. Chandra. 2018. Effect of next generation higher alcohols and calophylluminophyllum methyl ester blends in diesel engine. *Journal of Cleaner Production* .180:50–63.
- [21] Selvaraj, K., and Thangavel, M. 2019. The effect of fuel injection pressure on combustion and emission characteristics of a diesel engine using frying oil methyl ester. *Energy Sources, Part A: Recovery, Utilization, and Environmental Effects*. DOI: [10.1080/15567036.2019.1675818](https://doi.org/10.1080/15567036.2019.1675818).

Chapter 10. Combustion and Emission Characteristics in Biodiesel Water Emulsions

10.1. Introduction

In this chapter, combustion and emissions from biodiesel water fuel emulsions will be discussed. Emulsions of water in diesel or biodiesel are defined as an emulsion of water in the oil (diesel oil or biodiesel oil) with specific additives, surfactants, in order to stabilize the system [1]. The concept of biodiesel water emulsions is defined as water inside the oil in the form of micrometer-sized droplets has a good effect on the combustion in the engine. Water is covered by oil droplet resulting in micro-explosion diesel that surrounded by water particle. The micro-explosion appears if the low boiling point of liquid or water is surrounded by the high boiling point of liquid like biodiesel oil or diesel oil. The low boiling point liquid as water is becoming unstable when the heat transfer occurs in the diesel during the compression stroke in the engine. This condition may lead to micro-explosion that would better in the fuel mixing with air. Therefore, NO and PM emissions would decrease and water- in-diesel oil or biodiesel oil emulsion can run in the engine without making any modification [2].

10.2. Materials and Method

10.2.1. Materials

Biodiesel cooking oil was purchased from PT. Bali Hijau Biodiesel Company and the emulsions were obtained from Mechanical engineering Department Trisakti University Jakarta [3]. In this study, there are four fuels were considered, pure diesel oil which our base fuel, biodiesel cooking oil blended with 5% diesel oil, biodiesel cooking oil blended with 10% diesel oil and biodiesel water emulsions (10% water and 18.7% emulsions) blended with 5% diesel oil. The emulsion was 18.7% because in that value the emulsions can be merged together with water, biodiesel and diesel oil. Nevertheless, the emulsions were less or higher than 18.7%, the water cannot merge perfectly with diesel and biodiesel and turn to be milky. This condition can be dangerous to the engine because water is not merged together and some troubles may occur in the engine.

10.2.2. Experimental Method

The experiment was conducted on four-cylinder, four stroke, air-cooled direct injection diesel engine. The experiments were conducted in various loads (6 kW, 9kW and 15 kW) and constant speed of 1500 rpm. The loads were connected to 6 kW air heater and 9 kW water heater. These loads were arranged in the parallel set up with a stop contact for setting the load. A measuring cup was used to measure the fuel consumptions and a stopwatch was used to measure the time consumed every 10 ml of

oil. Exhaust gas analyzer KEG-500 was used to measure the emissions from the exhaust pipe from the engine. The NHT-6 opacimeter was used to measure the opacity from the exhaust pipe of the engine. The schematic diagram of the experimental apparatus can be seen in Figure 10.1. The experimental apparatus is indicated by capital letters. Capital letter A is indicated of diesel engine. Capital letter B is indicated of the air heater for the load. Capital letter C is indicated of water heater for the load. Capital letter of D is indicated of measuring cup and capital letter of E is indicated of the gas analyzer and opacity meter.

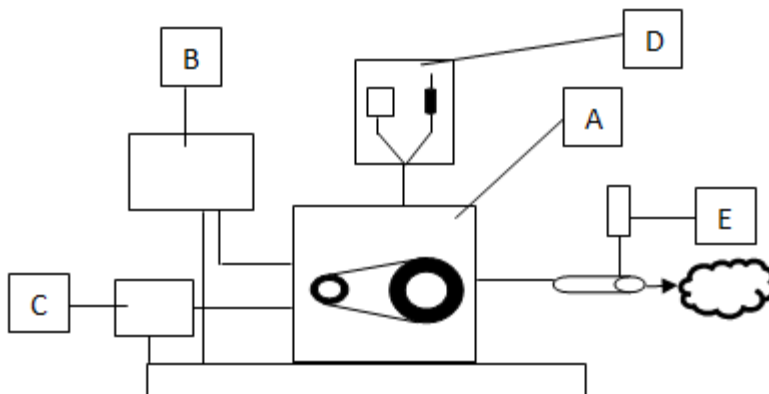


Figure 10.1. Experimental Set Up

Table 10.1. Engine specifications.

Items	Description
Brand	Yanmar
Model	4TNV84T-BGGE
Type	4 cylinder, four stroke, liquid cooled diesel engine
Combustion system	Direct Injection
Bore	84 mm
Stroke	90 mm
Displacement	1.995 L
Aspiration	Turbocharged
Rated speed	1500 rpm
Compression ratio	18.9 : 1

Table 10.2. Specifications measurement gases by exhaust gas and opacity

Name	Measurement	Resolution	Measureable range
Gas Analyzer KEG-500	CO	0.01%	0.00-10.0%
	CO ₂	0.1%	0.0-20.0%
	O ₂	0.01%	0.0-10.0%
Opacimeter NHT-6	Opacity	0.1%	0-99.99%

The experiment was conducted in the Laboratory of Mechanical Engineering at Trisakti University, Jakarta. The engine specification can be seen in Table 10.1. The experimental set up can be shown in Figure 10.1. Firstly, the engine was running for 20 minutes to make heating in the diesel engine. Secondly, data collections were taken three times in different loads (zero, 6kW, 9 kW and 15 kW) for every fuel or oil. The engine speed was constant about 1500 rpm and the collections data for fuel consumptions were taken every 10 ml of oil or biodiesel. The emissions were also taken by the time of the engine was running in different loads. The specifications measurement for emissions can be seen in Table 10.2. Lastly, after the data collections were done. The engine was left in no-load condition for cooling down and turns off.

10.3. Results and Discussions

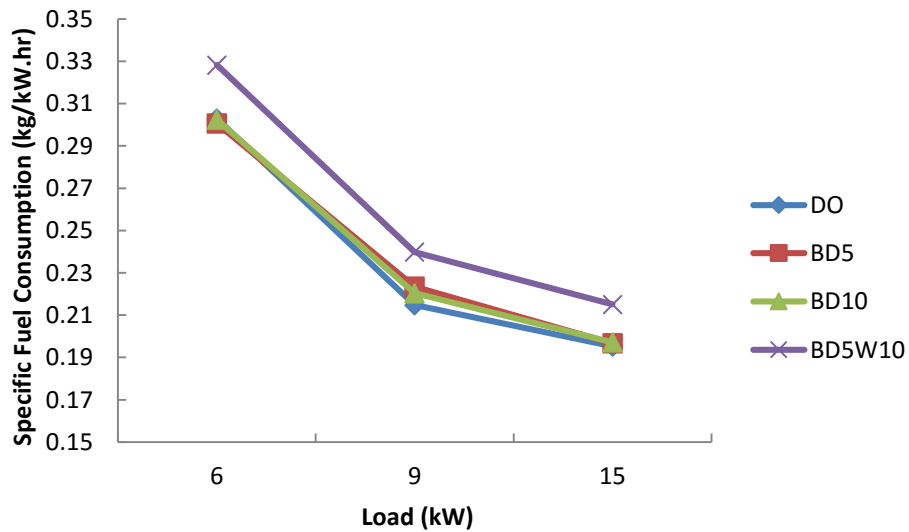
The fuel properties from different biodiesel and diesel fuel are presented in Table 10.3. From this table, it can be seen that water emulsions have effects in chemical properties in the fuel. Adding 10% water and 18.4% emulsions made high density, viscosity and flash point in the fuel. Nevertheless, 10% water and 18.4% emulsion have lower in heating value compared to DO, BD5 and BD10. However, high viscosity is not a problem for water- in-biodiesel oil or diesel oil emulsion. In fact, it has advantages in reducing emissions and gives lower NO_x and CO emissions [4].

Table 10.3. Fuel Properties from Various Fuels

Properties	BD100	DO	BD5	BD10	BD5W10
Density (kg/m ³)	881.6	820	825.4	833.6	842.9
Viscosity (cSt)	5.02	2.0	2.341	2.839	8.805
Flash Point (°C)	60	55	74	73	77
FAME content (% Vol)	93.88	-	5.23	10.01	3.96
Heating Value (MJ/kg)	38.191	45.572	45.493	45.328	38.299
Cetane Index	55	48	52	53	43
Distillation (°C):	350	340	335	325	337
T @ 90%	354	360	351	338	342
T @ 95%					

10.3.1. Engine Performance and emissions

10.3.1.1. Specific Fuel Consumption

**Figure 10.2.** Specific Fuel Consumption from Various Fuels.

The variation of fuels for specific fuel consumption (SFC) at different loads can be shown in Figure 10.2. In every load, specific fuel consumptions for BD5W10 are increased than DO, BD5, and BD10. It can be shown in Figure 10.2 that at low load (6 kW) BD5W10 is increased 8.37% compared to DO. While BD10 and BD5 are lower 0.14% and 0.744% than DO. At medium load (9 kW), BD5W10, BD10, and BD5 are higher 11.66%, 2.58% and 4.05% than DO. At higher load (15 kW), BD5W10 is increased up to 10.13% compared to DO and also BD10 and BD5 are higher 0.95% and 0.74% than DO.

The increased of SFC in BD5W10 are happened due to (i) the behavior of micro-explosions intensity, (ii) improved air-entraining in the spray, (iii) The combustion temperature is low, (iv) combustion premixed is high, (v) more result of burning gas because of quality of water in the emulsion [5, 6]. In addition, the high consumption in low load is happened because of the heat loss to the combustion chamber walls, whereas the high consumption at high load is caused by high friction [5].

10.3.1.2. Thermal Efficiency

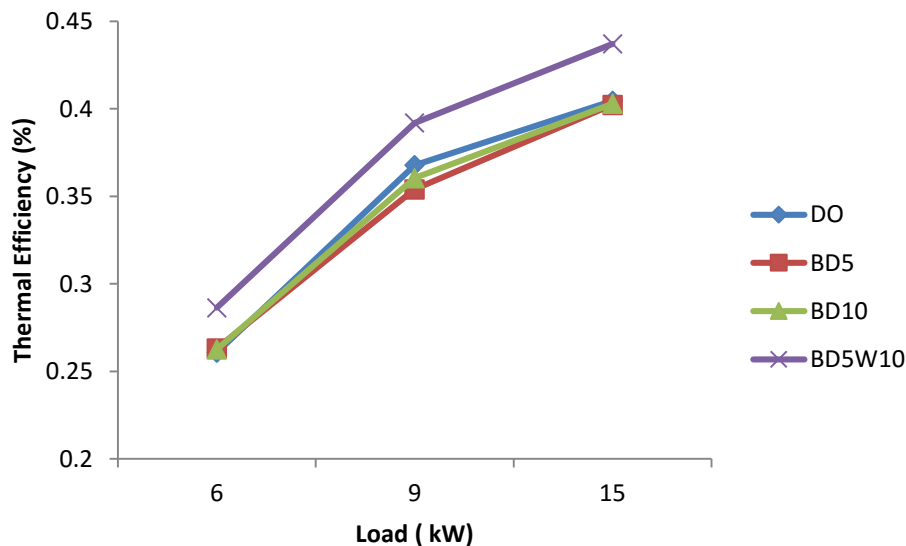


Figure 10.3. Thermal Efficiency from Various Fuels

Thermal efficiency from various fuels in different loads can be seen in Figure 10.3. Figure 10.3 shows that every load conditions the thermal efficiency of BD5W10 are higher than DO, BD5, and BD10. As can be seen in Figure 10.4 that at low load (6kW) the thermal efficiency of BD5W10 is higher 9.79% than DO. However, BD5 and BD10 are not having much differences in thermal efficiency compared to DO. Also at medium load (9 kW) BD5W10 can raise the thermal efficiency up to 6.5% than DO, while BD5 and BD10 are declined 3.73% and 1.99% than DO. At high load (15kW) BD5W10 is increased up to 8% compared to DO, whereas BD10 and BD5 only increased to 0.41% and 0.56%.

The improvement of thermal efficiency in BD5W10 is due to the micro-explosion phenomena and longer ignition delay. This also indicated that longer in ignition delay can occur the more amount of fuel wouldburn in the pre-mixed stage and has better thermal efficiency [7].

10.3.2. Emissions

10.3.2.1. CO Emission

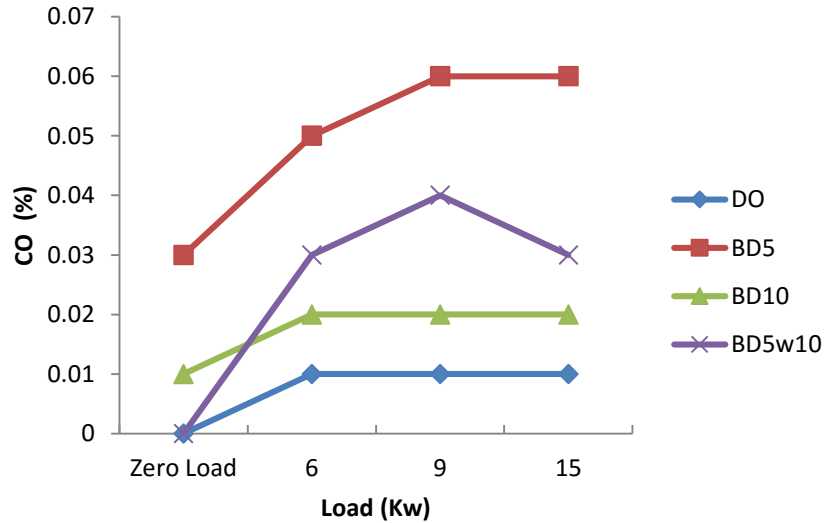


Figure 10.4. CO Emission from Various Fuels

Figure 10.4 shows CO emissions for BD5W10 are higher than DO and BD10 in medium and higher loads. As can be shown in Figure 10.4 that CO emission at low load (6kW) BD5W10, BD10, and BD5 are higher 0.02, 0.01 and 0.04 point than DO and BD10. At high load (9kW) the CO emission of BD5W10, BD10, and BD5 are also increased up to 0.02, 0.01 and 0.05 point compared to DO.

CO emission appears because of incomplete combustion, slow in burning and insufficient homogeneity in a diesel engine [5]. Higher in CO emissions also happened because of increasing ignition delay and the flame temperature was low [8].

10.3.2.2. CO₂ Emission

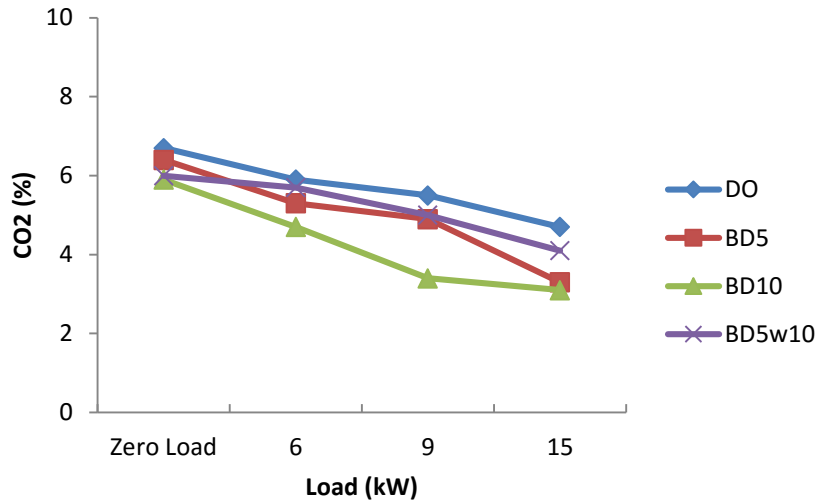


Figure 10.5. CO₂ Emission from Various Fuels

Figure 10.5 shows about CO₂ emission for various fuels. It can be seen that BD5W10 can be reduced the CO₂ emissions in every load compared to DO. CO₂ emissions of BD5W10 can reduce up to 12.8% than DO at high load (15 kW), whereas, at low load, BD5W10 can decrease CO₂ emission up to 10.4% than DO. Although the CO₂ emission in BD5W10 has limited effect in reducing CO₂, it is useful to environmental effect in reducing the level of NO_x and particulate matters (PM) [1].

10.3.2.3. Smoke Opacity

It is seen in Figure 10.6 that the biodiesel water emulsions is very effective in reducing smoke opacity. At high load (15 kW), it can be seen that BD5W10 can reduce the smoke opacity up to 67.64%, whereas BD10 can be reduced only 52.64% than DO. Also, the same in a middle load(9kW) that BD5W10 can cut the smoke opacity up to 84.25% than DO. While BD5 and BD10 can only cut the smoke opacity 74.07% and 76.85% compare to DO. Reducing in smoke opacity in water biodiesel oil or diesel oil emulsion is due to micro-explosion phenomenon may become an important role to control the smoke opacity in the engine [9].

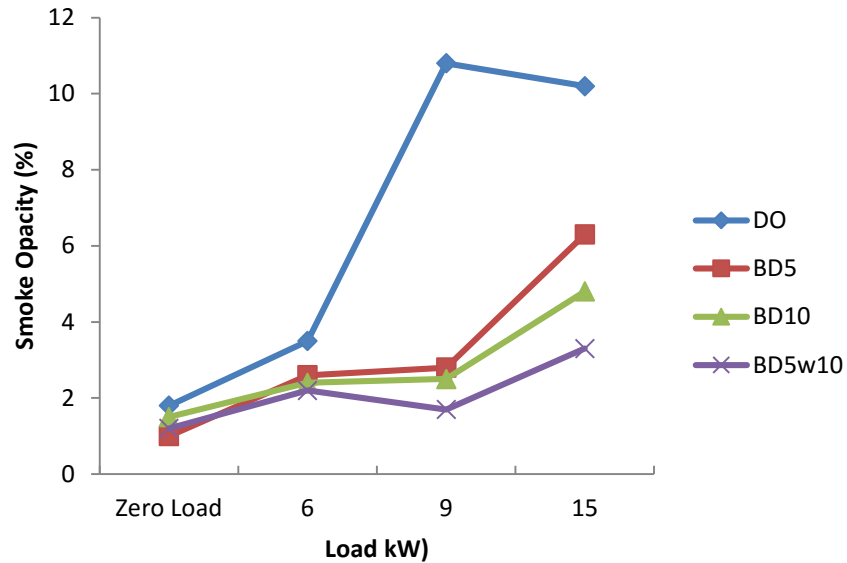


Figure 10.6. Smoke Opacity from Various Fuels

10.4. Conclusions

The following conclusions are presented based on the experimental results from comparing four sample fuels of DO, BD5, BD10, and BD5W10.

The specific fuel consumption of BD5W10 in every load is higher than DO. At low load, the specific fuel consumption of BD5W10 is increased 8.37% than DO and at high load, BD5W10 is higher 10.13% than DO. However, the thermal efficiency of BD5W10 is higher than DO in every load. At high load, the thermal efficiency of BD5W10 is higher up to 8.04 % than DO and at low load, BD5W10 is higher 9.79% compare to DO.

Biodiesel water emulsion is also effective in reducing the emissions. In high load, BD5W10 can reduce CO₂ emission up to 12.8% than DO. Although CO emission in BD5W10 is higher than DO, BD5W10 can cut the smoke emission up to 84.25% in middle load compare to DO.

The water in biodiesel oil or diesel oil can affect the combustion because of the micro explosion phenomenon that the different volatility between oil and water. From this study, the water biodiesel oil emulsion can be an alternative source to replace petroleum fuel in the future.

10.5. References

- [1] Lif, A., Holmberg, K. 2006. Water-in-diesel emulsions and related systems, *Advances in colloid and interface science*. 123-126: 231-239.
- [2] Ravikumar, T.S., P.D. Basar, and M. J. Attfield. 2001. Emulsified diesel-an immediate and effective solution for diesel exhaust emission reduction. Society of automotive engineers. *SAE paper no.* 2001-28-0037.
- [3] Hafnan M. 2008. Patent registered no. P00200800511. 1st August.
- [4] Lin, C.Y., Wang, K.H. 2003. The fuel properties of three-phase emulsions as an alternative fuel for diesel engines. *Fuel*. 82: 1367-1375.
- [5] Abu, Z. M. 2004. Performance of single cylinder, direct injection diesel engine using water fuel emulsions. *Energy Conversion and Management*. 45:697-705.
- [6] Tsukahara, M., Yoshimoto, Y., Murayama, T. 1989. Influence of emulsified fuel properties on the reduction of BSFC in a diesel engine. *SAE Technical Paper* 891841.
- [7] Vellaiyan, S., Amirthagadeswaran, K.S. 2016. The role of water-in-diesel emulsion and its additives on diesel engine performance and emission levels: a retrospective review. *Alexandria Engineering Journal*. 55: 2463-2472.
- [8] Koc, A.B., Abdullah, M. 2013. Performance and NO_x emissions of a diesel engine fueled with biodiesel-diesel-water nanoemulsions. *Fuel Process Technology*. 109: 70-77.
- [9] Subramanian, K.A. 2011. A comparison of water-diesel emulsion and timed injection of water into the intake manifold of a diesel engine for simultaneous control of NO and smoke emissions. *Energy Conversion and Management*. 52:849-857.

Chapter 11. Conclusions

11.1. Summary of the Present Work

Biodiesel is one of the promising alternative fuel in the future. Biodiesel is made from the trans-esterification process that uses methanol or alcohol and catalyst. The use of biodiesel in the diesel engines have some advantages such as high cetane number, oxidation stability and can reduce the emissions. However, higher viscosity, boiling temperatures and surface tension in biodiesel may affect the spray characteristics compared to diesel oil. To overcome the unbenefited in biodiesel, therefore, the fuels designed to a new method that high-boiling point fuel in jatropha methyl ester is mixed to n-tridecane which is a low-boiling point fuel in order to improve the properties in jatropha methyl ester. Moreover, biodiesel from waste cooking oil, bio hydro-finned diesel oil and biodiesel water emulsions were investigated.

The first part of the work is concerning to the chemical analysis from all fuels tested. The fuels are jatropha methyl ester (JME) blended to n-tridecane by volume (25:75, 50:50, 75:25 and 0:100), biodiesel fuel 100% (BDF), bio hydro-finned diesel oil (BHD), and biodiesel water emulsions (BWE). It was observed that adding n-tridecane in jatropha methyl ester can affect chemical properties in the fuel. The higher percentage of n-tridecane in jatropha methyl ester can make lower in boiling point, reduce the viscosity and surface tension. Moreover, bio hydro finned diesel oil (BHD) is a second-generation oil that not using the trans-esterification process but using hydro finning process shows that can improve the density and viscosity while biodiesel fuel (BDF) shows higher in viscosity, density and boiling point. This happened because Biodiesel fuel (BDF) is the first-generation oil that using methanol and KOH as a catalyst. Furthermore, biodiesel water emulsions are made from waste cooking oil 5%, water 10%, diesel oil 100% and emulsions 18.7% shows higher viscosity, density and lower in caloric value compared to diesel oil.

The second part of the work measurement of non-evaporating spray characteristic including spray tip penetration, spray cone angle and droplet size measurement by using shadowgraph photography for and super spatial resolution photography. Non-evaporating sprays are investigated in vessel chamber under room temperature with different injection pressures (50, 100 and 150 MPa) and the fuels are JME25 (JME 25: tridecane 75), JME 50, JME75, BDF and BHD. The results show that higher percentages of tridecane in JME, the spray tip penetration becomes lower as compared to lower percentages of tridecane. Same results for spray tip penetration of BDF compared to BHD. Spray tip penetration of BDF is larger than BHD and tridecane due to high viscosity, density, poor atomization, and

less momentum exchanged between the fuel spray and air. In sauter mean diameter (SMD) results show that the increase of injection pressures makes increase the spray tip penetration, spray cone angle and decreases overall SMD synchronously.

The third part of work is measuring the evaporating spray characteristics in the vessel chamber under injection pressure at 100 MPa and 400, 500 and 600 K. In evaporating spray, lower in ambient temperature (400 K), fuels that have higher boiling point temperature and distillation such as JME75 and BDF are resulting to have higher spray tip penetration and narrower spray angle as compared to other fuels. As ambient temperature increases at 600 K, the spray characteristics and deployment are improved due to micro-explosion occurred in the fuels. In sauter mean diameter (SMD) results show that at higher ambient temperature, SMD of all fuels is decreased. This happened due to the improved spray characteristics in fuels.

The fourth part of the work involved Laser-Induced Scattering (LIS) of non-evaporating spray by using sheet scattered photography. The condition was in the room temperature with an injection pressure of 150 MPa. The results show that with the percentage of JME increased, the shape of spray cross-section becomes sharp and penetration of spray trend to be longer. This happened due to constant injection pressure, spray tip penetration decrease and spray width increase with the rising of viscosity caused by the percentage of n-tridecane decreases.

The fifth part of the work is regarding the performance and emissions characteristics in BDF and BHD as compared to diesel oil. The experiments were investigated by single cylinder 4 stroke engine, in low and partial load, at EGR 0, 10, and EGR 20%. The results show that BHD has the highest thermal efficiency compared to diesel oil and BDF in low load with EGR zero and 10%. The thermal efficiency can reach to 2.28 to 8.1% as compared to diesel oil and BDF. The using of EGR have several advantages, at low load and EGR 20%, the thermal efficiency of diesel oil and BDF can be raised to 0.84 to 2.83% comparing to EGR zero. Moreover, at low and partial load adding EGR can reduce NO_x and THC emissions. Nevertheless, at partial load, the using of EGR can increase the CO and smoke emissions. Therefore, for the emissions control, using EGR is effective in low load than partial load. In addition, the performance and emissions also have been done in different injection pressure in EGR zero. As the fuel injection pressure increases, the brake thermal efficiency increases and the fuel consumption decreases. In higher injection pressure can improved the atomization in the fuel. Therefore, the emissions can also be decreased such as smoke and THC. However, NO_x is the biggest problems because it can be increased by the increase of injection pressure. However, combining between EGR and higher injection pressure are recommended in achieving good atomization and reducing the NO_x emissions.

The sixth part of the work is concerning the performance and emissions characteristics in biodiesel water emulsions (BDWE). The experiment was conducted in 1500 rpm with low, medium and high load. The results showed that at low load, the thermal efficiency of BDWE is reached up to 8.92% than diesel oil. At medium load, the specific fuel consumption of BDWE is increased to 11.66% compared to diesel oil. Moreover, CO₂ emissions in BDWE can be reduced to 12.8% than diesel oil at high load. The opacity of BDWE at middle load can cut up to 84.25% compared to diesel oil. The combustion efficiency is improved when water is emulsified with biodiesel. This is a consequence of the micro-explosions that facilitate atomization of the fuel.

11.2. Contributions from the Present Work

1. Detail characterization of JME and its blends, BHD, and BDF under non-evaporating and evaporating conditions. The experimental data on JME, BHD and BDF are useful to the technical literature.
2. The experimental data to the technical literature from the combustion and emissions of BHD and BDF. BHD is the second generation fuel that has some advantages such as the fuel properties has nearly the same as JIS. Moreover, the oxygen content in the fuel can improved the combustion characteristics in the fuel and reduced the emissions.
3. The experimental data to the technical literature from biodiesel water emulsions. Biodiesel water emulsions reached higher thermal efficiency. This because the micro-explosions in the fuel due to mixing between biodiesel fuel, water and emulsions can improved the combustion and reducing the emissions.

11.3. Direction for Future Work

This study of spray combustion and emissions from JME and its blends, BHD, BDF and biodiesel water emulsions have been investigated. However, in this study there are many future work that should be investigated. The future works are analyzing the JME and its blends, BHD, and BDF with LIF (Laser Induced Fluorescence) , LIEF (Laser Induced Essence Fluorescence) and flame in order to understand more detail in the combustion characteristics from fuels. Moreover, the simulation of combustion and emissions are also important to undertake to improve the work is significant close with the results from the simulations.

List of Publications

Annisa Bhikuning, Naoki Matsumoto, Tomoyuki Mukayama, Eriko Matsumura, and Jiro Senda. 2017. Analysis of Non-evaporating Spray Characteristics from Jatropha Methyl Ester and its Blend. *19th ILASS Asia, Jeju Island, South Korea*.

Annisa Bhikuning, Eriko Matsumura, and Jiro Senda. 2018. A Review: Non-Evaporating Spray Characteristics of Biodiesel Jatropha and Palm Oil and its Blends. *International Review of Mechanical Engineering*, 12 (4), 364-370.

Annisa Bhikuning, Eriko Matsumura, and Jiro Senda. 2018. Fuel Analysis of Jatropha Methyl Ester and n-Tridecane as an Alternative Fuel for the Future. *Matec Web of Conferences*, 153, 01002.

Annisa Bhikuning, Eriko Matsumura, and Jiro Senda. 2019. Performance and emission characteristics of biodiesel waste cooking oil water-emulsions under varying engine load condition. *Energy Sources, Part A: Recovery, Utilization, and Environmental Effects*. Published online 23 October 2019.

Annisa Bhikuning, Xin Li, Shoi Koshikawa, Eriko Matsumura, and Jiro Senda. 2019. An Experimental Investigation of Bio-Hydro Fined Oil and Waste Cooking Oil in Direct Injection Diesel Engine. *The Harris science review of Doshisha University*. 60 (3), 19-26.

Annisa Bhikuning, Xin Li, Shoi Koshikawa, Eriko Matsumura, Jiro Senda. 2019. The Experimental Investigation of the Performance and Emissions Characteristics of Direct Injection Diesel Engine by Bio-Hydro Fined Diesel Oil and Diesel Oil in Different EGR. *SAE Technical Paper*, 2019-32-0595.

Xin Li, Annisa Bhikuning, Eriko Matsumura, and Jiro Senda. 2019. Effect of Jatropha Methyl Ester Mixed with n-Tridecane on Spray Characteristics. *20th annual Conference of ILASS Asia, Yamaguchi, Japan*.

Annisa Bhikuning and Jiro Senda. 2020. The Properties of Fuel and Characterization of Functional Groups in Biodiesel-Water Emulsions from Waste Cooking Oil and Its Blends. *Indonesian Journal of Science and Technology*, 5 (1), 95-108.